

Probabilistic Modelling of Sensitivity in Fire Simulations

by

Kathrin Grewolls

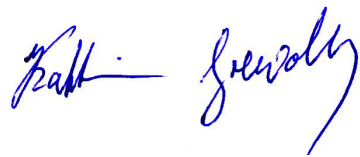
A thesis submitted in partial fulfilment for the requirements for the degree of
Doctor of Philosophy
at the
University of Central Lancashire

July 2013

Declaration

I declare that while registered as a candidate for the research degree, I have not been a registered candidate or enrolled student for another award of the University or other academic or professional institution.

I declare that no material contained in the thesis has been used in any other submission for an academic award and is solely my own work.

A handwritten signature in blue ink, appearing to read "Kath. Grewalt", written in a cursive style.

.....
Signature of Candidate

Type of Award: Doctor of Philosophy
School: University of Central Lancashire, School of Forensic and Investigative Sciences

Abstract

The objective of this thesis is to apply probabilistic sensitivity analyses to the emerging field of toxic hazard simulation in fire science. Fire simulation based on computational fluid dynamics (CFD) plays an important role in performance-based fire design. However, the thermal-physical process of material decomposition in fires and the chemical reactions of fire effluents are not well enough understood to make useful predictions about their burning behaviour. Input parameters are subject to uncertainties which can cause deviations in the results. Conventional engineering approaches are not suitable for reliable prediction of effects of input uncertainties on the results. In this work, probabilistic sensitivity analysis based on random sampling is used to determine the most important input variables and how uncertainties in their value influences the output.

The theoretical basis for hazard analyses is summarised and uncertainties are described which typically influence the results of fire tests and numerical fire simulations. The simulations are run with the Fire Dynamics Simulator (FDS), version 6. The proposed method was used for both mixing-controlled and finite-rate combustion with Large-Eddy- and Direct Numerical Simulation. Results of three different sensitivity analyses, each based on up to 500 samples are presented. The input parameter sets were systematically generated using advanced Latin Hypercube Sampling. The results of the sensitivity analyses were evaluated using the Metamodel of Optimal Prognosis which provides a measure of the predictability of the simulation that can be applied as an indicator for model quality. The results allow conclusions to be made, which quality of prognosis can be achieved using current fire simulation technology. The most influential parameters have been identified. Based on these simulation results a recommendation is made as to how the technology of probabilistic fire simulation and sensitivity analysis can be developed further in order to allow material parameter identification as a basis for the prediction of toxic effluents from solid fuels.

Contents

Acknowledgment	IX
List of Figures	X
List of Tables	XII
1 Introduction	1
2 Basics	3
2.1 Hazard Prediction	3
2.1.1 Fire Hazard Assessment	3
2.1.2 Socially Accepted Risk	5
2.1.3 Smoke Obscuration	6
2.1.4 Toxic Hazard Prediction	6
2.1.5 Fire Simulation within the Process for Hazard Prediction	9
2.2 Fire Simulation	11
2.2.1 Theroretical Basis and Numerical Methods	11
2.2.2 Modelling of Turbulence	13
2.2.3 Modelling of Solid Phase Pyrolysis	14
2.2.4 Modelling of Gas Phase Combustion	16
2.3 Experiments and Fire Tests	20
2.3.1 Purpose of Experiments and Fire Tests	20
2.3.2 Bench Scale Tests	20
2.3.3 Large-Scale Experiments	23
2.3.4 Full-Scale Experiments	23
3 Uncertainties and Sensitivity	27
3.1 Uncertainties	27
3.1.1 Introduction	27
3.1.2 Uncertainties in experiments	27
3.1.3 Uncertainties in Calculated Quantities from Measured Parameters	31
3.1.4 Uncertainties in Fire Models	32
3.1.5 Uncertainties of Input Parameters	33
3.2 Probabilistic Simulation of Sensitivity	37
3.2.1 Sensitivity Analyses of Fire Simulation in Literature	37

3.2.2	Basics of Sensitivity Analysis	38
3.2.3	Theoretical Basis	42
3.2.4	Metamodel of Optimal Prognosis	43
4	Simulation	46
4.1	Fire Simulation: The Fire Dynamics Simulator (FDS)	46
4.1.1	Basis, Model Assumptions, Simplifications	46
4.1.2	Finite-Rate Combustion Model for Propane and Tracked Species	46
4.2	Sensitivity Analysis with OptiSLang	47
4.3	Sensitivity Analysis of a Bench-Scale Tubular Furnace Test	48
4.3.1	Objective	48
4.3.2	Model Description	48
4.3.3	Sensitivity Analysis TF1: Simple Chemistry Model	49
4.3.4	Summary of findings from TF1	58
4.3.5	Sensitivity Analysis TF2: Finite Rate Combustion	58
4.3.6	Summary of findings from TF2	67
4.4	Sensitivity Analysis of ISO-9705 Room-Corridor test	70
4.4.1	Introduction	70
4.4.2	Model description	70
4.4.3	Summary of findings from Room Corridor Test	74
5	Conclusions	80
5.1	Uncertainties and Probabilistic Sensitivity Analyses	80
5.2	Simple Chemistry or Single Mixing-Controlled Reaction.	81
5.3	Finite-Rate Combustion.	82
5.4	Turbulent Combustion	83
6	Guideline to sensitivity analyses	85
	References	87

Acknowledgment

First, I would like to express my sincere gratitude to Professor T. Richard Hull, Research Co-ordinator and Professor of Chemistry & Fire Science at the University Of Central Lancashire's School of Forensic and Investigative Sciences / Centre for Fire and Hazard Science for his help and support. Second, I would like to thank Professor David Purser for his advice as second supervisor. Finally, I thank my family for their encouragement, understanding and support.

This thesis is the result of research activities which I carried out in addition to my work as a certified expert in protective fire engineering. All technical equipment was provided by my own consulting company in Germany. The simulation cluster which was required to run the sensitivity analyses has been designed specifically for numerical fire simulations and can carry out many jobs simultaneously. It has been developed and improved in the context of many projects for my customers.

List of Figures

2.1	Scheme of the process of hazard analyses including fire simulation.	4
2.2	Hazard analyses: Severity vs. probability of occurrence and social acceptance of risks.	6
2.3	Fire simulation within the process of performance-based design.	10
3.1	Illustration of parameter sampling with Latin Hypercube.	40
4.1	Tubular furnace model: Dimensions (in mm) and positions of the sensors for gas temperature, mass fractions of species and FED.	49
4.2	Results of the mesh convergence study with the tubular furnace model using LES with grid sizes of 1.25, 2.50 and 5.00 mm.	50
4.3	Tubular furnace analysis TF1 with simple chemistry: Gas temperature (in °C) in the steady state after 5 s	52
4.4	Tubular furnace analysis TF1 with simple chemistry: Coefficient of Prognosis for heat release per unit area (HRRPUA)	52
4.5	Tubular furnace analysis TF1 with simple chemistry: 3D response surfaces of the metamodel of optimal prognosis.	54
4.6	Tubular furnace analysis TF1 with simple chemistry: Anthill plots and CoP graphs of ambient oxygen mass fraction vs. simulated oxygen concentration (above) and vs. gas temperature at the fire centre (below).	55
4.7	Tubular furnace analysis TF1 with simple chemistry: Anthill plot of CO mass fraction vs. CO ₂ mass fraction.	56
4.8	Tubular furnace analysis TF1 with simple chemistry: Anthill plots of CO, CO ₂ and O ₂ mass fractions vs. CO yield (above) and calculated gas temperature (below).	57
4.9	Tubular furnace analysis: <i>A posteriori</i> mesh quality metrics by the MTR criterion shown as time history for two measurement points which are situated vertically above the right edge of the fire surface, in heights of 2cm and 4cm and a centered MTR slice contour in the steady state after 5 s.	63
4.10	Tubular furnace analysis TF2: Coefficient of Prognosis for ambient temperature (TMPA). Comparison of finite-rate combustion with Large Eddy Simulation (LES), left vs. Direct Numerical Simulation (DNS), right, with 2.5 mm mesh resolution.	64

4.11	Tubular furnace analysis TF2: Coefficient of Prognosis for the concentration exponent of oxygen in reaction R1 of propane combustion, NS_O2_R1 (see 4.1.2), and anthill plot vs. max. total heat release rate.	65
4.12	Tubular furnace analysis TF2: Coefficient of Prognosis for the activation Energy in reaction R1 of propane combustion, E_R1 (see 4.1.2). The marked area in the Arrhenius graph is the parameter range covered in the sensitivity analysis TF2.	66
4.13	Tubular furnace analysis TF2: Coefficient of Prognosis for the initial mass fraction of CO ₂ , IMF_CO2, and anthill plot vs. the CO mass fraction at position 1.	67
4.14	Tubular furnace analysis TF2: Coefficient of Prognosis for the concentration exponent of CO, NS_CO_R2, and for the activation energy for the reaction R2, E_R2 (right) (see 4.1.2)	68
4.15	Tubular furnace analysis TF2: 3D response surfaces of the metamodel of optimal prognosis.	69
4.16	Geometry and measurement points of the room corridor simulation model	71
4.17	Gas temperature results (in °C) for the reference run of the room corridor model after 30, 60 and 350 s.	75
4.18	Room corridor sensitivity analysis: Coefficients of Prognosis for HRRPUA calculated with the metamodel of optimal prognosis.	76
4.19	Room corridor sensitivity analysis: Coefficients of Prognosis calculated with the metamodel of optimal prognosis.	77
4.20	Room corridor sensitivity analysis: MOP Response Graphs.	78
4.21	Room corridor sensitivity analysis: 3D Response Surfaces of the MOP for CO (left) and CO ₂ (right) at measurement point GS_20.	78
4.22	Room corridor sensitivity analysis: Linear correlation coefficients of soot yield.	79
5.1	Borgh-Peters Diagram	84
6.1	Process of sensitivity analysis and parameter identification.	86

List of Tables

2.1	Purser furnace results from Stec [76]	22
2.2	Results measured 200 s after ignition in the first floor (Bénichou et al. [19])	24
3.1	Example of given standard uncertainties of measured values from an ISO 9705 compartment fire test [47]	30
4.1	Input and output parameters of the tubular furnace sensitivity study TF1 with simple chemistry model. Descriptions correspond to the FDS6 User's Guide [25].	51
4.2	Input parameters of the tubular furnace sensitivity study TF2 with finite rate combustion model. (Descriptions according to the FDS6 User's Guide [25]).	61
4.3	Output parameters of the tubular furnace sensitivity study TF2 with finite rate combustion model and Direct Numerical Simulation (DNS). The output parameter values are the statistical results of 144 simulations, each of them using a different input parameter set. Values in the same line generally originate from different variants.	62
4.4	Input parameters of the room corridor sensitivity study with simple chemistry model. (Descriptions according to the FDS6 User's Guide [25]).	70
4.5	Output parameters of the room corridor sensitivity study with simple chemistry model. (Descriptions according to the FDS6 User's Guide [25]). The output parameter values are the statistical results of 96 simulations, each of them using a different input parameter set. Values in the same line generally originate from different variants.	72
5.1	Comparison of different combustion and turbulence models with regard to their applicability on different scales	83

Chapter 1

Introduction

The objective of this thesis is to investigate how toxic hazard simulation for fire science can be improved. An important step towards this improvement is to identify weaknesses in the simulation model. One such weakness is the reliability of input parameters which are subject to scatter. Understanding the influence of the uncertainties in the input parameters on the results is a key to identify which parameters deserve more precise determination before being employed for predictions. Due to the numerous non-linear relationships between input parameters and responses, answers to this question can only be found by multiple simulations of the same model while varying the input parameters. An appropriate approach to examine statistically relevant response of the model on variations in input data are sensitivity analyses which are based on probabilistic methods. Chapter 2 provides an introduction into the fundamentals of fire hazard assessment. The state-of-the-art of science and technology on toxic hazard prediction and fire simulation is described. Further, standardised experiments and tests to gain toxic yield data are explained.

Since it is of great interest how accurately a computer model can predict the consequence of a fire, chapter 3 gives an overview about uncertainties in experiments, measured quantities, simulation models and input variables. The differences between the predictions of a fire model and experimentally measured values for a specific fire scenario are based on the following uncertainties:

- Uncertainties of the computer model and the input parameters,
- Uncertainties arising from the setting of the experiment and the measurement method.

Subsequently, a literature review on sensitivity studies and an approach to probabilistic simulation of sensitivity with Latin Hypercube (LH) is proposed.

In chapter 4, an attempt is made to answer the following questions about the applicability of numerical fire models by probabilistic, simulation-based sensitivity studies:

- Is it possible to estimate fire toxicity with a simple fire model and a known heat release rate?
- Which are the parameters of importance included in the fire model?

- What influence do the most important parameters have on fire toxicity?

In chapter 4 "Simulation", results of different sensitivity analyses are presented which are based on Latin Hypercube Sampling, a method which allows a significant reduction of required samples compared to classical Monte Carlo Simulation.

The sensitivity analyses presented in chapter 4 were based on two different model scales: First, a small furnace of 5 x 11 x 5 cm with a specimen of 1 cm³ was simulated as a bench-scale investigation.

The performance of the simple chemistry combustion model with a Large-Eddy-Simulation was tested on the bench-scale model with 500 different samples. More simulations were carried out with same model using the finite rate combustion model using Large-Eddy-Simulation and Direct Numerical Simulation, both with 144 different samples.

Second, the half-scale room corridor test with outer dimensions of 2.30 x 4.80 x 1.20 m was subject to a sensitivity study with 96 different samples.

The results are discussed in chapter 5. Different combustion and turbulence models are compared with regard to their applicability on different scales.

In chapter 6 a guideline is proposed for the process of sensitivity analyses.

Chapter 2

Basics of Hazard Prediction, Fire Simulation and Fire Tests

2.1 Hazard Prediction

2.1.1 Fire Hazard Assessment

For most people in the world, their home is a place where they feel safe and protected. But the cosy furniture is a source of toxic hazard - in the case of a fire. A range of different ignition sources like equipment, candles and cigarettes may be nearby. A single technical or human failure may be enough to ignite upholstery or textiles, with disastrous consequences.

The probability to die in a house fire is relatively low. The way people see the risk of an event is strongly subjective according to personal experiences, education and social integration of people and far out of proportion to the actual risk. For example, people perceive the very low risk of terrorist attack as comparable or greater than the very high risk of being involved in a road traffic accident. The assignment of fire protection engineering is the identification of inherent hazards and the realistic, quantitative assessment of the risks.

Any harm or adverse health effect on people exposed to fires as well as damage to property are regarded as fire hazards. Possible fire hazards result from thermal exposure to flames or radiation, oxygen deficiency (asphyxiation) through smoke inhalation.

In ISO 13571 [39], four life-threatening components of fires are defined:

- inhalation of asphyxiant fire gases,
- exposure to eye and upper-respiratory tract irritants,
- exposure to radiant and convective heat,
- visual obscuration due to smoke.

Fire hazard assessment is based on the identification of inherent hazards, and their expected effects, in connection with the probability of the scenarios. It is based on three elementary questions [82]:

- What could occur?
- Which consequence would that cause?
- How likely is that scenario?

Any conditions that have the potential to cause an unwanted fire is a fire hazard. Therefore a fire hazard is present when combustible materials, ignition sources and oxygen are simultaneously present. Depending on the size of the ignition source and the type and distribution of combustibles, fire growth and the production rate of hazardous products will be different. The consequences to people are strongly dependent on the fire growth rate and yield of toxic gaseous products, linked to the number of people and their properties (e.g. age, health) in the exposed volume, and the time needed for evacuation. Developed fires also cause damage to property and the environment. The basic concept of hazard assessment is to link the consequences of certain scenarios with the time period in which they will occur statistically. The danger or risk is a combination of the hazard resulting from the consequences of gas effluent composition and the probability of this scenario. The identified risk may be considered acceptable, but in general an acceptable level of risk to society in general does not exist. It is always found in comparison to the model risk that is laid down through legislation by public authorities and with regard to the group of people that are threatened e.g. children or disabled people (see Figure 2.1).

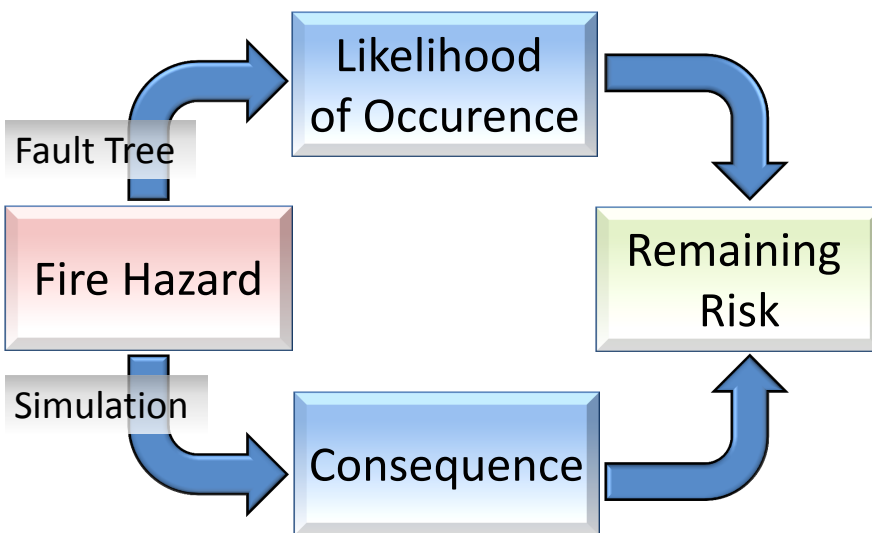


Figure 2.1: Scheme of the process of hazard analyses including fire simulation.

Techniques to assess fire hazards have been included in the safety process for mass transportation vehicles such as airplanes, trains and ships. Considering that passengers of commercial aviation are exposed to high risks in case of failure it is understandable that the Federal Aviation Administration (FAA) was the first organisation to include

the process of fire hazard assessment into the regulation in order to achieve a general acceptable risk for all passengers [16].

2.1.2 Socially Accepted Risk

The economic goal within the construction process is to build a cost-effective building. Therefore the costs for mounting and service of fire protection measures have to be reduced to a minimum, while the fire protection measures have to provide the minimum safety for people. A perceived failure following a fire could result in catastrophic claims for damages. This statement sounds rather simple but to specify the socially accepted risk in legal terms is rather difficult.

Fischer et al. [24] undertook a financial analysis of Switzerland's willingness to pay more for the purpose of saving additional lives. Switzerland was in 2005 ranked 2nd in the life quality index (LQI) with a score of 8,068 which was based on the subjective life-satisfaction surveys of different countries. The willingness of the Swiss society to pay for a higher fire security standard in order to save at least one person's life was considered to be dependent on wealth, life expectancy and a demographic factor. This was estimated at about five Million Euro per year. Statistical data must be used as input to these calculations. However, it can be used to express the willingness of the society to pay for additional obligations, but this data gives no useful information on the socially accepted risk for a single particular building.

For example, considering that 24 people die in house fires in Switzerland per year, between 2 and 7 lives could be saved through the use of compulsory installation of smoke detectors and alarms. Therefore the average costs for smoke alarm installation is about € 14 M per life saved, which is not considered worthwhile [24].

Generally it is assumed that the existing law reflects the socially accepted risk for unwanted fire. The safety level is laid down in each regulatory measure in prescriptive codes. Given that the safety level is always a holistic combination of many different measures it can only be regarded in its entirety.

The socially accepted risk for non-residential buildings specifies that people must be able to leave the fire room and the building without severe injuries no matter where and how a fire starts.

That implies that the level of safety has to be proven for the most likely and the most severe fire scenarios. In Figure 2.2, the black area designates the socially accepted probability of occurrence for hazards of different severity levels. According to the public opinion, cases of damage with high consequences (CC3, e.g. immediate fatalities, large amounts of loss, destroyed buildings) cannot be excluded but have to be reduced to a minimum. For cases with rather low consequences (CC1) which at the same time have a low probability of occurrence, the public opinion covers a wider range; therefore the black area is wider in the lower left corner of Figure 2.2.

This has the clear implication that the toxic hazard prediction and the tenable exposure time for all different people's escape abilities has to be demonstrated.

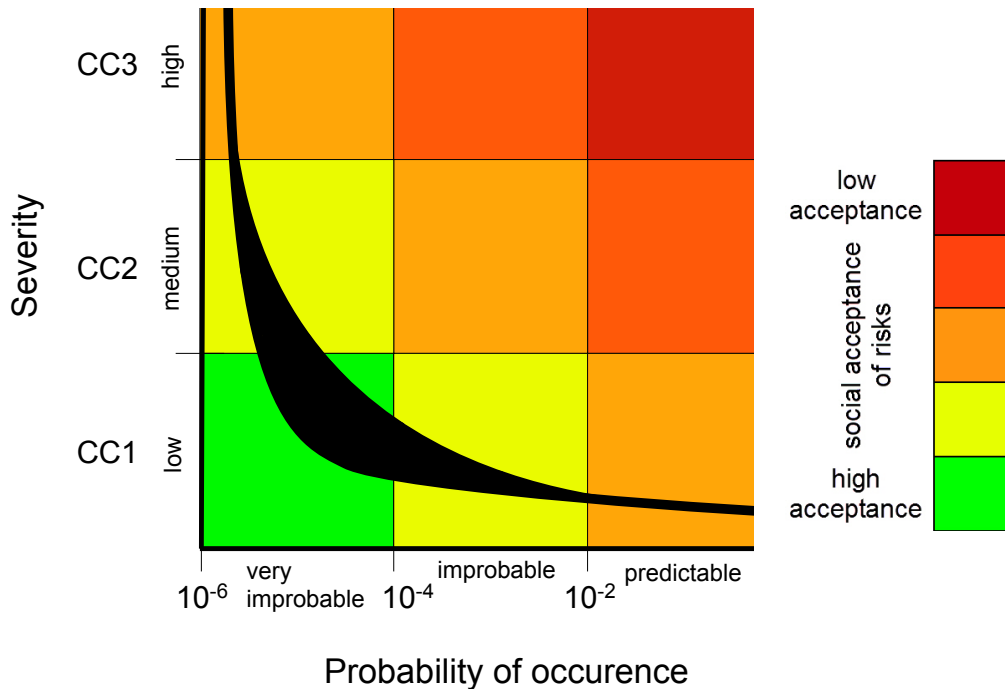


Figure 2.2: Hazard analyses: Severity vs. probability of occurrence and social acceptance of risks.

2.1.3 Smoke Obscuration

Fire effluents reduce the visibility and irritate the eyes, when aggregated in a room they blur the vision, make colours pale and contours blur till disorientation is reached. This is the point of incapacitation. Purser [67] explains the impact of smoke on the evacuation process and the walking speed. Lack of orientation as a result of reduced sight increases evacuation time and thus exposure time, irrespective whether persons are familiar with the building or not. Under conditions with extremely low visibility, they rather turn back than keep moving towards the exit.

Jin and Yamada [42] reported the observation of psychological effects of people exposed to smoke. Although most people seemed to get used to the smoke over the exposure time they still showed difficulties in concentration.

Two variables are important for the assessment of evacuation circumstances: smoke density and visibility. From a distance of 6 to 15 m people without seeing disabilities are able to read exit signs [41]. Non-illuminated exit signs seem to disappear at the presence of smoke while illuminated signs are still visually perceived. The presence of soot particles in the air absorbs light, therefore emergency signs may be visually recognised but are not readable. Carbon dioxide concentrations can be used to estimate smoke density and visibility.

2.1.4 Toxic Hazard Prediction

Most people exposed to fire die from smoke inhalation. Below some important relations of toxic hazards arising from fires are given. The book "Fire Toxicity" [78] is a compendium

that gives detailed information, for instance about the effects on fire victims (Shepherd [75]), animal exposure studies (Pauluhn [59]) and their application for fire safety (Purser [66]).

Alarie [1] distinguished between hazards in the room of fire origin and remote rooms. As a result of complete or incomplete combustion the room of fire origin starts to accumulate many different toxic gaseous compounds, burned and unburned hydrocarbons (such as alkanes, aldehydes or aromatics), carbon dioxide and water vapour. Already 30 seconds after ignition organic and inorganic gases such as hydrogen chloride (HCl), hydrogen fluoride (HF) and hydrogen bromide (HBr) and smoke have sensory effects on the eyes and the respiratory tracts, and lead to an impaired vision. Within a few minutes asphyxiant gases are produced. The combination of carbon monoxide (CO) and hydrogen cyanide (HCN) prevents oxygen from getting to the vital cells of the body. Alarie reduces the lethal hazards in rooms remote to the fire room to obscuration and irritation effects and asphyxiation from the concentration of carbon monoxide and hydrogen cyanide (HCN).

Various studies confirm the occurrence and severity of these toxic agents and some complete this list by adding nitrogen oxides (NO and NO₂) formaldehyde (HCHO), acrolein (CH₂CHO) or sulphur-dioxide (SO₂) depending on the composition of the burning material.

Additionally to the lethal effects Jin and Yamada [42] reported the observation of psychological effects of people exposed to smoke. Although most people seemed to get used to the smoke over the exposure time they still showed difficulties in concentration. Those effects increased the escape time and therefore the exposure time.

Studies on the effects of concentration of irritants or asphyxiant gases for incapacitation or death have been carried out on animals and on fire victims (e.g. Alarie [1], Stec and Hull [78] or Babrauskas et al. [8]). However, the applicability of animal exposure data to humans is limited. In particular, laboratory animals are generally chosen as healthy, young adults, while fire victims are usually very old, very young, or in some way incapacitated. Therefore it is not possible to define a certain range of exposure times and concentrations for all kind of victims that have to be considered as tenable based solely on such data. The personal dose of incapacitation is dependant on the health, age and the condition of the human body. Therefore the models assessing the effects of fire toxicity on humans estimates which assume a healthy population.

The complexity of experiments also increases with every toxicant that has to be assessed. As several hundred toxicants have been identified on burning a single polymer product, the research was directed to identify the most toxicologically significant elements that determine the toxicity of the smoke. The description of key species laid down the fundamentals for the N-gas model. Hartzell et al. [31] developed the fractional effective dose (FED) as an accumulation concept to model the effect of intoxication by one or multiple gas species.

LC₅₀ is the general term used to express toxic potency. It defines the mass of product that killed half of a rat population in a standard test. The N-gas model consists of a limited number of "N" toxic species, accounting for the biggest part of the toxic potential. The fractional effective dose (FED) is defined as the accumulated ratio of the atmospheric concentration C_i of any key species (i) at any point of time and its lethal concentration

at 30 minutes exposure time LC_{50} :

$$FED = \sum_i \frac{C_t}{LC_{50}(i)}.$$

The basic empirical N-gas model is based on 6 species (carbon monoxide, carbon dioxide, oxygen depletion, hydrogen cyanide, hydrogen chloride and hydrogen bromide) [9]:

$$FED_{NIST} = \frac{m \cdot c_{CO}}{c_{CO_2} - b} + \frac{21 - c_{O_2}}{21 - LC_{50,O_2}} + \frac{c_{HCN}}{LC_{50,HCN}} + \frac{c_{HCl}}{LC_{50,HCl}} + \frac{c_{HBr}}{LC_{50,HBr}}.$$

The constants m and b are empirical values accounting for deaths occurring within a period of 30 minutes of exposure and 14 days of post-exposure time. For CO_2 concentrations up to 5 % $m = 18$, $b = 122,000$ and above 5 % $m = 23$, $b = -38,600$.

Babrauskas et al. [9] propose LC_{50} values for HCN of 150 ppm ($LC_{50,HCN}$), HCl of 3,800 ppm ($LC_{50,HCl}$) and HBr of 3,000 ppm ($LC_{50,HBr}$). At a value of $FED_{NIST} = 1.0$ the 50 % lethality level is reached. To satisfy small variations the 95% confidence interval (± 0.2) assumes that at a value of $FED_{NIST} = 1.1$ half the animals would die.

For values of $FED_{NIST} < 0.8$ all laboratory animals survived and for $FED_{NIST} > 1.3$ all animals died within the 30 minutes exposure time.

Levin et al. extended this formula to cover nitrogen dioxide (NO_2). Nitrogen dioxide is highly toxic. Several hours after inhalation fire victims show poisoning symptoms like lung oedema and die. The following equation accounts for the effect that the simultaneous presence of nitrogen dioxide, carbon monoxide and carbon dioxide increases the toxic potential of all three gases. It shows the same effect for oxygen depleted situations [45]:

$$FED_{NIST} = \frac{m \cdot c_{CO}}{c_{CO_2} - b} + \frac{21 - c_{O_2}}{21 - LC_{50,O_2}} + \left(\frac{c_{HCN}}{LC_{50,HCN}} \cdot \frac{0.4c_{NO_2}}{LC_{50,NO_2}} \right) + 0.4 \left(\frac{c_{NO_2}}{LC_{50,NO_2}} \right) + \frac{c_{HCl}}{LC_{50,HCl}} + \frac{c_{HBr}}{LC_{50,HBr}}.$$

Using the same data set, Purser [65] introduced a similar model. However, this took the increase of the respiration rate from CO_2 to increase the uptake of all toxicants, not just CO and transferred it into an incapacitation model for humans.

Which means that when $FED_{Purser} = 1.0$ exposed people fail to escape because of unconsciousness. To account for 95 % of the population a much lower critical value should be chosen, e.g. $0.1 < FED_{Purser} < 0.3$. FED_{Purser} is based on the fact that different exposure doses of carbon dioxide, hydrogen cyanide and irritants are suitable for being summed up. Purser also accounts for increasing intakes through hyperventilation due to carbon dioxide exposure. Purser assumes that this effect is common in addition to the asphyxiation effect. Different forms of expressing FED can be found in literature, the equations below may also be found in [26]:

$$FED_{Purser}(t) = \max \left\{ \sum_{t=0}^{t^*} \left[(F_{CO}(t) + F_{HCN}(t) + F_{LD,irr}(t)) \cdot V_{Hyp}(t) + F_{O_2}(t) \right], \sum_{t=0}^{t^*} F_{CO_2}(t) \right\}.$$

The coefficient of carbon monoxide intake is derived by multiplying the carbon monoxide concentration of the air with the volume of breath per minute (RMV). In the blood carbon monoxide and haemoglobin forms carboxyhemoglobin (COHb) in the blood preventing oxygen transport by blood within the body. Fire victims with blood concentrations of COHb of 40 % are considered to be unconscious, but even lower concentrations of about 30 % COHb can lead to incapacitation especially for people with comprised cardiac function [64]. COHb concentrations of 50 to 70 % or even lower are reported as lethal.

$$\begin{aligned} \text{FED}_{\text{CO}}(t) &= \frac{3.317 \cdot 10^{-5} \cdot \text{BMV} \cdot c_{\text{CO}}^{1.036}(t) \cdot \delta t}{\text{COHb}_{\text{incap}}}, \\ \text{FED}_{\text{HCN}}(t) &= \frac{\delta t}{e^{5.396 - 0.023c_{\text{HCN}}(t)}}, \\ \text{FLD}_{\text{irr}}(t) &= \sum_{i=1}^n \text{FLD}_{\text{irr},i}(t) \frac{\delta t}{e^{5.396 - 0.023c_{\text{HCN}}(t)}}, \\ \text{V}_{\text{Hyp}}(t) &= e^{0.2c_{\text{CO}_2}(t)} \quad \text{with } c_{\text{CO}_2}(t) \text{ in vol-\%}, \\ \text{F}_{\text{O}_2}(t) &= \frac{\delta t}{e^{8.13 - 0.54(20.9 - c_{\text{O}_2}(t))}} \quad \text{with } c_{\text{O}_2}(t) \text{ in vol-\%}, \\ \text{F}_{\text{CO}_2}(t) &= \frac{\delta t}{e^{6.1623 - 0.5189(20.9 - c_{\text{CO}_2}(t))}} \quad \text{with } c_{\text{CO}_2}(t) \text{ in vol-\%}. \end{aligned}$$

2.1.5 Fire Simulation within the Process for Hazard Prediction

Fire Safety Design. For many years preventive fire protection was based only on prescriptive regulations. Those national or regional building regulations have evolved over time which means that regulations evolved as a response to disastrous fires. Often the given specifications are inappropriate to modern architectural design. Therefore another method is needed. Performance-based design combines engineering analyses and assumptions about likely fires to calculate fire safety. One of the reasons to use performance-based design is that an architectural design cannot meet the mandatory requirements. More often financial incentives lead to computer modelling of fire behaviour in order to lower construction costs. The solution found with the help of performance-based design is customer-fit and that is why that process can lead to lower construction costs without compromising the safety level. On the other hand performance-based design can also be used to increase the safety level as a process of security optimisation.

In recent years performance-based design has been accepted as an equivalent solution to meet regulatory requirements. The task of the fire protection engineer is to meet the given safety objectives outlining the socially acceptable level of risk. In the process of performance-based design the safety objectives such as:

- life safety - safe escape and rescue of people and animals,
- property protection - effective fire fighting measures.

have to be transformed into design objectives for fire protection and design criteria. A current method used in performance-based engineering is to model the architectural design (Figure 2.3b) and the correspondent design according to building regulations (2.3c). After selecting an appropriate design fire scenario, both designs are simulated. The results from the prescriptive design model are set as an upper limit (Figure 2.3c). For the architectural design the results (2.3e) are sufficient if the upper limit (2.3c) is not exceeded.

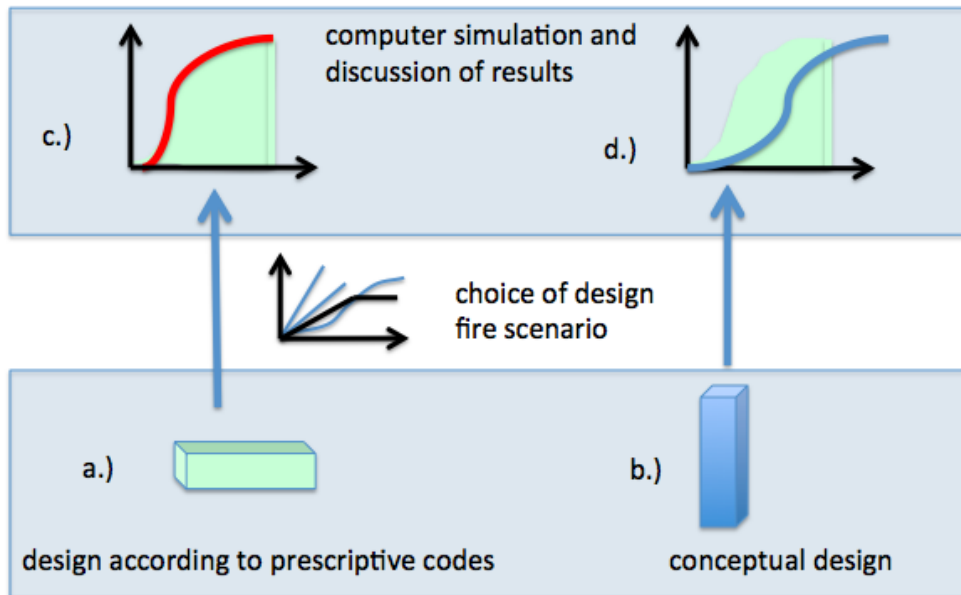


Figure 2.3: Fire simulation within the process of performance-based design.

For example, in order to prevent fire spread from the room of fire origin (design objective) the maximum temperature rise in the fire room over a certain time (performance criteria) has to be set. For safe evacuation of a hall (safety objective), the design criteria could be adequate evacuation routes and no smoke logging of escape routes within the evacuation time. This design criterion could lead to performance criteria for evacuation like maximum density of the flow of people and duration as well as criteria for influences on the evacuees like presence of smoke or toxicants in the smoke free layer, distance to smoke layer or maximum temperature.

According to these design criteria, and the scope of the project, the design fire scenarios have to be selected. Given that the number of fire scenarios that could possibly occur is almost unlimited, in order to complete the project in a timely and economic manner, only the most relevant fire scenarios can be considered. The "most relevant scenarios" which are used to assess the safety for building design must be appropriate for this purpose. The average fire scenario may be an underestimate while the worst-case scenario may be an overestimate of the consequences. Therefore these scenarios are not the best choice. The fire scenarios considered should not only have a reasonable likelihood of occurrence, but unlikely scenarios that represent failure events with disastrous consequences should also be considered. In each design fire scenario many single fire scenarios with similar characteristics are embedded in order to define fire protection measures. The underlying

assumption is that the results of a set of fire scenarios with only slightly different input parameters are similar within a certain range. No interactions between input parameters are taken into account in this method.

Assessing the ability of a fire model to predict fire toxicity and temperature rise is therefore crucial. The robustness of a model must be tested to understand the impact of certain changes or uncertainties in the input parameter on the result.

Fire Investigation. Fires lead to property damage and financial loss but it is even worse when people suffer serious injury or even death. Forensic investigations of fire incidents have to address the question of criminal responsibility; if the fire was of malicious arson or gross negligence. Therefore the origin, cause and the progression of fire is of certain interest. Professional in-situ examinations in combination with expertise provide a phenomenological approach. In addition, fire modelling provides technical references including smoke obscuration and asphyxiation. Almost all fire victims have their blood analysed to find the carboxyhemoglobin concentration (COHb) - surprisingly this is possible even from very badly charred bodies.

The modelling approach in fire investigation is for example:

- verification of assumed fire spread,
- computation of fire load and ventilation needed to create the scorch marks found,
- estimation of FED.

According to the available evidence, a set of most relevant fire scenarios that could have possibly occurred has to be chosen. Like in performance-based design, each fire scenario that is chosen as an example to be modelled within the investigation process represents a set of possible fire scenarios with similar characteristics and input parameters that ought to produce similar results.

2.2 Fire Simulation

2.2.1 Theroretical Basis and Numerical Methods

The theory for the description of fires is based on several disciplines among which fluid mechanics, thermodynamics and fire chemistry are the most important. Numerical simulation has become a very efficient method of investigation in many scientific and technical areas. Today, simulation technology is very advanced, powerful and efficient in many fields of technology. Also in fire simulation advances have been made; however, research is still concentrating on fundamental ways to describe the extremely complex processes occurring during a fire. Despite these open questions, it is possible to simulate the fluid dynamics and gas temperatures of typical fires with good precision. However, the correct simulation of toxic combustion product generation is not sufficiently advanced due to the need to integrate detailed chemical kinetics and fast chemistry into models of fluid dynamics [38, 49].

Fire simulation is carried out in order to determine those physical quantities which are important to assess effects of the fire on humans or animals and on building structures. For humans and animals, safe evacuation is most important and for buildings static strength under fire-induced thermal loads as well as possible damage by soot deposition. For fires in buildings, calculations of fluid flows and their physical properties in three-dimensional space are required to get reliable results. The discipline which develops solutions for this task is the Computational Fluid Dynamics (CFD). It is based on three physical conservation principles:

- The conservation of energy.
- The conservation of mass.
- The conservation of momentum.

These principles are mathematically described by the Navier-Stokes equations. The conservation equations of energy, mass and momentum form a system of coupled, non-linear, partial differential equations. As differential equations describe only relations between alterations of variables, the initial conditions from which these alterations start must be known, as for instance the ambient temperature or oxygen concentration. Additionally the conditions at boundaries of the system need to be defined.

The system of differential equations is to be solved under the given initial and boundary conditions. A closed solution - "analytical" by a hand calculation - is not possible because no closed solutions exist for these differential equations even for simple building geometries. The results can only be found by numerical methods, using powerful computers.

CFD simulation software differs by the numerical method which is applied, the majority of currently available CFD codes are based on one of the following methods:

- the Finite Element Method (FEM),
- the Finite Volume Method (FVM),
- the Finite Differences Method (FDM).

Several variants and combinations of these methods were developed to improve efficiency and precision.

All three methods require a geometrical discretisation of the computational space, i.e. the volume is divided into small cells or elements by a numerical grid or mesh. For simulation of transient currents such as occur in building fires, the time from beginning of the fire until the end of the simulation is also divided in small time steps - increments - which are sequentially computed.

In the Finite Differences Method (FDM) the Partial Differential Equations (PDE) are converted into a set of difference equations solved for every node of a continuous mesh. In the Finite Volume Method (FVM) the volume integrals in the partial differential equations are converted into surface integrals. The Finite Element Method (FEM) discretises a model into a number of finite elements. The Partial Differential Equations (PDE) are

solved for every element by means of an approximation function. The global solution is found by connecting all element equations in one system of equations.

The three methods do not only differ with regard to the applied algorithms and approaches but also with respect to their flexibility of use and precision. For example, the Finite Element Method (FEM) allows relatively precise mapping of complex geometrical shapes, where in fluid dynamics, the precision of results will be reduced by use of the Finite Differences Method (FDM). In FDM, curved geometry is mapped more coarsely than in FEM but for planar geometry the reliability of results is generally higher because FDM ensures that the conservation equations are automatically satisfied. In the field of fire protection engineering, mainly fires in buildings are simulated, and the walls and components are not inclined or curved but parallel to the coordinate planes. Here the application of the Finite Differences Method is appropriate [29].

For the simulation carried out for this thesis, the software Fire Dynamics Simulator (FDS) was used, which was developed by the National Institute of Standards and Technology (NIST, USA) in collaboration with the VTT Technical Research Centre of Finland. It uses the Finite Differences Method for the solution of the Navier-Stokes equations and a modified Finite Volume Technique to solve the radiation equation. More details on FDS are described in section 4.1.

2.2.2 Modelling of Turbulence

For the modelling of flows it is important to distinguish between laminar and turbulent flows. In *laminar flows* there are no measurable swirls or turbulences; fluid movements perpendicular to the direction of motion do not occur. The fluid moves in parallel layers. Such flows are typical for small velocities, at high viscosity and over sufficient distance to avoid geometrically disturbing influences such as sharp edges. In building fires, only a small part of the flow fulfills these conditions. Hence the turbulence of the flow has to be taken into account. Turbulent flows are characterised by vortices which cause state variables like velocity and pressure to change chaotically and irregularly. The spatial extent of the vortices comprises all possible orders of magnitude of the model, there are small ones at small openings or other geometric irregularities like ceiling beams or pillars and also vortices with the maximum dimensions of the simulated room.

Not only does turbulent flow accelerate the mixing of different components or species within the fluid, like mixing of soot particles with air - the vortices transform mechanical flow energy into thermal energy. The correct modelling of turbulence therefore has a great influence on the result. The method of Direct Numerical Simulation (DNS) works with mesh refinement down to the size of the smallest vortices of interest in order to include the effects of turbulence. Due to the limitations of current simulation hardware, this method cannot be applied to building fires because simulation times would be unacceptably long. Therefore different methods have been developed in order to describe the effect of turbulence in fluid dynamics approximately.

To do this, a typical property of the flows occurring in burning buildings can be utilised: they are normally driven by convection only, hence they move relatively slowly. This fact leads to important simplifications: the model of incompressible flow can be applied and modelling of vortices can be restricted to those with relatively large dimensions. This

simplification is referred to as "Large Eddy Simulation" (LES).

2.2.3 Modelling of Solid Phase Pyrolysis

Gasification of solid fuels is described with the help of pyrolysis models that couple the heating of the sample onto the pyrolysis of condensed phase. The process of pyrolyses is complex, and not well understood. Typically, the fuel of an unwanted fire is a polymer consisting of a long chain molecule of 100,000 atoms. In order to volatilise this chain must break down into smaller fragments. To predict pyrolysis, the heat transfer through this changing matrix must be known. Even the gasification of polymethyl methacrylate (PMMA) which has been for since about 80 years in many products and buildings defies prediction. The same generic material in different experiments showed a different number of reaction steps or behaviour. It can be concluded that the chemical equations to describe the pyrolysis and gasification of solid materials are not sufficiently understood. Fire modellers typically use experimental estimates of the gasification rates based on data from thermogravimetric analysis, fitted to the Arrhenius equation (2.1), such as the pyrolysis model in the Fire Dynamics Simulator (FDS).

The very complex interactions between the chemistry of combustion and dynamics of fire are explained in detail in Drysdale [23], Marquis and Guillaume [49], Quintiere [70]. Below there are only some important phenomena extracted.

The process of materials under fire conditions has to be separated into solid phase reactions and gas phase reactions.

The thermal decomposition of materials under fire is called "pyrolysis"; and is generally independent of the availability of oxygen.

It is common sense that fuel exposed to a heat source heats up. It is irrelevant if this process is initiated by an external heat source or the thermal feedback of an exothermic reaction. The phenomenon of transporting the heat absorbed on the surface into the solid is defined by the thermal conduction. The energy absorbed starts and drives the chemical and physical processes of thermal decomposition. The process starts generally when surface temperatures of 200 to 400 °C are reached. When a critical flux to the gas phase occurs, the criteria for ignition are met - the heat feedback from the flame is sufficient to replace the fuel generating it. General mechanisms of thermal decomposition of polymers have been described by Troitzsch [81]. A general simplification is that the oxidative process occurs only at the surface of the solid (e.g. rubbers). More detailed models take volume change and heat diffusion into account or include the formation of char on the surface, which reduces the rate of discharge of volatile pyrolysis products.

The breakdown of polymer composites depends on the structure, on the radiative properties, its emissivity and its transmissivity. Oxygen depletion changes the gas phase flaming process physically through flame extinction and chemically. The time to ignition increases with decreasing oxygen concentrations so the flame spread rate decreases. In addition the process of decomposition slows down, which also results in decreasing mass loss rate. Troitzsch explains that the process of pyrolysis and devolatilisation of polymers consists of hundreds of endo- and exothermic reactions appearing simultaneously only dependent on the fuel, thermal conditions and the thermal stability of the fuel. Most models subsume those multi-reaction kinetics into a single global reaction.

Another constraint in the accuracy of predicting thermal decomposition is that the physical properties of each material, such as density, thermal conductivity, specific heat capacity and the permeability are temperature-dependent. To get information about the temperature dependencies and to account for the temperature ranges of these parameters in the model is not easy. This is even more complicated for multi layer materials. Therefore often a global property is used. Instead of multiple specialised bench-scale property tests Lautenberger introduced a different method to account for these dependencies with the help of a numerical optimisation routine.

Pyrolysis models have to concentrate on a simplified mechanism that is based on a small number of empirical parameters, such as single or two-step reactions, for a specified range of conditions (e. g. oxygen concentration and temperature). Single-step reaction models are based on non-isothermal thermogravimetric (TG) data [34].

In contrast to the commonly used pyrolysis models that focus on the total mass loss, predicting the actual escape of flammable volatiles is another promising approach [44]. This is important because some mass loss produces volatiles which are not combustible (e.g. H_2O , CO_2) and some even react as inhibitors (e.g. hydrogen halides HCl, HBr from fire retardant additives).

Two types of pyrolysis models have been established.

- Semi-empirical pyrolysis models (macro-scale description) that relate material properties directly to equations of burning behaviour found in bench-scale fire tests.
- Comprehensive pyrolysis models. These models are more advanced and include at least some details of microscopic processes appearing within the solid.

An advancement to the single-step reaction are the multi-step reactions based on thermogravimetric mass loss data and numerically iterated kinetics. The various steps of thermal decomposition are defined by the Arrhenius equation but for a complex system such as a decomposing polymer the kinetic parameters A and e are empirical values.

The process of pyrolysis is very complex and particularly unsteady especially in the area of char and cracks. During the process many changes in variables take place, for example an increase in enthalpy, mass transfer and devolatilisation, heat transfer through convection and conduction, and evaporation of moisture. All pyrolysis models are based on homogeneous materials, rather than actual fuel in unwanted fires, such as layered materials in fabricated foam furniture or composites.

A flame above the material will only be stabilised if the mass flow of combustible gas is sufficient. In addition, for ignition to actually occur a heat source is needed to provide the critical concentration of free radicals needed to indicate flaming combustion. This provides the minimum activation energy needed to start burning. The lowest temperature at which ignition will occur above the surface of a solid is the so-called ignition temperature. It depends most on the shape and size of the material and the parameters discussed above like oxygen concentration, temperature, pressure.

2.2.4 Modelling of Gas Phase Combustion

Once the sample is heated above its ignition temperature and an energy source provides enough free radicals for ignition, the gaseous fuel will radiate heat back enough for self-sustained burning. The ignition temperature is a function of the ambient oxygen concentration and the sample geometry and orientation.

The fuel mass flow increases with increasing surface temperature of the sample which accelerates the process of thermal decomposition and gasification and drives flame propagation across a combustible surface.

The exothermic process of combustion releases heat at a certain rate, with the formation of more stable molecules by breaking and reforming molecular bonds. The amount and kind of species produced in the fire is not only dependent on the fire conditions (temperature, oxygen concentration and pressure) and the decomposition process (charring or non-charring material behaviour) it is also dependent on molecular structure and the composition of the material and the decomposition mechanisms of the products released. The simplification of the ideal combustion model is that carbon and hydrogen form carbon dioxide and water vapour respectively with ambient oxygen. In reality, some radical species combine and agglomerate instead of reacting with oxygen, which results in the formation of other products of incomplete combustion (carbon monoxide and hydrocarbons). Furthermore the molecular structure plays an important role in the reactions occurring in the burning process which also defines the fire growth, heat and smoke release as well as the flame height.

The amount of toxic species produced, such as the main asphyxiants, carbon monoxide and hydrogen cyanide (HCN), is strongly dependent on the ventilation conditions of the burning material. The less oxygen available the bigger the yields of carbon monoxide (CO) and hydrogen cyanide (HCN) that will be released from the fuel.

Pitts [63] described the use of the global equivalence ratio concept (GER) that linked the mass of species produced to the mass of fuel consumed in the reactive volume and the burning conditions.

The global equivalence ratio concept (GER) can be defined as the proportion between the actual fuel mass flow to air flow ratio to the corresponding stoichiometric ratio:

$$\phi = \frac{\frac{\dot{m}_f}{\dot{m}_{\text{air}}}}{\left(\frac{\dot{m}_f}{\dot{m}_{\text{air}}}\right)_{\text{stoic}}} = \frac{\left(\frac{\dot{m}_f}{\dot{m}_{\text{air}}}\right)}{r},$$

with

$$\left(\frac{\dot{m}_f}{\dot{m}_{\text{air}}}\right) \quad \dots \text{ actual ratio of fuel mass flow } (\dot{m}_f) \text{ to air mass flow } (\dot{m}_{\text{air}}),$$

$$\left(\frac{\dot{m}_f}{\dot{m}_{\text{air}}}\right)_{\text{stoic}} = r \quad \dots \text{ stoichiometric fuel-to-air ratio.}$$

The global equivalence ratio concept (GER) can also be expressed in terms of the the ideal heat release rate of the fire (\dot{Q} in kW) and the air flow rate (\dot{m}_a in kg/s) as follows

[28]:

$$\phi = \frac{\dot{Q}}{\dot{m}_{\text{air}}} \cdot \frac{1}{3,030}.$$

To solve this question no knowledge about the fuel chemistry is needed. The ideal heat release rate (\dot{Q}) is determined by multiplication of the mass loss rate and the heat of combustion.

For stoichiometric burning conditions ϕ equals 1.0. Larger values of ϕ represent under-ventilated or fuel-rich burning conditions, while values smaller than 1.0 indicate well-ventilated or fuel-lean conditions.

The general approach of the GER concept for fire hazard assessments has been determined normalised species yields. Forell [26] compared the results for yields of carbon monoxide from 7 different experimental studies, e.g. Beyler [10], Hosser and Blume [35]. He came to the conclusion that after 20 years of research there is still a lack of understanding and a lack of documentation of the main phenomena important for the comparability of the test results.

Forell therefore identified three major problems:

- The accuracy of measured mass flows of fuel and air. When steady state conditions are not achieved, the air mass flow values were averaged over different time intervals or calculated from exhaust gas flows.
- Identification of the temperature and the value of GER for the transition point between the minimum basic yields of CO which are unaffected by ϕ , and GER dependent yields.
- The observation of secondary combustion in the upper layer away from the main fire plume and their influence on CO yield.

The accuracy of GER is strongly influenced by the accuracy of the measured parameters. But the basic concept of choosing the important parameters is not always the same. Steady state conditions are needed to account for GER but for solid or liquid fuels, for example, steady state conditions are hard to achieve. Therefore the mass loss rate is often averaged over different intervals. Another example reported was that the mass flow of freely ventilated experiments often varied considerably and the fire condition was therefore amended after the experiment.

The temperature dependency found for different values of ϕ is not assimilable between all experiments. Some of the reported values of upper layer temperatures (T_{ul}) at the transition point between the minimum basic yields of CO and increasing CO yields depending on the GER values are summarized below:

- $550\text{K} < T_{\text{ul}} < 850\text{K}$ (Beyler [11]),
- $T_{\text{ul}} < 800\text{K}$ or $T_{\text{ul}} > 900\text{K}$ (Gottuk and Lattimer [28]),
- $T_{\text{ul}} < 700\text{K}$ or $T_{\text{ul}} > 900\text{K}$ (Pitts [63]).

These findings are not taken into account in the "simple chemistry" combustion model of FDS 6 where constant yields of CO and soot are defined as input parameters.

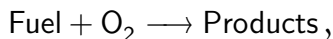
Forell also reported that external or secondary combustion of exhaust gases away from the main fire plume in these experiments had been interpreted in different ways. It is often reported that burning at the interface of hot upper layer will reduce the yield of carbon monoxide. However, Wieczorek reported increasing yields of carbon monoxide because his method of correlating the species concentration was based on measurements within the burning layer.

Even simple fuels decompose within a large number of intermediate reactions, which are often extremely fast and occur simultaneously. These elementary reactions are only identified for simple fuels like methane or hydrogen [46]. Therefore often one global reaction may be used that approximates all decompositions into a single equation.

To model the reactions and transport of fuel, air and combustion products, different options are possible in FDS, from the "simple chemistry" approach with only a single mixing-controlled reaction over complex stoichiometry (mixing-controlled with multiple reactions) up to finite-rate combustion. FDS solves the mass transport equations by default for fuel, air and products only, each of these three represent a lumped species consisting of multiple components. However, it is possible to track multiple species. In this case the transport equations must be solved again for each additional species which requires roughly 5% more computational cost per species [25, 55]. In order to investigate the distribution of toxic combustion products, both modelling of multiple reaction steps and multiple species transport are important. Finite-rate combustion is a more precise description of reality than the simplification of the mixing-controlled approach.

Rate of combustion. The rate of combustion is the time derivative of the fuel concentration. It is proportional to the concentrations of fuel and oxygen with the reaction rate constant $k(T)$ as a proportionality factor:

For the combustion reaction



the reaction rate is

$$v = \frac{d\hat{C}_{\text{Fuel}}}{dt} = k(T) \left(\hat{C}_{\text{Fuel}}\right)^{N_{\text{Fuel}}} \left(\hat{C}_{\text{O}_2}\right)^{N_{\text{O}_2}}.$$

The dependency of reaction rates on temperature is realised via the temperature dependency of the rate constant in the Arrhenius equation:

$$k(T) = A e^{-E/RT}, \quad (2.1)$$

with

A ... Pre-exponential factor,

E ... Activation energy,

- R ... Universal gas constant, $R = 8.314[\text{Jmol}^{-1}\text{K}^{-1}]$
T ... Absolute Temperature in K.

Using this definition for $k(T)$, the reaction rate becomes

$$v = Ae^{-E/RT} (\hat{C}_{\text{Fuel}})^{N_{\text{Fuel}}} (\hat{C}_{\text{O}_2})^{N_{\text{O}_2}}. \quad (2.2)$$

2.3 Experiments and Fire Tests

2.3.1 Purpose of Experiments and Fire Tests

In order to predict toxic hazards of fires it is necessary to understand burning behaviour of different materials. The models of chemical and physical processes are often empirical or semi-empirical, thus they are based on hypothetical parameters that are obtained through experimental observation.

Therefore fire tests are required to obtain experimental data in order to form hypotheses and to test them against other experiments for the purposes of

- understanding the thermal breakdown of materials,
- knowing which species are evolved under fire conditions,
- observing the burning process as a whole.

2.3.2 Bench Scale Tests

The toxicity of smoke is a function of the type of product that is burning, on the conditions in which it is decomposing and the presence of oxygen during flaming combustion. The burning rate is dependent on the ventilation, which will also affect the degree of oxidation or combustion efficiency of the burning material. The decreasing oxygen concentration in a burning room leads to incomplete combustion, and therefore to increasing yields of toxic products (particularly CO and HCN) and soot (unburned carbon). Most of these parameters may be obtained from bench-scale tests.

As conditions of burning in real scale fires can rapidly change from smouldering to burning with flames, while the surrounding conditions such as oxygen concentration or gas temperature will also change, it is important to minimise the impact of these changes. Therefore bench scale tests have been developed to study defined phenomena under quasi-steady state conditions, representing different stages of fire under defined conditions. Bench scale tests used to investigate toxic gas and smoke generation as a function of the surrounding gas temperature and available oxygen have shown that usually these are the two most important parameters.

Objectives of bench scale fire experiments are to determine:

- thermal material behaviour like decomposition, gasification and ignition,
- char formation and
- volatile pyrolysis products.

Benefits of bench scale tests are:

- processes can occur under controlled conditions (esp. oxygen concentration and temperature),
- therefore the results are more reproducible and

- the experimental conditions are better defined.

The constraints of bench scale experiments are the limitations in the sample sizes, as they are too small for some large scale fire phenomena to occur. Some typical examples of bench scale tests have been described.

Cone Calorimeter (ISO 5660). Cone calorimeter tests have become an established small-scale standard test to determine heat release and mass loss rate under well ventilated conditions. The main parts of a cone calorimeter are the load cell which records the mass of the sample and the conical electrical heater above the sample. Additional informations can be deduced from measured heat release and mass loss rates providing important data for numerical models, like fire growth rate, critical heat flux for ignition and charring behaviour [37, 71]. Surface temperature measurements at the sample provide information about the critical surface temperature for ignition and char forming processes.

Hot effluent streaming upwards is collected via an exhaust hood. Gas samples are extracted from the duct and the concentration of oxygen, carbon monoxide, carbon dioxide and smoke density is measured. In addition, grab samples can be obtained from the flame zone.

A refinement to this apparatus is the controlled atmosphere cone calorimeter. In this setup sealed cubicle is fixed around the load cell and the heater through which a controlled volume of air may flow which makes it possible to conduct experiments under reduced ventilation. The simple principle is to allow less oxygen into the cubicle than the sample needs for stoichiometric burning. Mulholland et al. [52] reported broad results for CO₂ and CO yields within under-ventilated burning conditions. Several designs of apparatus exist, and standardisation of the method has been attempted.

German Tube Furnace (DIN 53436-3). A tube furnace contains an electric heating device that surrounds a tubular cavity which moves over the sample inside a quartz tube. It may be used to force burning under controlled, and well defined conditions. Since the sample decomposes in the apparatus under controlled conditions it will reach a steady temperature with a constant oxidiser flow.

Steady State Tube Furnace (BS 7990 and ISO TS 19700). The steady state tube furnace (BS 7990 and ISO TS 19700) or Purser furnace is a further development of the German tube furnace and has additionally a moving test specimen and a longer, static furnace. It has been used specifically to replicate the conditions of underventilated fires. It is a standard test method as well as a research tool to test fire behaviour of polymer materials in the different stages of a fire from:

- smouldering (non-flaming),
- after ignition (well-ventilated, flaming),
- ventilation controlled (under-ventilated, flaming) or

Table 2.1: Purser furnace results from Stec [76]

Material	ϕ	CO ₂ /CO ratio	CO ₂ [vol.-%]	CO [vol.-%]
LDPE	$\phi = 1.0$	30	2.8	0.02
	$\phi = 1.5$	10	2.0	0.12
	$\phi = 2.0$	9	1.5	0.12
PA 6.6	$\phi = 1.0$	50	2.8	0.01
	$\phi = 1.5$	8	1.3	0.12
	$\phi = 2.0$	2	1.0	0.20
Polystyrene	$\phi = 1.0$	50	2.8	0.06
	$\phi = 1.5$	12	2.1	0.10
	$\phi = 2.0$	12	1.8	0.09

- fire load controlled (well-ventilated, flaming).

As the test specimen moves through the tube furnace the temperature and the air flow are controlled. This test was used to establish toxic product yields as a function of the fuel air ratio (equivalence ratio). These yields are in good agreement with those measured in real scale fires. The furnace results are mostly reported as yields at particular values of the equivalence ratio ϕ or the furnace temperature. Stec [76] tested common single unadulterated polymers like Low Density Polyethylene (LDPE), Polystyrene (PS) and Nylon 6.6 (PA 6.6). Most polymers show a consistent and progressive decrease of the CO₂ /CO ratio with increasing values of equivalence ratio which results in decreasing CO₂ concentrations and increasing CO concentrations.

The fuel in unwanted fires often contains many different polymers. For practical solutions of fire engineering problems the combustion properties of such mixed fuels are usually replaced by one single fuel with averaged properties of the materials involved. The yield of carbon monoxide is one of the input parameters in simple chemistry models which is defined as constant and independently of the equivalence ratio ϕ to calculate CO₂ and CO concentrations.

As shown in table 2.1, Stec [76] discovered increasing concentrations of CO with increasing values of ϕ , with especially large changes for values of ϕ between 1.0 and 1.5 which reflects conditions found in room fires. Progressively decreasing CO₂ concentrations for values of ϕ between 0.5 and 1.5 lead to decreasing CO₂ /CO ratios. These results gained in bench-scale tests may be used to verify simulation results.

Results from Bench-Scale Tests. Typical results reported from bench-scale tests are mostly derived from steady state burning conditions. Most real scale fires undergo different conditions at different times. To adopt those bench scale yields for numerical simulations the following restrictions have to be considered. The values of the different yields are dependent on:

- the composition of the burning material,
- oxygen availability (ϕ),

- the temperature in the burning room.

Those conditions may change rapidly during the burning process.

2.3.3 Large-Scale Experiments

Babrauskas [6] postulated in 1992 that the CO yields of real-scale fires are not related to the yields found from bench scale experiments because of the oxygen supply and the plume temperature play an important role in the generation process. These bench scale test methods have improved over the last two decades, and now bench scale testing provides important yield data. Large scale experiments are much more conspicuous and expensive than bench scale tests but they provide important information about naturally occurring conditions within a fire compartment. Some tests need a large scale set up, because of the nature of the fire test; for example flame spread tests. Others need a large flaming volume in order to make the heat flux large enough to drive the underventilated flaming reaction.

Numerous large-scale fire tests have been used to measure toxic species evolution over decades. Blomqvist and Simonson-McNamee [12] give a detailed description of large-scale generation of fire effluents.

ISO 9705 Room Corner Test. The ISO 9705 room corner test is a reference test used to classify building materials. In order to determine heat release rates, measurements of oxygen, carbon monoxide and carbon dioxide are made. The dimensions of the room are 3.60 m long and 2.40 m wide with a door opening of 0.80 x 2.00 m. The height of the room is 2.40 m. Above the door opening an exhaust hood of 3.00 m² collects the smoke. The fire is located in a corner opposite to the door. The ventilation conditions can be modified by changing the width of the door opening. One of the restrictions of this test setting is that it is hard to determine the air in- and outflow, making estimation of the equivalence ratio difficult.

A variation to the standard ISO room corner test is the 1/2 scale room and corridor test. The room compartment has a size length of 1.80 m, a width of 1.20 m and height of 1.20 m. The room is extended by a corridor which is 4.80 m long and divided into two horizontal partitions along its full length. This horizontal partition separates the incoming air supply from the exhaust gases. Between the fire compartment and the corridor is an adjustable door installed to vary the ventilation conditions in the room of fire origin. This experiment is based on a half linear scale ISO 9705 room with corridor test.

2.3.4 Full-Scale Experiments

Real-scale experiments are often executed in existing or identical rebuilt flats or houses in order to simulate conditions as realistic as possible. However, such tests are non-standard, so they are more often employed to verify a particular hypothesis than for fundamental research. They are also very important in of fire investigation. Some examples of real-scale experiments are given below.

Table 2.2: Results measured 200 s after ignition in the first floor (Bénichou et al. [19])

Species		Door, open	Door, shut
Carbon monoxide	[vol.-%]	1.2	0.1
Oxygen	[vol.-%]	15	20
Carbon dioxide	[vol.-%]	3	1

Large-Scale Test Series. Observing realistic conditions produced in a fire room is only possible using large scale tests. There have been different test series with single rooms (e.g. Purser and Purser [68] and NIST [17]), flats and even houses. An outstanding research project with several tests in a two-storey single-family house was initiated by the National Research Council of Canada (NRC). The research project investigated the tenability (or time to escape) from fires starting in the basement of the house for occupants on a upper floor. Temperature rise, optical density and concentrations of carbon monoxide, carbon dioxide and oxygen as well as activation times of smoke alarms have been compared [19].

Two of several tests of fast growing fires, starting in the exposed ceiling joist basement were carried out to compare the time for untenable conditions in the upper level. The only difference between the tests was whether the door between the basement and the first floor was shut or open [19]. In those experiments the fire load was recorded but the heat release rates were not. Due to the difference of temperature rise in the room of fire origin it can be concluded that even if the two tests had the same setups the heat release rate for the fire was quite different. While the temperature in the basement with the door open had reached 800 °C within 200 s, the same fire load within the closed basement only reached 600 °C in the same time. Due to oxygen depletion this test never reached 800°C. Concentrations of oxygen, carbon monoxide and carbon dioxide are measured, an example is shown in table 2.2. After three minutes, a clear difference is observed between the results of the test with an open door and those with the door shut. The open door test shows high values of CO and CO₂ concentrations while the oxygen concentration has significantly decreased. In the other test only some fire effluents penetrated the door to the basement that was shut. The oxygen supply to the room of fire origin was limited by the leakage of the door. This can be concluded from the remaining oxygen concentration in the upper floor.

Although velocity measurements were mentioned the results were not reported or discussed. The difference between the two experiments for the conditions at the staircase in the first floor 200 s after ignition, is that the tenability limit ($FED = 0.3$) for carbon monoxide and related carbon dioxide hyperventilation is reached at 205 s when the door is open or at 466 s when the door to the basement is shut. This is very important as it shows that despite underventilated flaming having higher toxic product yields, the overall effect is that more ventilation leads to more rapid fire growth, and hence a shorter time to reach untenable conditions.

The test report describes in detail the construction of the house and ventilation openings, the type and location of the fire load and its ignition as well as the position of

measurement points. Limited information is given about the uncertainties arising from the measurements and the equipment. Only the general uncertainty in the calculation of FED is discussed in reference to ISO 13571. The fire load representing the furniture of a house is given as 190 kg of wood and 9 kg of polyurethane foam blocks but no information is given about air flow rates in openings, the mass loss rate or the resulting heat release rate.

Bounagui et al. [13] used the Fire Dynamics Simulator (FDS) to build a numerical model of the fire house. The reported simulations were executed with different peak heat release rates but only with a propane burner. The goal of this research was to find the best grid resolution; in this report this was a fine grid with a 10 cm cell length. As no information is given about additional yield input parameters it can be concluded that only the default reaction of propane was used. Given that the fire in the test, with the door kept closed, was clearly ventilation controlled the assumption of complete combustion cannot be justified.

Although the report was not published to compare simulation results to the measured experimental values it is remarkable that peak heat releases of 2,500 kW and 3,000 kW showed carbon dioxide concentration in the first floor (the door to the fire room was shut) that were still tenable ($FED < 0.3$) within the first 280 s after ignition while the same tenability limit in the experiment was reached about 320 s after ignition. In the simulations and the experiment with the open door, on the first floor values of carbon dioxide concentration of about 2.0 vol.-% were reported 200 s after ignition. At the same point of time concentrations of carbon monoxide were reported as 0.7 vol.-% for the simulation and 1.2 vol.-% for the experiment.

The NRC two-storey single-family house fire tests were initiated to test conditions that are naturally developed in the first and second floor of the house in order to get better knowledge about times remaining for escape. Among the detailed test reports there are only a few hints given that numerical analyses would follow. In a paper concerning grid optimisation the set-up was modelled and used to define the basics for a numerical study to optimise grid resolution and simulation times. In these reports there is no discussion of how the results of the experiment burning PU and wood differ from the simulation results where only a propane burner was used.

Round Robin Studies in Fire Science. In order to assess and improve the quality of measuring methods, DIN EN ISO/IEC 17025 classified laboratories are obliged to run tests regularly. The characteristics of the tests is that many laboratories have to run the same test independently and show agreement in output quantities. The test results will be compared and discussed by a supervisory board. Completely published round robin tests are of great value because of the unbiased comparison between the single results and the variation. Unfortunately most of the data is reserved only for internal use. Even worse are those publications presenting only "selected" results which directs the reader towards a predefined, and possibly misleading conclusion.

About 40 fire laboratories did flammability tests of common materials when Harvards's Prof. Emmons arranged a round robin test in 1968. From the large differences in the test results arose a critical discussion about fundamentals of flammability tests [72]. There are only a few publications about round robin tests for fire simulations, and even then

only part of the results are publicly available.

The goal of round robin fire simulation tests is that as many different engineers with different simulation tools calculate independently the same output quantities based on the same information about a common scenario. According to ASTM E 1355 [3], there are three different ways these tests may be conducted:

- Blind or *a priori* tests: only basic information about the compartment, the furniture and the technical equipment is provided,
- Open or *a posteriori* tests: additional to the information about the scenario, the measured results are provided,
- Specified tests: the ready-to-run input file is provided to the test person.

While *a priori* tests are conducted to assess the ability of different users to predict realistic output quantities such as temperatures without the possibility of adjusting the results. In *a posteriori* tests the measured values are known to the test participants. Therefore, the intent is to test the capability of adjusting a scenario to the target. Specified tests only check the hardware performance or the influence of compiling options on the result. Tests on round robin studies of fire modelling are often based on large scale fire tests in real buildings that are scheduled for demolition (e.g. the "Dalmarnock fire test one" in the UK or "Lehrter Brandversuche" in Germany). The benefit is a realistic fire scenario that is produced and measured. Rein et al. [72] presented a valuable *a priori* round robin study where international teams of different researchers and fire protection engineers experienced. The goal was to create a model of the test compartment and to "translate" the given furniture and ignition source into a realistic fire scenario in order to predict the time to flashover and to calculate plots close to the measured ones, unknown to the participants. The documentation given to the participants contained complete geometrical data, the point in time for forced, mechanical window breakage and points of measurements. Photographic documentation of the furnished and equipped room was provided, together with information about the fire load density and the ignition source. The test set up was arranged to generate a robust respectable scenario. Many measurement points assured sufficient comparability with different grid solutions. Altogether this provided an outstanding quantitative description of a compartment, more complete than a fire investigator will ever have. Nevertheless, the results predicted wide ranging differences in fire growth rate and time to flashover. Rein et al. [72] outlined the results as a wide scatter of predicted fire behaviours. The difficulty in predicting the fire growth is made clear by comparing the computed heat release rate (HRR) which lies in a range of 30 to 90 % of underprediction to 100 % of overprediction. This results of course in a wide range of predicted temperatures, roughly scattered about $\pm 80\%$ around the measured values. Rein et al. [72] summarised that out of ten values five did not meet the scenario at all.

Another result was that the only participant to adequately predict the heat release rate and the wall heat fluxes failed to predict other local quantities with same precision. In order to explain the scatter in the results of these tests, fundamental knowledge about sensitivity of input parameters is necessary.

Chapter 3

Uncertainties and Sensitivity

3.1 Uncertainties

3.1.1 Introduction

For many fields of application it is of great interest to know how accurately a computer model can predict the consequence of a fire. Therefore the accuracy of a fire model is mostly quantified by comparing the predictions against experimentally measured values for a specific fire scenario [3].

The difference between the results is based on the following uncertainties:

- Uncertainties of the computer model and the input parameters,
- Uncertainties arising from the setting of the experiment and the measurement method.

A total measurement uncertainty composed of different, single measurement uncertainties is very useful for the comparison of simulation results. But this presumes a broad documentation of the experiment and the measurements as well as a quantitative statement of its uncertainties. The confidence level of the measurement is mostly expressed as expanded uncertainty. The chosen expansion factor defines the size of the expanded bounds of the confidence level. The uncertainty related to the standard deviations (factor 2) corresponds to the confidence level of 95%.

An overview on the treatment of uncertainties in fire engineering calculations is given by Notarianni [56].

3.1.2 Uncertainties in experiments

The difference between a measured value and its true value is called measurement error. It is common sense that the repetition of measurements mostly shows at least tiny differences in the measured values. Systematic and random errors are always inherent in a measurement process.

Depending on the method used, there are two types of uncertainties [80]:

- Systematic errors through instrument uncertainty (e.g. thermocouples or gas analysers) and
- Random errors spreading the measured results and affecting repeatability.

Measurement errors that arise from instrument uncertainty are mostly systematic. They are mostly constant or proportional to the unknown true value. The bias depends on the instrument or method used for the measurement and is a degree for the trueness of measurements, whereas random error only adds a scattering effect to the measured values.

The standard deviation and the bias must be discussed in order to better assess the accuracy of values, their trueness and their precision. Information about those parameters may be found in the manuals of the measurement equipment, gained from repeated measurements and by observing the process and making expert judgements.

In typical room fire tests the temperature of the room, the air flow, the oxygen, carbon dioxide and carbon monoxide and other species concentrations are measured. Some examples are given below.

Uncertainties in Measured Temperature Values. For most temperature measurements thermocouples are used. The technique is quite simple. The potential voltage difference at the open end of two dissimilar metal wires in contact with each other at a certain temperature may be related to the temperature of the junction. Although this technique allows measurements of high accuracy, the uncertainty arises from the fact that the junction may not have the same temperature as the surrounding gas. Several sources of errors have been investigated by Moffat [51].

Pitts et al. [62] reported significant systematic errors of bare-bead thermocouple measurements under predicted temperatures in long term measurements. Owing to radiation loss, the recorded temperatures reached only about 70 % of the absolute temperature, although this radiation error may be reduced by approximately 80 % for double-shielded, aspirated thermocouples. Depending on the position of the opening the ambient temperature was underpredicted between 25 to 75°C. The indicated temperatures of the aspirated thermocouples was about 90°C higher than of the bare-bead ones.

NIST stated that significant improvements to measurement in fire conditions are needed to advance the validation of analytical tools and performance based design methodologies. To deepen the research of large scale fires, a new National Fire Research Laboratory (NFRL) had to be constructed [50]. The new laboratory should not only give NIST the possibility of testing real-scale structures under combined structural and fire load, it may also house a significantly improved measurement techniques. In order to fulfil all requirements of this huge project, which ought to be completed in 2013, a technology review had to be made. Thermocouple measurements are widely-used but every thermocouple has to have its own wire therefore new techniques were investigated. A demonstration test showed promising results for temperature measurements by digital image correlation and fibre-optic methods. Fibre-optic sensors (DSS sensors) measure temperature anywhere along the length of a fibre. The DSS measurement is based on Raman or Rayleigh scatter measurement and optical frequency domain reflectometry (OFDR). One of the fibre-optic systems discussed is based on a Rayleigh OFDR along a 70 m long fiber. The

reported spatial resolution is of the order of 0.01 m or ± 1 °C uncertainty. Lönnermark et al. [48] compared temperatures measured in an experimental tunnel fire with gas temperatures below 300 °C. The values measured by Fibre Bragg Grating sensors were within approximately 25 °C of the calculated gas temperature. Thermocouples measurements were significantly lower by up to 75 °C [50]. These results demonstrate the need for further research of thermocouple and fibre-optic gas temperature measurements in real fire conditions with time-varying gas temperatures.

Uncertainties in Measured Velocity Values. Most of the traditional flow meters are based on the Pitot tube concept of flow measurement, with an accuracy of about 10 %.

The velocity in room and corridor fire tests at the University of Central Lancashire was measured by an air velocity transducer which uses a velocity sensor as well as a temperature sensor to accurately measure air velocity. The manufacturer states the accuracy of the general-purpose air velocity transducers (FMA-900) used in the experiments as $\pm 1.5\%$ for room temperature and additional $\pm 0.5\%$ for a wider temperature range from 0 to 50 °C. Measurements of velocities below 5 m/s have an accuracy of $\pm 1\%$. The disadvantage of this method is the single point measurement that cannot replicate the complete flow field. Phenomena like counter flow or its three dimensional character can not be identified with this method. This lowers the accuracy of the measurement.

To overcome these problems, Bryant [15] reported a new approach to ventilation measurements for enclosed fires using stereoscopic particle image velocimetry (SPIV). The biggest benefits of stereoscopic PIV is that this technique allows measurements of thousands of sampling points over openings and the resolution of the flow velocity into the components of each dimension, (v_x, v_y, v_z) . The technique is completely independent of temperature and differential pressure measurements because it uses an optical imaging technique that optically identifies the displacement of tracer particles in a flow which is recorded with a camera. Scattering light around the tracer particles makes it possible to identify their displacement. The flow velocity for each dimension is computed from the optically measured displacement. Bryant [15] reported a relative uncertainty of the measured displacement of less than 0.02 for displacements as small as 1 mm.

Uncertainties in Measured Species Concentrations. Discharged volatile pyrolysis products are continuously monitored or grab sampled in an analysis unit connected to the experimental unit. These analysis units are:

- Fourier transformed infrared spectroscopy (FTIR),
- Gas chromatography (GC),
- Mass spectrometry (MS),
- Non-dispersive infrared analysis (NDIR).

Often a combination of gas chromatography and mass spectrometry (GC-MS) is used. Many more measurement units like electrochemical cells, wet chemical analyses or paramagnetic

Table 3.1: Example of given standard uncertainties of measured values from an ISO 9705 compartment fire test [47]

Quantity	Total Expanded Uncertainty (k = 2)
Temperature	-20% to +6%
Heat Flux	-16% to +20%
Soot Mass Fraction	± 6
Measured Heat Release Rate	± 14
Ideal Heat Release Rate	± 6

analysers are used within fire experiments. Those techniques are widely described in literature and not discussed here.

For FTIR, a beam of infrared light containing many frequencies at once is passed through the sample gas where different molecules will absorb different amounts of energy. This process is repeated many times with the next beam of light containing a different set of frequencies. Every time the returning light passes a certain configuration of mirrors (Michelson Interferometer) each wavelength is periodically blocked and transmitted. With the help of a Fourier transformation algorithm the absorption of each frequency may be calculated. Tolerance of the measured species is about 3 to 10 %.

In contrast to FTIR, non-dispersive infrared analysis (NDIR) measurements of CO and CO₂ concentrations use measurements of absorption over a single frequency often using simple fillers and fairly broad frequency ranges. In contrast to FTIR, where appropriate algorithms can be used to separate other species that absorb at the same frequency, in FTIR it is not possible to compensate for such interference.

A common method to separate the compounds of volatile mixtures is gas chromatography. One of the advantages of this method is its short processing time which makes it possible to get results from many samples. Bundy et al. [18] reported an uncertainty of ± 10 % for a measurement of the gas chromatograph with flame ionization detector (FID). However, the retention time alone is not regarded as positive identification.

Lock et al. [47] conducted an experimental study of the effects of fuel type, fuel distribution and vent size on an ISO 9705 compartment fires and discussed connected uncertainties. Some example of standard uncertainties of measured values are shown in table 3.1. The total expanded uncertainty for temperature measurements is -20 to $+6$ % including calibration and random errors as well as radiative cooling. The total expanded uncertainties for heat flux -16 to $+20$ % includes soot deposition, cooling water, calibration and random errors. Lock et al. [47] specify the total expanded uncertainty for the gas analysers used to be in a range of ± 12 including errors caused by the zero and span gas, the equipment uncertainty, the mixing and averaging and random errors.

3.1.3 Uncertainties in Calculated Quantities from Measured Parameters

In many experiments and calculations the heat release rate or the peak heat release rate prove to have the biggest influence on temperature, and also on the production of toxic species.

Axelsson et al. [4] published a survey about the uncertainty of each factor included in heat release rate calculations and discussed the uncertainties found for the standard ISO Room/Corner test with two different heat release rates.

The combined expanded relative standard uncertainty ($k = 2$) for the measurement of the heat release rate was calculated to be 7.1 % (peak heat release rate of 1 MW) and 10.6 % (peak heat release rate of 150 kW). The factors that contributed to the combined uncertainty are listed below (in order of decreasing importance):

- Oxygen concentration,
- Amount of energy released per kilogram oxygen consumed (E-factor),
- Mass flow in the exhaust duct,
- Molecular weight of the gas species,
- CO₂ concentrations,
- Humidity,
- Ambient pressure.

Independent of the quantity of the heat release rate the combined uncertainty was significantly influenced by the oxygen concentration, the E-factor and the mass flow in the exhaust duct. The uncertainty of the oxygen concentration in the duct decreases with increasing heat release rates because of the decreasing difference between the ambient and the duct concentration.

The E-factor is unknown if the material used for the test consists of several fuels (e.g. furniture). Axelsson et al. [5] state that for most common organic fuels the E-factor is about 13.1 MJ/kg_{O2} with a variation of 5 %. With a triangular distribution implied a relative standard uncertainty of 2 % is received.

The uncertainty of the mass flow measurement is a combination of uncertainties listed below (in order of decreasing importance):

- Velocity decay constant (k_p),
- Ratio of the average volume flow to the volume flow in the centre of the exhaust duct (k_t),
- Density of the exhaust gas in the duct (fixed factor of 22.4),
- Temperature,
- Cross section area (A),

- Pressure difference.

The combined expanded relative standard uncertainty ($k = 2$) was determined to be $\pm 3.2\%$.

This short excursion to experimental uncertainties was made to demonstrate that a difference between computed and measured values of about ± 10 to $\pm 20\%$ could still indicate excellent agreement taking uncertainties of each measured value into account for fire tests.

3.1.4 Uncertainties in Fire Models

In publications that compare measured values with simulation results, often only graphs of measured and computed results are plotted versus time. Sometimes these graphs are close to each other, sometimes they reveal large differences, but as long as the computed solution is not trivial they are never in excellent agreement.

Even if all the input parameters were exact and without any uncertainty, the prediction by a fire model would still not be exact. This is based on the intrinsic uncertainty of the fire model which is composed of:

- Physical and mathematical assumptions that are part of the model formulations (e.g. turbulence model or layer height assumption),
- Small numerical errors made in each differentiation and approximation process and
- One programming error within every thousandth program line [32, 33],
- Errors due to insufficient discretisation in space and time, for example by inadequate mesh density or too large time increments.

Several ways to assess model uncertainties have been reported in literature. Simulations often require many input parameters but only a few of them have a high impact on the result. The identification of those parameters with the biggest influence on the simulation results is therefore of high interest. Reducing the number of parameters to only a few contributes to lower research cost for parameter measurement material testing and improves the reliability of simulation results. It is often stated in literature that the "selection problem" of input parameters, the so-called subset selection, is one of the most fundamental and widespread model selection problems in statistics. The Bayesian treatment is only one example among possible methods to treat model uncertainties. Droguett [22] and Clyde and George [20] described the Bayesian method as one possible approach of selecting the best predictor subset for a variable of interest in expressing more precise objectives.

Once the input parameters of high interest are found, a method to describe the importance of each parameter is needed in order to assess its contribution to the final result. The sensitivity analyses which are described in this thesis fulfil this purpose.

3.1.5 Uncertainties of Input Parameters

In order to assess the exact model error in predicting a specific result from an experiment, by disregarding the measured uncertainties, it would be necessary that all essential input parameters are documented in the original test reports. But some of these quantities are difficult to determine because they are not measured (e.g. radiation loss). Therefore estimations have to be made.

The model input uncertainty is caused by input parameters that are derived from experimental measurements. Uncertainties of the following groups of parameters can occur:

- Thermal properties of solid surfaces of the compartment,
- Chemical properties of the fuel,
- Yields of fire effluents,
- Heat release rate of the fire.

The uncertainty of input parameters for simulation models in fire protection design is even bigger because:

- The fire that is chosen is only hypothetical,
- The building has often not been built at the time of simulation and
- The ventilation depends on daily conditions.

Uncertainties in Setting the Boundary Conditions and Structure Components.

The ambient temperature is the temperature of the air in the fire room and its surroundings at the beginning of the simulation, and that of the inflowing air at any time during the simulation. It depends on the room utilisation (sleeping or living room), the season (summer or winter), the location of the fire compartment (room inside a house or test room inside a fire test building) and the region (e.g. Finland or Italy). The common ambient room temperature is between 16 and 26°C.

The atmospheric pressure is the force per unit area that the weight of the air imparts to the ground. The normalised air pressure background at sea level is about 101 325 Pa. The atmospheric pressure fluctuates between 92 500 Pa in low pressure areas in summer time and 107 000 Pa in high pressure areas in winter.

The dimensions of building elements can be extracted from plans or measured directly. Smaller variations may accrue during the construction process. It is quite common that walls in a building differ from their supposed length up to 0,01 m. For air intake or smoke flow, voids in the structure play an important role. In contrast to the practice used for zone models, an aerodynamic opening cannot be defined by the user. Only the geometrical opening may be defined, using the horizontal and vertical lines of the grid. The amount of air flowing through a certain intake or exhaust opening can differ from those flowing through the openings in the test even when the pressure differences are the same. The difference may be caused by the geometry of the opening (sharp edges

or the system of levers of a smoke vent). The air flow through an opening has therefore to be investigated.

Münch [53] reported a critical influence of model boundaries, defined as open. The flow through open boundaries is not unaffected. A weak bouncing effect may influence output quantities close to the boundaries.

Any obstacles defined in the model may be heated or cooled in the simulation which influences the process. Only surfaces defined as "inert" or "adiabatic" do not gain or lose heat. In contrast to adiabatic surfaces, heat transfer to inert obstacles is calculated even when the obstacle itself does not warm up. Most of the following material parameters are temperature-dependent and define the heat transfer to obstacles:

- Thickness
- Thermal conductivity
- Density
- Specific heat
- Ignition temperature

Conductivity and specific heat may be defined as functions of temperature in an FDS-Simulation. These material parameters are product-specific and may be drawn from the respective technical data sheet. Some examples are given below.

The thermal conductivity (λ) of a material describes its ability to conduct heat. Because of its strong temperature-dependence, the values given in literature often refer to a temperature below fire temperatures. For example:

- $\lambda > 40 \text{ W}/(\text{m} \cdot \text{K})$: steel,
- $2 < \lambda < 3 \text{ W}/(\text{m} \cdot \text{K})$: concrete, granite, sand-lime brick, marble,
- $\lambda < 1 \text{ W}/(\text{m} \cdot \text{K})$: porous concrete, brick, wood, glass,
- $\lambda < 0.1 \text{ W}/(\text{m} \cdot \text{K})$: thermal insulating material,
- $0.02 < \lambda < 0.04 \text{ W}/(\text{m} \cdot \text{K})$: customary rigid polyurethane foam, expanded polystyrene insulating material.

The values of these parameters change significantly with temperature and for porous or cellulosic materials, with moisture content.

Below there are some examples of density for customary construction material given:

- $\rho > 7000 \text{ kg}/\text{m}^3$: steel,
- $2000 < \rho < 7000 \text{ kg}/\text{m}^3$: concrete, sand-lime brick,
- $400 < \rho < 2000 \text{ kg}/\text{m}^3$: porous concrete, brick, wood,
- $\rho < 350 \text{ kg}/\text{m}^3$: customary thermal insulating material,

- $15 < \rho < 30 \text{ kg/m}^3$: customary expanded polystyrene insulating material.

The density of a material is also dependent on the porosity of the material. A figurative example to this problem is a brick wall. Different bricks contain a different amount of voids or even long holes. If the density of solid brick material is about $1,600 \text{ kg/m}^3$ the total density without the volume of the voids may be around 20% less.

Typical values for specific heat or heat capacity of construction materials are given below:

- $c_p < 0.5 \text{ kJ}/(\text{kg} \cdot \text{K})$: steel,
- $1 < c_p < 2 \text{ kJ}/(\text{kg} \cdot \text{K})$: wood,
- $0.8 < c_p < 1.0 \text{ kJ}/(\text{kg} \cdot \text{K})$: concrete, sand-lime brick, marble,
- $0.6 < c_p < 0.8 \text{ kJ}/(\text{kg} \cdot \text{K})$: glass.

The values of these materials are highly dependent on their composition and their aggregates, and change as a function of temperature.

Radiative heat transfer into a material with an opaque surface is defined by the absorptivity, emissivity and reflectivity of the material.

The emissivity coefficient (ϵ) for common materials is a function of the ambient temperature, examples for room temperature are given below:

- $0.2 < \epsilon < 0.8$: steel,
- $0.8 < \epsilon < 1$: wood,
- $0.6 < \epsilon < 0.9$: concrete,
- $0.92 < \epsilon < 0.94$: glass.

The emissivity of steel building material was shown to increase by 20 % when heated up to about 200°C [58].

Uncertainty in Defining a Fire. Solid and gas phase reactions are discrete models implemented in FDS. There are several possibilities to model a fire. The applicability of the chosen model is dependent on available material data.

The most simple way to specify a fire is by defining a heat release rate (HRRPUA) or the mass release rate per unit area (MRRPUA) and the chemical formula of the fuel that is burning. This simple pilot-controlled burner model is based on a single, mixing-controlled reaction for combustion. Because this model does not account for the pyrolysis process and thermal conditions driving pyrolysis, no additional material properties needs to be defined.

This simple fire model is one of the most important utilities for numerical fire safety design. The heat release rate and the conditions of a fire can be assessed within a certain range even if these parameters are hard to assess. In contrast, the burning material is very difficult to predict before the fire happens.

The heat release rate of fabricated materials such as upholstered furniture depends on the materials, the layering of the materials, the burning conditions, the ignition and the

position in the room. "Identical" armchairs burnt under "identical" conditions in tests do not show identical heat release curves. Different armchairs may show similar heat release rates, but even different constructions using the same materials may give very different results. These differences are not only due to measurement uncertainties.

Below, input parameters to the simple fire model are listed:

- Heat release rate,
- Heat of combustion,
- CO and soot yield.

Babrauskas and Peacock [7] stated in their article about "Heat release rate: The single most important variable in fire hazard" that the 180 s average heat release rate of bench scale tests are comparable to the peak real-scale heat release rate. The exemplified peak heat release rates of multiply furnished rooms varied from 220 to 1,790 kW, and CO yields varied between 0.14 and 0.23 kg/kg.

Information about yields gathered from bench-scale tests are found in literature (e.g. Babrauskas et al. [8], Forell [26], Stec [76, 77]). One important question on the use of fire simulation models is: How are the results of the simple fire models influenced by the given yields?

In the simple pyrolysis model there are only few parameters controlling the burning rate itself. If an experimental burning rate should be adopted, the heat release rate must be customised. This can be done by defining a fire spread rate or the progression of the heat release. The following thermal parameters specifying the burning object may be defined to control the burning rate:

- The thickness of the object or layer,
- Heat of vaporisation (account for the energy used to vaporize the fuel)
- Its ignition temperature (delays ignition until the required temperature is reached).

For the fuel the following material properties may be specified:

- Thermal conductivity,
- Specific heat,
- Density.

These parameters may be measured or estimated. This leads to a particular kind of uncertainty in the simulation results.

The heat of vaporisation, enthalpy of vaporization or heat of evaporation (ΔH_{vap}) defines the amount of energy required to transform a liquid fuel into a gas. The heat of vaporisation is temperature and pressure dependent. Dependent on the instruments used for the temperature and pressure measurement, for a typical liquid fuel, the test result will be precise to about $\pm 3 \text{ J mol}^{-1}$ which leads to an uncertainty of about $\pm 0.01 \%$.

Piloted ignition temperatures of typical materials used in domestic properties vary from about 200 to 500 °C. Even though this range is fairly large the ignition temperature of some fuels can be specified as closely as ± 5 °C.

The questions for the applicability of numerical fire models arising from this point of view are:

- Is it possible to estimate fire toxicity with a simple fire model and a known heat release rate?
- Which are the parameters of importance included in the fire model?
- What influence do the most important parameters have on fire toxicity?

In the next chapter "simulation", an attempt is made to answer these questions by probabilistic, simulation-based sensitivity studies.

3.2 Probabilistic Simulation of Sensitivity

3.2.1 Sensitivity Analyses of Fire Simulation in Literature

In the literature, various sensitivity analyses of fire simulation models have been described. Some of them are described briefly below.

In literature, sensitivity analyses of fire models are often described as a test of the model, to predict output parameters based on different mesh sizes. Others use an arbitrary change in the input data set as one-factor-at-a-time simulations [14]. A frequent conclusion is that the output parameters show a significant sensitivity to a high number of input parameters.

More advanced studies are rarely found in literature. Qu [69] used a response surface model of Monte Carlo fire data to identify some aspects of safety indices, in order to develop a methodology that can be used with minimal effort in fire protection design. The focus was placed on temperature and time to reach incapacitation.

In several published sensitivity studies, deterministic sampling methods are applied. Parameter ranges are often defined by a fix percentage from which upper and lower limits are calculated, e.g. nominal or mean value ± 20 %. Mostly, these analyses are just based on samples generated by selecting different combinations of the minimal or maximal values of input parameters. Some of them simulate the sensitivity of one-dimensional material models in an environment with external heat source. Galgano et al. [27] analysed the sensitivity of a predictive model for fire response using a glass-fibre/polyester-Vermiculux sandwich exposed to a hydrocarbon flame. The influence of variations of ± 25 % of the main input parameters and of different model assumptions were taken into account.

Stoliarov et al. [79] and Witkowski [84] investigated the sensitivity of the burning rate to different input variables of the numerical pyrolysis model "ThermaKin". The parameters used in this semi-empirical model are obtained from direct property measurements. Stoliarov et al. [79] used 12 data sets containing all possible combinations of three different values of radiative heat flux and of four different values of the initial thickness. Witkowski

[84] analysed sensitivity based on variations of all 29 input variables but in each sample just one parameter value was increased or decreased by 5 %.

As a reaction to the results of the Dalmarnock round-robin study [72], Jahn et al. [40] carried out sensitivity analyses with deterministic sampling for combustion parameters, fire size and location, convection and radiation parameters. Koo et al. [43] developed a method which calculates multiple possible scenarios out of two measured fires generated with the Monte-Carlo method in order to identify input parameters for the prediction of real fire conditions.

Hostikka et al. [36] introduced a two-model Monte Carlo approach in order to use advanced simulation techniques like CFD for large compartments more effectively. The scope of this method is to determine the factor of over- or underprediction of simple zone models in order to identify input parameters for advanced CFD models by scaling the results.

Albrecht and Hosser [2] published results of a response surface methodology study used on parameters involved in assessing evacuation time and tenability limits. The response of the fire simulation model to the possible variation of input parameters is not obvious because of the strongly restricted number of parameters used for the pre-study of fire simulation.

All sensitivity studies cited above were limited either in the number of input and output variables involved, or in the number of samples or they do not systematically exclude linear correlation of input parameters. One important reason for the restricted investigations is the very high computational capacity required for fire simulation with CFD and the long simulation times. Due to the rapid development of hard- and software for numerical simulation, sensitivity analysis could be considerably faster and more reliable in the near future.

In this thesis, an approach is proposed to overcome these limitations and to use currently available simulation software to perform sensitivity analyses on gas phase reactions with all variables of potential influence, and with many random samples, under the condition of excluding correlations between input parameter sets. As a part of this work, results of probabilistic sensitivity studies for the parameters of wood as solid fuel, using FDS 5 for simulations of the room corridor test have been published in [30].

3.2.2 Basics of Sensitivity Analysis

The quality of results which are produced by fire simulation depends very much on the quality of the applied models and of the input data. Input data for simulations are usually mean values which were identified by regression from measurement results. Geometrical dimensions are taken from plans but in the real structure they can be built with a certain precision which can only be expressed as a probability distribution. Consequently, simulation results based on mean values are mean values as well. This is obvious; but mostly the influence variations of *one specific model property or material parameter* have on the results is unknown. However, this is valuable information which can be used to estimate the influence of uncertainties, to facilitate design optimisation and to improve models and input data. A method to measure these relationships qualitatively and quantitatively is sensitivity analysis. For sensitivity analysis, from input data which is uncertain, a set

of input parameters is defined, and results which are expected to depend on the input parameters are set as output parameters. Sensitivity analysis is the study of how the uncertainty in the output of a model can be apportioned, qualitatively or quantitatively, to different sources of variation in the input of a model [74]. The uncertainty of each input parameter is described by a parameter range and a probability distribution function, e.g. normal or uniform distribution. Within this space of parameters, different sets of parameter values - samples - are selected which represent in the best possible way the complete parameter space (Figure 3.1). These sets are found by random sampling.

The classical method for random sampling is Monte-Carlo simulation. For a Monte Carlo simulation with multiple parameters, a sample - i.e. a set of parameter values - is generated by assigning each parameter a random value from its predefined range. To achieve high precision with Monte Carlo simulation, a very large number of samples is required, often of the order of 10^4 to 10^5 . Therefore the classical Monte Carlo approach is not appropriate for time-consuming fire simulation as the CPU time for one study with the required number of simulations would considerably exceed acceptable values. An efficient way to solve this problem is to use Latin Hypercube Sampling (LHS) which allows a significant reduction of samples required for the same quality of results.

The concept of Latin Hypercube Sampling is:

1. The probability distributions for each input parameter must be known or needs to be assumed. Every input parameter range is divided into a number of segments, each having equal probability of occurrence. This can be visualised in a probability density diagram (Figure 3.1). For uniform distributions the probability density function is constant and each segment has equal width to fulfill this condition. For normal distributions, like Figure 3.1, segments become wider towards the maximum or the minimum of the parameter range in order to have equal probability to values from the ranges in the middle. The segment between B and C is narrower than the other ranges, and all segments have equal area, i.e. equal probability, here 0.2.
2. To generate parameter sets (the samples), random values are generated by uniform selection within the segments. The number of segments is always equal to the chosen number of samples. Each parameter has the same number of segments; the segments are enumerated.
3. A parameter set consists of random values from the predefined segments, meeting the condition that each segment number is represented once in each set. The effect is visible in Figure 3.1, the random values (blue points) are combined in a way that from each of the five segments one value is present in the sample. By combining the parameter values in this way, linear correlations between input parameters are minimised and the whole parameter space can be covered.

In comparison to Monte Carlo simulation, Latin Hypercube Sampling allows statistically valid results to be produced with a much smaller number of samples which is acceptable even from the perspective of fire simulation. Therefore this method was selected for the

investigations of this work. The sampling was performed with the commercial software optiSLang, which also controlled the simulation runs, see also section 4.2.

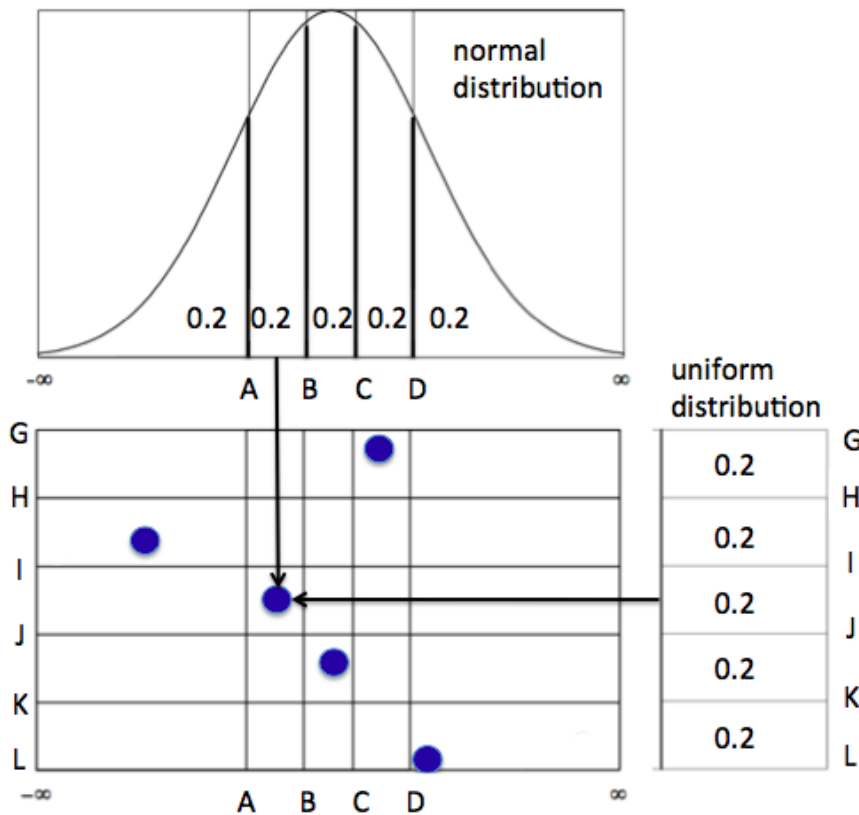


Figure 3.1: Illustration of parameter sampling with Latin Hypercube.

The number of samples required to produce statistically valid results is dependent on the specific problem. For scenarios with many strong non-linearities, a higher number of samples may be required than for scenarios with linear dependencies and relatively low sensitivity of output versus input parameters. There is no universally applicable law to calculate the required number of samples. One way to verify if the number of samples is sufficient is to carry out several analyses with different numbers of samples and to compare the results. However, in this work the number of samples was chosen to be as large as possible to allow simulation within an acceptable time (1-3 weeks per study). The number of samples for all studies carried out in this work meets the guidance given in the optiSLang Documentation [57] for LHS. It recommends setting the minimum number of samples as a function of the number of input parameters n_i and output parameters n_o :

- Monte-Carlo sampling: $N_{\text{required}} = (n_i + n_o)^2$
- Latin Hypercube Sampling: $N_{\text{required}} = 2(n_i + n_o)$

For the sensitivity studies in chapter 4, the number of samples is greater by factors between 2 and 18 than specified by this guidance. Studies with deterministic sampling - e.g. different variants based on arbitrarily selected parameter values, can deliver information on sensitivities. However, possible linear or other correlation of the manually defined input value sets worsens the reliability of such results. Latin Hypercube Sampling (LHS) is a way to ensure that the entire parameter space is investigated *systematically*. For the sensitivity studies of this thesis, an *advanced* Latin Hypercube Sampling was applied (as an option of the optiSLang software) which uses an additional numerical optimisation procedure to minimise spurious linear correlations between different input parameter samples automatically. The effect of this operation is especially visible if only a small number of samples can be investigated despite many random variables (i.e. input and output parameters) are of interest. It generally increases the reliability of the results. In comparison to deterministic studies, Latin Hypercube Sampling takes into account the probability distribution functions. This means that parameter values with a higher probability of occurring in reality also occur more often in the samples. Therefore this type of random sampling generally delivers much more reliable sensitivity information than a deterministic variant study with the same number of samples.

The results of a sensitivity study are valuable to assess fire simulations because:

- Optimisation of design is only efficient if the number of design variables is reasonably small. Using sensitivity analysis these can be reduced to those few parameters with greatest influence. This result is especially important for numerical optimisation methods which work much more efficiently with few design parameters. Simulation-based optimisation is a possible way to identify material parameters in order to overcome the lack of reliable material and chemical reaction parameters with influence on toxic gas production (cf. chapter 6).
- Linear and non-linear correlations between several input parameters and one output parameter have been determined and shown graphically. These results help to understand the physics and mode of operation of the model.
- Correlations are not only detected between input and output parameters, but also between different output parameters; this additional information helps in understanding how the model works.
- Many parameters have to be determined by experiments which are often expensive and time-consuming. Sensitivity analysis provides the basis to decide which of the input parameters require high precision and which do not need to be determined precisely as they do not have a measurable influence.
- The results provide the basis for assessing the model's quality, and to detect model errors systematically by use of the "Metamodel of Optimal Prognosis" (cf. section 3.2.4).

3.2.3 Theoretical Basis

In order to understand and discuss the simulation results in chapter 4, a number of terms and definitions from statistics and theory of sensitivity analyses are needed. Most of these definitions are general knowledge and can be found in mathematical standard literature. Therefore they will not be discussed here in detail.

Mean Value μ . The arithmetic mean value is calculated by

$$\mu = \frac{1}{N} \sum_{i=1}^N x_i.$$

Expected Value E. The expected value of a random variable X is the sum of all its possible values x_i , each weighted with its probability p_i of occurrence.

$$E(X) = \sum_{i=1..N} x_i p_i.$$

The expected value of test results with uniform probability distribution is the arithmetic mean value μ .

Variance. The variance is defined as

$$\sigma_{x_i}^2 = \frac{1}{N-1} \sum_{i=1}^N \left(x_i^{(k)} - \mu_{x_i} \right)^2.$$

Regression. In order to evaluate the statistical contents of the probabilistic sensitivity analysis, linear and quadratic regression is performed, for input/output, input/input and output/output parameters. In a quadratic regression, the coefficients of the quadratic polynomial

$$x_j = A_i + B_i x_i + C_i x_i^2 = \hat{y}(x_i).$$

are determined by the method of least squares, in order to minimise the squared difference between the regression function $\hat{y}^{(k)}(x_i)$ and $x_j^{(k)}$ for the samples $k = 1 \dots N$.

Coefficient of Determination, CoD, R^2 : The regression function \hat{y} and the simulated response values y_j are used to define the Coefficient of Determination (CoD):

$$R_j^2 = \frac{\sum_{k=1}^N \left(\hat{y}_j^{(k)}(x_1, x_2, \dots, x_i, \dots, x_n) - \mu_{y_i} \right)^2}{\sum_{k=1}^N \left(y_j^{(k)}(x_1, x_2, \dots, x_i, \dots, x_n) - \mu_{y_i} \right)^2},$$

with

$$\begin{aligned} i &= 1 \dots n && \dots && \text{Index of independent or input variables } x_i, \\ j &= 1 \dots M && \dots && \text{Index of response variable } j, \\ k &= 1 \dots N && \dots && \text{Index of sample, number of samples: } N. \end{aligned}$$

The Coefficient of Determination (CoD) measures the portion of the variation of one response variable y_j which can be explained by the statistical model based on the regression function \hat{y} . Its values lie between 0 and 1. If all response values are exactly calculated by the regression function \hat{y} , the CoD has the value 1.

Coefficient of Importance: In order to assess the particular influence of the input parameter x_l on the response parameter y_j , the Coefficient of Importance (Col) is defined. It is the difference between CoD and the portion of variance in the response which can be explained by all other input parameters except x_l :

$$R_{j, X \sim i}^2 = R_j^2 - \frac{\sum_{k=1}^N \left(\hat{y}_j^{(k)}(x_1, x_2, \dots, x_{l-1}, x_{l+1}, \dots, x_n) - \mu_{y_i} \right)^2}{\sum_{k=1}^N \left(y_j^{(k)}(x_1, x_2, \dots, x_{l-1}, x_l, x_{l+1}, \dots, x_n) - \mu_{y_i} \right)^2},$$

with

$$\begin{aligned} i &= 1 \dots n && \dots && \text{Index of independent or input variables } x_i, \\ j &= 1 \dots M && \dots && \text{Index of response variable } j, \\ k &= 1 \dots N && \dots && \text{Index of sample, number of samples: } N, \\ l &&& \dots && \text{Index of a single input parameter } x_l. \end{aligned}$$

Note that in the numerator of the second term, the contribution of x_l is missing in the summation of the regression function, i.e. the terms depending on x_l are eliminated, whereas the denominator is the same as in the definition of CoD. As result of the subtraction, that portion of variance in the response $y_j^{(k)}$ is obtained which can be explained by x_l only [57].

3.2.4 Metamodel of Optimal Prognosis

The simulation of systems that require complex models containing a high number of variables is mostly time-consuming and needs high computational capacity. In areas where many runs of such simulations are needed, the approach of meta-modelling is a widely-used strategy to reduce the problem to the content of interest and to allow much faster simulations with less resources. A metamodel is a surrogate model which represents a subspace of the original model containing only those properties which are essential. For engineering simulation models, this can be realised through approximating the results by a multi-dimensional response surface. Operations for sensitivity analysis or simulation-based optimisation are then performed on the response surface and not with the original model.

A metamodel offers another benefit as well: The quality of a metamodel which is generated by selecting the optimal regression function for the data to be approximated can be

used as a measure for the quality of the underlying model. The justification is that most processes which are modelled in engineering are continuous in the sense of continuum mechanics, and the responses can be described by a smooth surface based on one analytical function, or by piecewise approximation with multiple analytical functions. For fire simulations, it is generally expected that continuous changes of input parameters, such as ambient conditions or heat of combustion, do not produce discontinuous changes in the results as local singularities, sharp jumps or bifurcation problems. Exceptions can be observed for situations where kinds of thresholds are investigated, such as ignition or extinction.

For the generation of the best possible metamodel, two important questions must be answered: 1. Which is the best regression model to approximate the data?, and 2. What is the best technique to filter out irrelevant input variables? A useful criterion to answer these questions is the Coefficient of Prognosis (CoP), which is also beneficial for the evaluation of sensitivity analyses and for the assessment of the quality of the underlying model.

Coefficient of Prognosis (CoP): The Coefficient of Prognosis measures the ability of the metamodel to predict responses for randomly occurring input parameter sets. It acts like a test for the metamodel, represented by the response surface which was found using a set of simulation input and output data of the original model. The CoP evaluates whether the metamodel is able to predict any additional results generated with different input parameter sets. These additional data sets are called test data. The CoP is a measure for the agreement between the response predicted by the metamodel and the response simulated by the original model. In the optiSLang Documentation [57], it is defined as

$$\text{CoP} = \left(\frac{\mathbf{E} \left[Y_{\text{test}} \cdot \hat{Y}_{\text{test}} \right]}{\sigma_{Y_{\text{test}}} \sigma_{\hat{Y}_{\text{test}}}} \right)^2 = \left(\frac{\sum_{k=1}^N \left(y_{\text{test}}^{(k)} - \mu_{y_{\text{test}}} \right) \left(\hat{y}_{\text{test}}^{(k)} - \mu_{\hat{y}_{\text{test}}} \right)}{(N-1) \sigma_{Y_{\text{test}}} \sigma_{\hat{Y}_{\text{test}}}} \right)^2 ,$$

with

$\mathbf{E} [Y_{\text{test}}]$... Expected value of the test data,

$\mathbf{E} [\hat{Y}_{\text{test}}]$... Expected value of the metamodel estimates,

$\sigma_{Y_{\text{test}}}$... Standard deviation of the test data,

$\sigma_{\hat{Y}_{\text{test}}}$... Standard deviation of the metamodel estimates.

It can be expected that for all response variables which have a high Coefficient of Prognosis (> 70-80 %), the model is able to produce reliable predictions for any valid input parameter set. Valid input parameter sets are based on the parameter ranges for which the CoP was determined.

The expectation that CoP is a sign of model quality is based on the above mentioned assumption that continuous changes in input parameters lead to continuous changes of output parameters. If so, a valid metamodel of optimal prognosis can be determined;

i.e. a smooth response surface with little deviation from the response data exists which leads to high CoP values and thus to high predictability. If the simulation model tends to produce results which deviate from the continuous relationship between input and response, the CoP is decreasing. Reasons for a low Coefficient of Prognosis can be:

- Input and response are independent of each other or are only very weakly correlated.
- The real parameter range of the input parameter is unknown and therefore assumed too large. If the input parameter is highly correlated to the investigated response, then random selections of parameter values from the unrealistically large range can lead to extremely large jumps in the output.
- There are intentional non-linearities in the model which cause discontinuities in the response. Examples are ignition or extinction, abrupt changes in ventilation by sensor-controlled switches.
- The model predicts non-linear responses which do not correspond to reality but result from errors. Examples are: inappropriate mesh density or topology, incomplete models of chemical reactions, simplified turbulence description neglecting too many significant effects. In these cases, the CoP can be applied as a measure of model quality because it will increase by improvement of the model.

Chapter 4

Simulation

4.1 Fire Simulation: The Fire Dynamics Simulator (FDS)

4.1.1 Basis, Model Assumptions, Simplifications

The Fire Dynamics Simulator (FDS) is software for numerical simulation of fluid dynamics which solves the Navier-Stokes equations for typical fire-driven flows of low speed. Typical tasks that can be solved with FDS are the calculation of transient smoke and heat distribution from fires.

FDS was developed by the National Institute of Standards and Technology (NIST, USA) in collaboration with the VTT Technical Research Centre of Finland and is free software. It uses the Finite Differences Method for the solution of the Navier-Stokes equations and a modified Finite Volume Technique to solve the radiation equation. Turbulence is approximated by the Large Eddy Simulation model (LES).

FDS is constantly being improved. Since 2012 Version 6 became available for beta-testing. This new version has some extensions which are favourable for fire and toxic hazard prediction. It allows modelling of transport and production of the toxicant CO and soot production, and includes reverse reactions which consume them. Many improvements for higher precision were implemented in Version 6. Therefore Version 6 was preferred to the previous version 5.5 despite its official "beta" status [54].

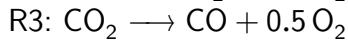
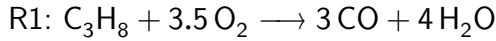
The simulations of the tubular furnace and the room corridor test, documented in sections 4.3 and 4.4, were carried out with FDS 6, Release candidate 3, published on 20 December 2012.

4.1.2 Finite-Rate Combustion Model for Propane and Tracked Species

The finite-rate combustion model of propane is used for simulations of the tubular furnace. The species fuel, oxygen, and the reaction products carbon monoxide and carbon dioxide are separately tracked, i.e. the mass transport equation has to be solved for each species, not just for fuel, air and products as in the default lumped species approach of

FDS.

Three reaction steps of the combustion are modelled with a finite combustion rate. The third step is the reduction of CO_2 to CO :



This is a simplification because in reality, each of these reactions is split up into many partial reactions. Combustion rates of the three reactions are described by Arrhenius equations.

The reaction rate of Propane combustion (reaction R1) is computed by

$$\frac{d\hat{C}_{\text{C}_3\text{H}_8}}{dt} = -A T^n \cdot \hat{C}_{\text{C}_3\text{H}_8}^{N_{\text{C}_3\text{H}_8}} \cdot \hat{C}_{\text{O}_2}^{N_{\text{O}_2}} \cdot e^{-E/RT},$$

where

A ... Pre-exponential factor,

$\hat{C}_{\text{C}_3\text{H}_8}$... Concentration of propane,

$N_{\text{C}_3\text{H}_8}$... Concentration exponent of propane,

\hat{C}_{O_2} ... Concentration of oxygen,

N_{O_2} ... Concentration exponent of oxygen,

E ... Activation energy,

R ... Universal gas constant, $R = 8.314 \text{ [Jmol}^{-1}\text{K}^{-1}\text{]}$,

T ... Absolute Temperature in K,

n ... Temperature exponent.

The temperature dependence of the pre-exponential factor is not included. The temperature exponent n is set to 0 [25, 83]. Then the equation corresponds to equation (2.2).

4.2 Sensitivity Analysis with OptiSLang

optiSLang, called by its authors "The Optimizing Structural Language" is software for sensitivity analysis, multidisciplinary optimization, robustness evaluation, reliability analysis and robust design optimization. It was developed by the dynardo Dynamic Software and Engineering GmbH, Weimar, Germany. It is a commercial code which is widely used in industrial and scientific areas, usually in domains where numerical simulation is efficient and highly developed.

For the fire simulations investigated, optiSLang is used to carry out sensitivity analyses on the basis of advanced probabilistic sampling methods. It provides the required algorithms to parametrise input and output files, automatic sample generation, scripts which control simulation, job execution and graphical results' evaluation.

4.3 Sensitivity Analysis of a Bench-Scale Tubular Furnace Test

4.3.1 Objective

The principal objective of the sensitivity analysis is to answer the following questions:

- What influences do the variations in experimentally determined input parameters have on the output quantities, in particular on toxic gas species yields?
- Which input parameters have the biggest influence on each output parameter?
- Are there flaws or errors in the simulation model (or in one of the various models which it contains) which lead to low Coefficients of Prognosis (cf. section 3.2.4)?

4.3.2 Model Description

In order to gain basic insights into the behaviour of the combustion model a study with a small room of simple geometry was first carried out. This approach intends to minimize influences of geometric dimensions and to exclude transient effects of smoke and heat spreading, which, for larger environments, require significantly longer simulation times for a steady state to be reached.

Bench scale measurements may be carried out in small furnaces, like the Steady State Tube Furnace (SSTF) in order to ensure complete mixing of fuel and oxidizer, as described in section 2.3.2. A small furnace with simple geometry and similar dimensions like the SSTF was modelled. With this model, a probabilistic sensitivity study was set up, where the essential input parameters of the combustion model were investigated for their influence on the variance of the results. Output parameters were mass fractions of CO, CO₂, O₂, FED, gas temperatures and total heat release rate.

The dimensions of the model are shown in figure 4.1. The outer walls form a tunnel of 110 mm length and 50 mm height. In the centre of the floor is a burning specimen, a cube of 10 mm edge length, on the top surface of which propane fuel is inserted. The top surface has an area of 0.0001 m².

Due to the finite differences method in FDS, the walls of all mesh cells need to be parallel to the coordinate planes. Therefore the tubular shape of the SSTF was modelled by a rectangular tunnel of comparable size.

The sensors for temperature, species mass fractions and FED were positioned at three locations: Position 1 vertically above the fire, position 3 near the open side and position 2 in the middle between 1 and 3. Position 2 is located in a region where high species concentrations were observed in the results of the reference run with nominal parameter values.

Mesh and simulation control parameters. A mesh convergence study was made before the different sensitivity analyses were started. It showed that the mesh size of 2.5

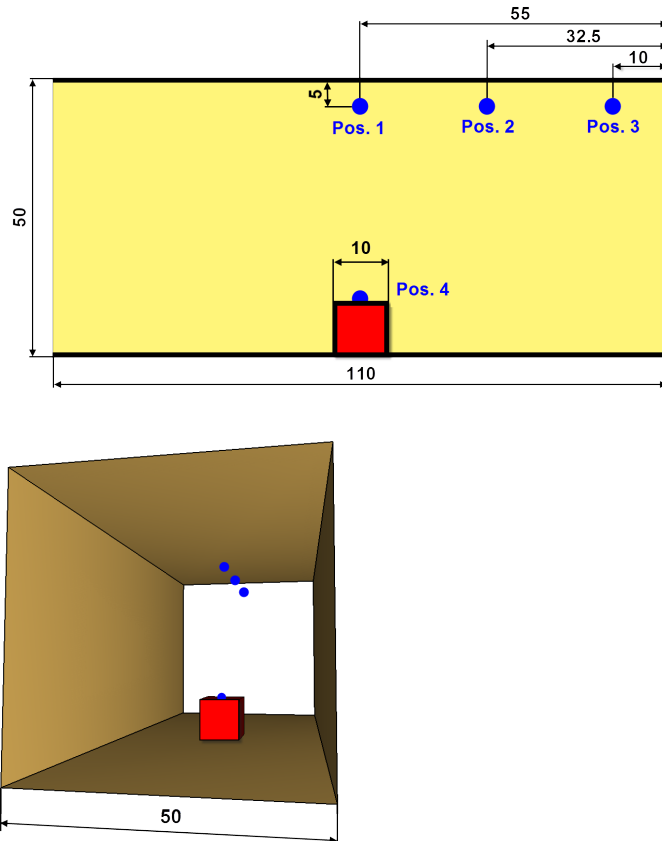


Figure 4.1: Tubular furnace model: Dimensions (in mm) and positions of the sensors for gas temperature, mass fractions of species and FED.

mm is sufficient and further refinements do not change the output parameters significantly (figure 4.2). The simulation can be stopped when a steady state is reached. The steady state is already reached after about 4s, the end time was set to 5s.

4.3.3 Sensitivity Analysis TF1: Simple Chemistry Model

Combustion Model for TF1. In the sensitivity analysis TF1, the tubular furnace test was simulated with the "simple chemistry" combustion model of FDS6. With the "simple chemistry" model, a single, mixing-controlled reaction is active for combustion. The energy produced by the reaction is specified by the input parameter HRRPUA, the heat release per unit area. Propane was specified as fuel, using the default properties within FDS. By use of the predefined default value for the heat of combustion of propane, FDS determines the mass flow of fuel which is needed to reach the desired HRRPUA. As an additional parameter, the heat of combustion (HOC) of the fuel can be specified explicitly, so the energy content per mass of fuel is modified. If HOC is decreased, the simulation code increases the mass flow of fuel accordingly, thus this parameter can influence gas mass fractions in the results.

The combustion for TF1 was defined by the following code lines:

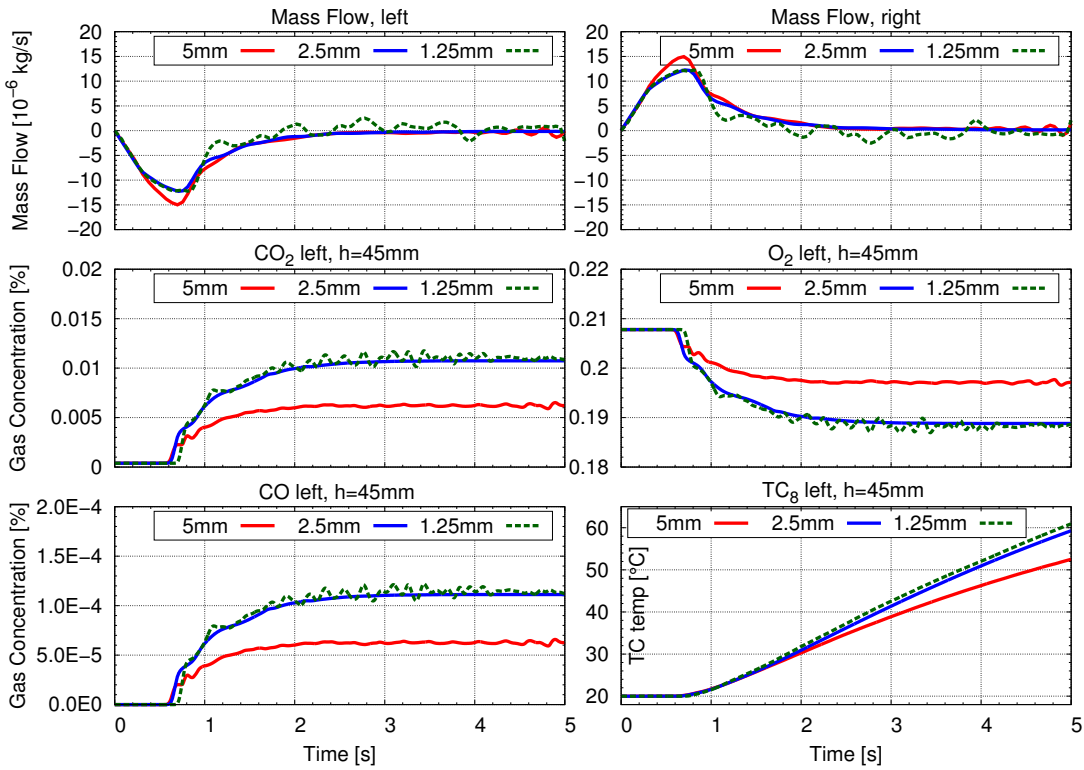


Figure 4.2: Results of the mesh convergence study with the tubular furnace model using LES with grid sizes of 1.25, 2.50 and 5.00 mm.

```

&REAC ID = 'R1'
  FUEL = 'PROPANE'
  CO_YIELD=0.00500
  SOOT_YIELD=0.010
  HEAT_OF_COMBUSTION=46334./

&SURF ID = 'HR_SURF', HRRPUA=300.0/
&OBST XB=-0.005,0.005,-0.005,0.005,0.0,0.01,SURF_IDS='HR_SURF','INERT','INERT'/

```

Input and output parameters for TF1.

For the study TF1, 500 different input parameter sets each with different parameter values were defined by advanced Latin Hypercube Sampling, using the parameter ranges shown in table 4.1. The output parameter values are the statistical results of 500 simulations, each of them using a different input parameter set. Values of output parameters in the same line generally originate from different variants.

Table 4.1: Input and output parameters of the tubular furnace sensitivity study TF1 with simple chemistry model. Descriptions correspond to the FDS6 User’s Guide [25].

Input parameter name	Description	Units	Lower bound	Upper bound
CO.YIELD	The fraction of fuel mass converted into carbon monoxide.	kg/kg	0	0.02
SOOT.YIELD	The fraction of fuel mass converted into smoke particulate.	kg/kg	0	0.02
HOC	Heat of combustion of propane	kJ/kg	44018	48651
HRRPUA	Heat release per unit area	kW/m ²	150	300
Y.O2.INFTY	Ambient mass fraction of oxygen (default: 0.232428 kg/kg)	kg/kg	0.17	0.232428
Y.CO2.INFTY	Ambient mass fraction of carbon dioxide (default: 0.0058 kg/kg)	kg/kg	0.0003	0.0058

Output parameter name	Description	Units	Results			
			Min	Max	Mean	Std.-Dev.
TC8_right	Gas temperature at position 3	°C	40.55	58.38	48.96	4.774
CO2_8right	Mass fraction of CO ₂ at position 3	kg/kg	0.00982	0.02076	0.01565	0.00239
CO_8right	Mass fraction of CO at position 3	kg/kg	9.08E-08	1.04E-04	4.29E-05	2.54E-05
O2_8right	Mass fraction of O ₂ at position 3	kg/kg	0.1495	0.2159	0.1839	0.0180
C3H8_8right	Mass fraction of propane at position 3	kg/kg	6.40E-11	9.26E-11	7.91E-11	9.79E-12
massflow	Mass flow through one side opening	kg/s	-8.40E-07	4.05E-08	-1.70E-07	5.90E-08
max_total_HRR	Maximal value of total heat release rate	kW	0.01504	0.03096	0.02293	0.00420
T_atfire	Gas temperature near fire surface	°C	179.6	1021.0	694.5	100.2

For max_total_HRR, the global maximum over the simulation time of 5 s was recorded; for all other output parameters the mean value of the last 0.5 s of simulation was used. Position 3 is marked in Figure 4.1.

Reference Run and Results Post-Processing for TF1. For each sensitivity analysis, a reference run was performed using the nominal values of all input parameters. The results which were to be processed by the sensitivity analysis, were saved as text files (comma-separated values). These data are further processed by scripts which calculate, from the time functions in the FDS output, the scalar values (for example maxima, minima, averages) that are applied as output parameters in the sensitivity analysis. For max_total_HRR (see table 4.1), the global maximum over the simulation time of 5s was recorded; for all other output parameters, the mean value of the last 0.5 s of the simulation was used. The gas temperature field of the reference run, in the section through the centre of the fire, is shown in Figure 4.3.

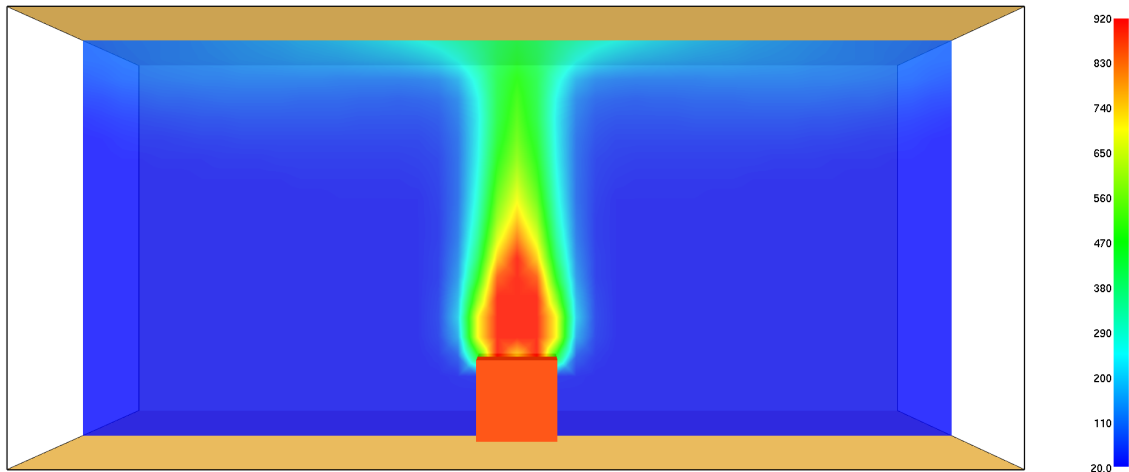


Figure 4.3: Tubular furnace analysis TF1 with simple chemistry: Gas temperature (in °C) in the steady state after 5 s

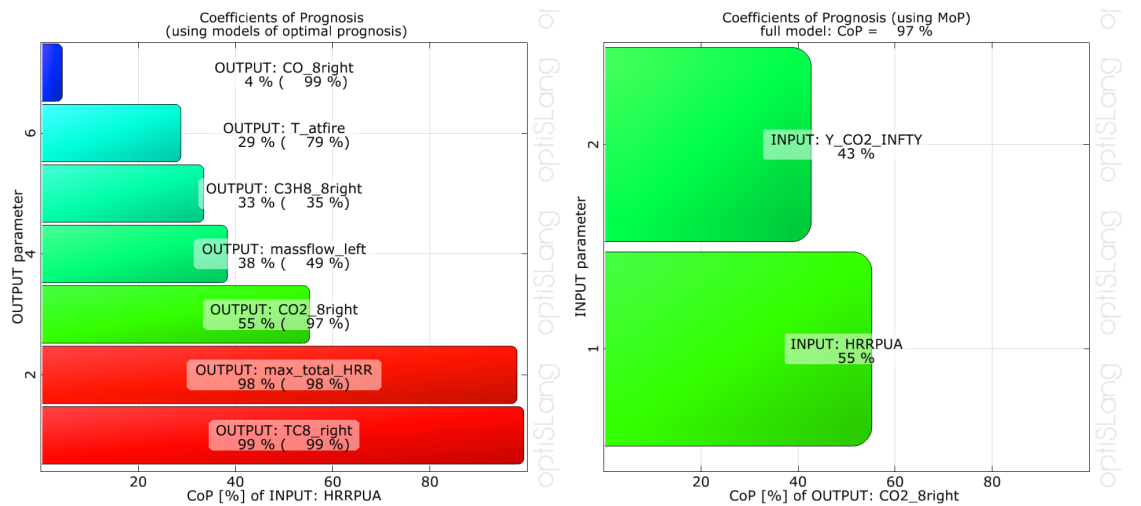


Figure 4.4: Tubular furnace analysis TF1 with simple chemistry: Coefficient of Prognosis for heat release per unit area (HRRPUA)

Sensitivity Analysis Results for TF1. The Coefficients of Prognosis shown in Figure 4.4 describe how well the variation in the output parameters can be explained by the metamodel which is based on 500 samples, and which portion of each parameter's variation can be explained by the variation of the heat release rate per unit area, HRRPUA. As expected, the biggest impact of HRRPUA is on the gas temperature and the maximum total heat release rate. These two CoPs reach very high values of almost 100% which designates an excellent ability of the metamodel to predict the influence of HRRPUA on these output parameters. The values on the green bar (CO₂_right) on the left chart "55% (97%)" mean: 55% of the variance in the CO₂ concentration can be explained by HRRPUA variance, and 97% of the variance in the CO₂ concentration are explained by the variance of all variables in the model together. The chart on the right indicates that the only other input variable with a significant contribution to the 97% is the ambient mass fraction of CO₂, "Y_CO2.INFTY", which explains 43%. The sum of both single CoPs in the chart on the right is 98%, the difference of 1% is the portion of variance in CO₂_right which can only be explained by HRRPUA and Y_CO2.INFTY together, i.e. only if both parameters change .

In Figure 4.5, 6 response surfaces are shown. They were calculated by optiSLang based on automatic selection of the optimal approximation method which leads to the highest CoP values. The surfaces in 4.5a, 4.5c, 4.5e and 4.5f are based on the moving least squares method, 4.5b is a linear regression and 4.5d a quadratic regression without mixed terms. These graphs contain helpful information to understand the model, for instance:

- Graph a): If the ambient oxygen mass fraction decreases below 19%, the temperature in the centre of the fire decreases, but only if HRRPUA is bigger than ca. 240 kW/m² (samples in the right lower corner). An explanation for this behaviour could be oxygen depletion.
- Graphs b) and d): Very high CoPs of 97 and 99% are determined for CO and CO₂ mass fraction dependent on HRRPUA and the predefined ambient mass fraction (CO₂) or yield (CO). In these relationships the model has high predictability, the results are plausible.
- Graph c): Ambient mass fraction of O₂ and HRRPUA have moderate influence on the mass flow at measurement point 8, changes are of the order of 10-15%. The CoP is 49% - only 49% of the variance in the mass flow can be predicted by the model. It corresponds to our experience that fluid dynamics has a strong influence on the mass flow, therefore the reason for the low CoP could be a too coarse mesh or flaws in turbulence modelling.
- Graph e): The values of mass fraction of propane at the right opening near the ceiling are very low (order of 10⁻¹⁰) because propane is almost completely burned in the fire. The maximum of left-over propane is found for high values of HRRPUA. As for higher HRRPUA higher temperatures and thus faster reaction rates should occur, this result is not expected but it possibly correlates with low temperature found for some samples with higher HRRPUA values in graph a). As the Coefficient of Prognosis is only 37%, the reason for the unexpected result could be too much simplification of the combustion process in the model.

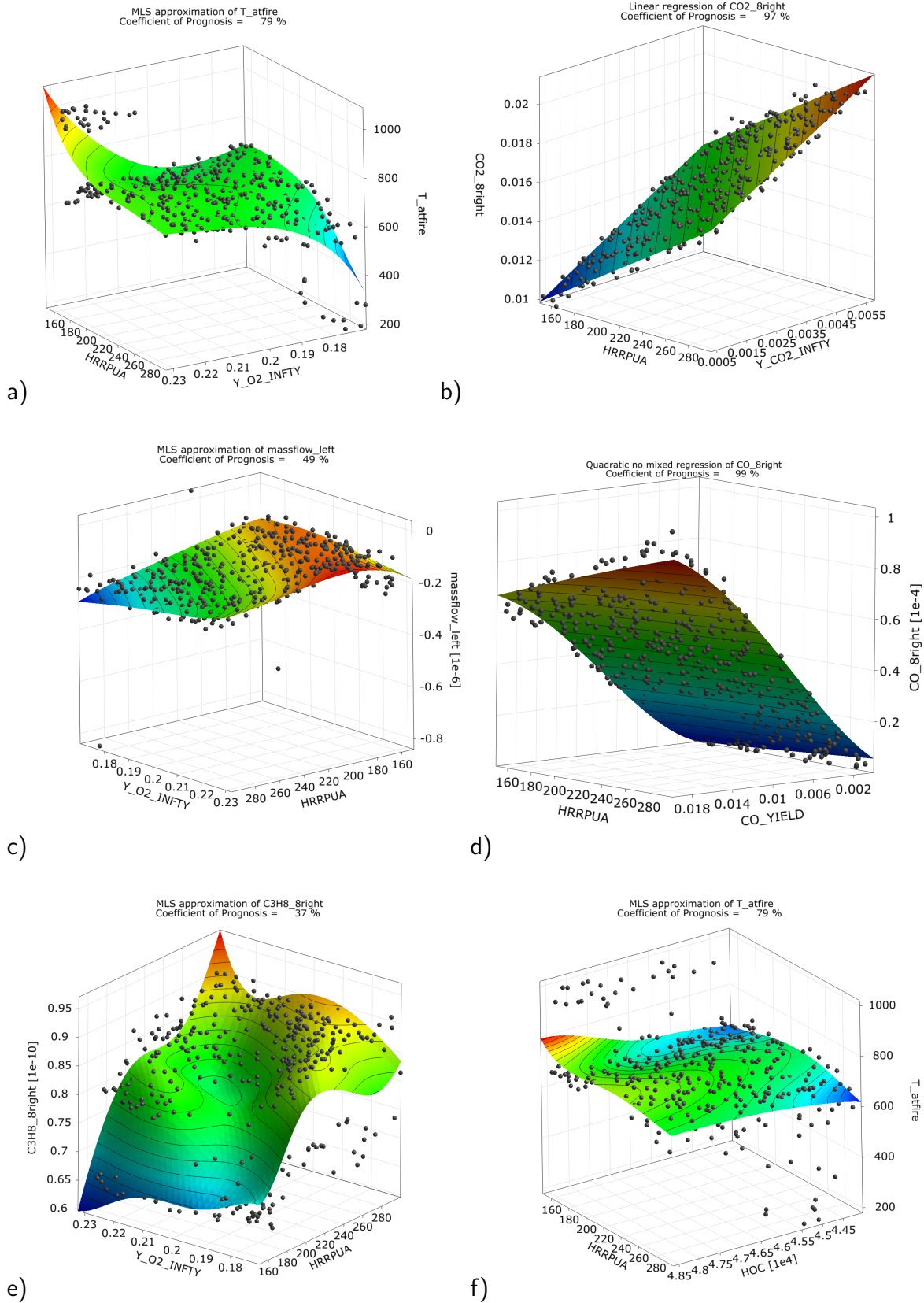


Figure 4.5: Tubular furnace analysis TF1 with simple chemistry: 3D response surfaces of the metamodel of optimal prognosis.

In Figure 4.6a linear correlation between the ambient oxygen mass fraction and simulated oxygen concentration is visible. The CoP for these 2 variables is 98%, the linear correlation coefficient is 0.992. This is an expected result. In Figure 4.6b all CoPs for the ambient oxygen mass fraction are shown, also the changes of the variables "T_atfire", "massflow_left" and "C3H8_8right" can partly be explained by the ambient oxygen mass fraction "Y_O2_INFITY". 58% of the variance in "T_atfire" can be explained by "Y_O2_INFITY", another major portion (19%) of the variance can be explained by the variance of the heat of combustion of propane, "HOC" (Figure 4.6d). About 2% of the explainable variance (79%) in "T_atfire" are not captured in the graph, these are small contributions from other parameters which are filtered out.

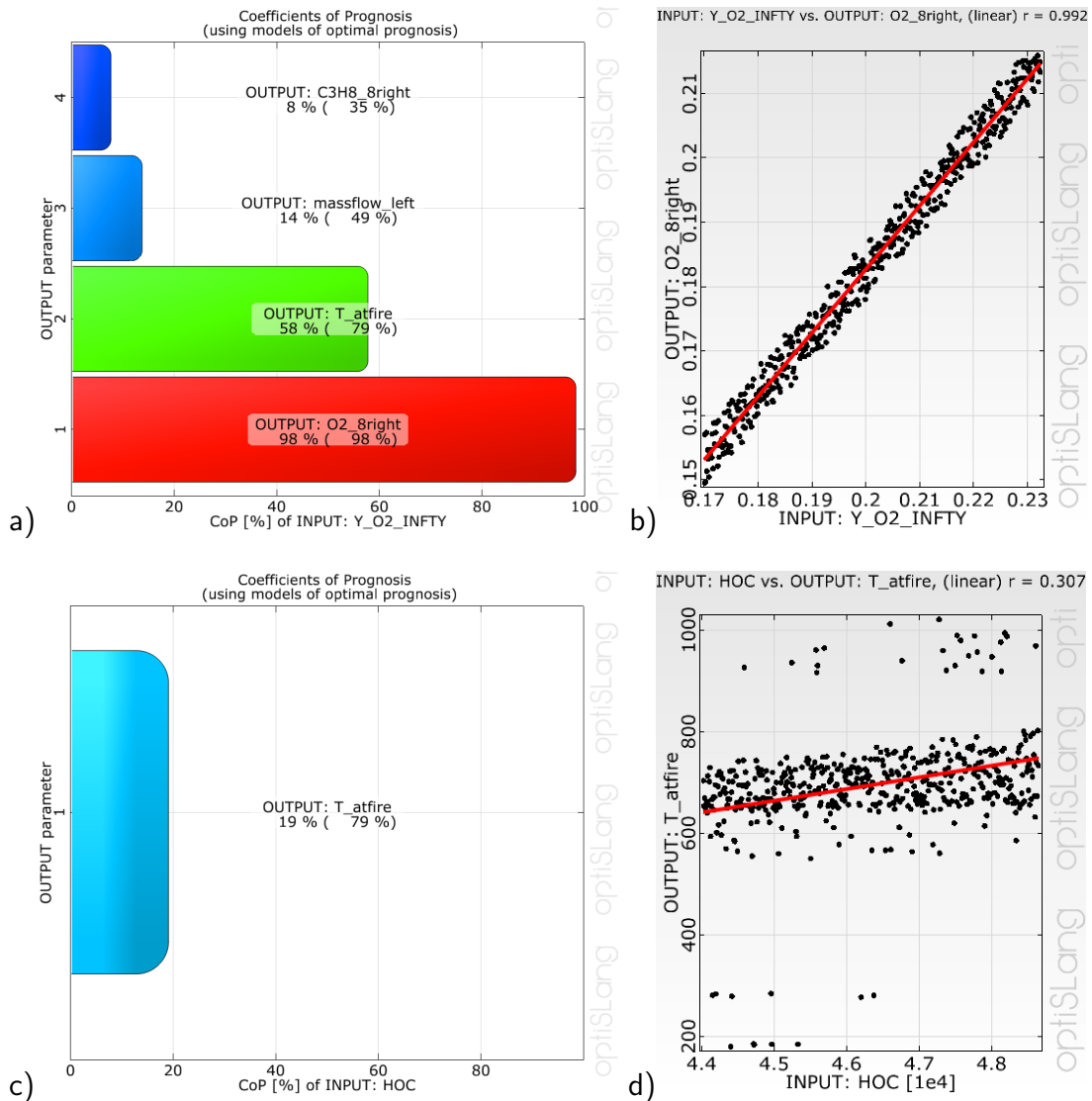


Figure 4.6: Tubular furnace analysis TF1 with simple chemistry: Anthill plots and CoP graphs of ambient oxygen mass fraction vs. simulated oxygen concentration (above) and vs. gas temperature at the fire centre (below).

The anthill plots in Figure 4.8 visualise how the results for mass fractions of CO, CO₂ and O₂ are related to the input parameter CO yield and the calculated gas temperature. As expected, the calculated CO concentration is linearly correlated to the specified CO yield, for higher CO yields the scattering range gets wider. CO₂ and O₂ mass fractions are independent of CO yield, the correlation coefficients are near zero. Comparing the calculated gas temperature with the mass fractions, it is found that CO is weakly ($r=0.236$) and CO₂ stronger ($r=0.736$) correlated to the temperature.

From the anthill plot in Figure 4.7 it can be concluded that CO and CO₂ production are almost independent of each other with the simple chemistry model. A small linear correlation coefficient of $r=0.167$ is calculated but the correlation is too small to produce any significant values of the Coefficient of Importance.

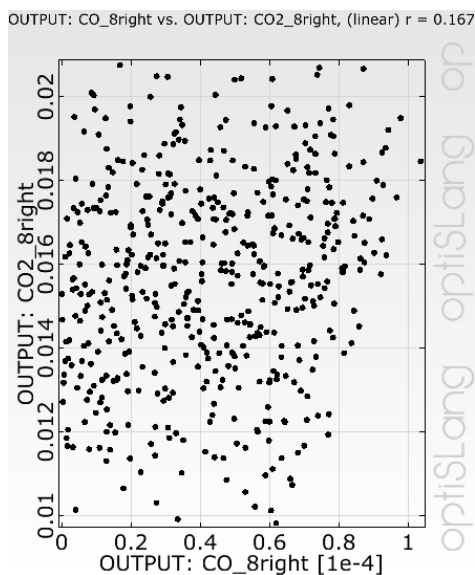


Figure 4.7: Tubular furnace analysis TF1 with simple chemistry: Anthill plot of CO mass fraction vs. CO₂ mass fraction.

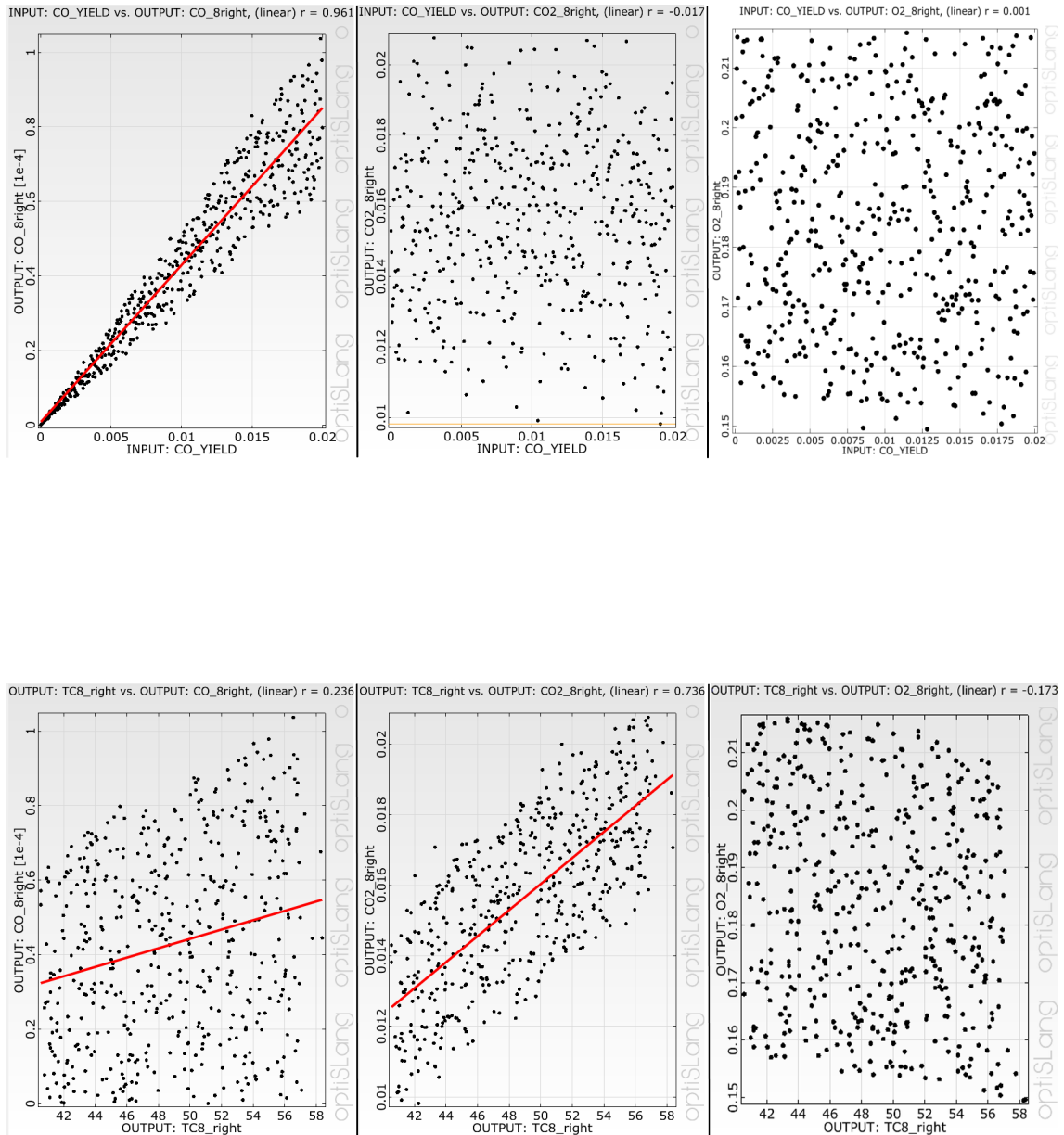


Figure 4.8: Tubular furnace analysis TF1 with simple chemistry: Anthill plots of CO, CO₂ and O₂ mass fractions vs. CO yield (above) and calculated gas temperature (below).

4.3.4 Summary of findings from TF1

The sensitivity analysis TF1 of the tubular furnace model with 500 samples using the mixing-controlled "simple chemistry" model and Large Eddy Simulation (LES), produced high Coefficients of Prognosis for most output parameters. Only the mass flow and the propane concentration show lower CoPs. From that it can be concluded that gas temperatures, CO and CO₂ concentrations and the total heat release rate are correctly modelled because their variations over all samples can be explained almost completely by variations of the input parameters. The most influential input parameter is, as expected, the heat release rate per unit area, HRRPUA. For further conclusions, see also section 5.2.

4.3.5 Sensitivity Analysis TF2: Finite Rate Combustion

Combustion Model for enhanced tube furnace model TF2. In the sensitivity analysis TF2, the tubular furnace test was simulated with the finite rate combustion model of FDS6RC3, where the reaction rate is controlled by an Arrhenius equation for each reaction (as described in section 4.1.2). Multiple reactions and multiple fuels can be defined.

The combustion for TF2 was defined by the following code lines:

```
&SURF ID = 'PROPANE_FIRE'
  SPEC_ID='PROPANE'
  MASS_FLUX = 0.006709158/

// SPECIMEN ON FIRE, A=1cm^2
&VENT XB=-0.005,0.005,-0.005,0.005,0.01,0.01,SURF_ID='PROPANE_FIRE' /
&OBST XB=-0.005,0.005,-0.005,0.005,0.0,0.01,SURF_ID='INERT'/Specimen Basis

/ Species Definition
&SPEC ID='NITROGEN', BACKGROUND=.TRUE./
&SPEC ID='OXYGEN', MASS_FRACTION_0=0.23054 /
&SPEC ID='WATER VAPOR', MASS_FRACTION_0=0.00626 /
&SPEC ID='CARBON DIOXIDE', MASS_FRACTION_0=0.00046 /

&SPEC ID='PROPANE' /
&SPEC ID='CARBON MONOXIDE' /

/Reactions
&REAC ID = 'R1'
FUEL = 'PROPANE'
SUPPRESSION=.FALSE.
EQUATION = 'PROPANE+3.5*OXYGEN=3*CARBON MONOXIDE+4*WATER VAPOR'
```

```

A = 1.0000e12
E = 125520.0
SPEC_ID_N_S = 'PROPANE', 'OXYGEN'
N_S = 0.10, 1.65
HEAT_OF_COMBUSTION=46000./

&REAC ID = 'R2'
FUEL = 'CARBON MONOXIDE'
SUPPRESSION=.FALSE.
A = 4.0000e14
E = 167360.0
SPEC_ID_NU = 'CARBON MONOXIDE', 'OXYGEN', 'CARBON DIOXIDE'
NU= -1, -0.5, 1
SPEC_ID_N_S = 'OXYGEN', 'CARBON MONOXIDE', 'WATER VAPOR'
N_S = 0.25, 1.00, 0.50 /

&REAC ID = 'R3'
FUEL = 'CARBON DIOXIDE'
SUPPRESSION=.FALSE.
A = 5.0000e8
E = 167360.0
SPEC_ID_NU = 'CARBON DIOXIDE', 'OXYGEN', 'CARBON MONOXIDE'
NU= -1.00, 0.50, 1.00
SPEC_ID_N_S = 'CARBON DIOXIDE'
N_S = 1.00 /

```

Turbulent combustion and mixing for TF2. In the Arrhenius model, temperatures are smeared out over the mesh cell and lead to lower average temperatures for the cells if the default Large Eddy Simulation (LES) is used (see 2.2.2). Therefore the User's Guide recommends the use of the finite-rate combustion model only with Direct Numerical Simulation (DNS) or to adapt some of the reaction parameters. DNS simulation requires a very fine mesh resolution with edge length $<1\text{mm}$ which is only suitable for small-scale models. The smallest mesh size for the tubular furnace model which produced results in acceptable time was 2.5 mm.

The mesh convergence study described in section 4.3.2 prove that a mesh size of 2.5 mm provides sufficient accuracy for LES simulations. A further refinement does not change the results significantly. The DNS simulation requires a mesh size that corresponds to the Kolmogorov scale which depends on the viscosity and the energy dissipation rate. As the energy dissipation rate is not precisely known the Komolgorov scale can not be determined reliably. According to the FDS technical reference guide [55] the Kolmogorov scale for fire scenarios is usually on the order of 1 mm. This corresponds to the results of the LES convergence study described above. Although LES and DNS are not directly

comparable it can be assumed that a mesh size of 2.5 mm is on the order of the Komolgorov scale for this experiment.

The simulations were run with this mesh size as DNS. In order to verify how strong the effect of the modified mixing in finite rate combustion is, the same sensitivity study was repeated as Large Eddy Simulation (LES). The turbulence resolution of the LES run was checked with the "Pope criterion" MTR (FDS6 User's Guide [25]) for a mesh resolution of 2.5 mm. The time history of MTR and the MTR slice contour in the steady state after 5 s are shown in Figure 4.9. MTR lies in the range of 0 to 1, and with MTR mean values near 0.2 satisfactory results were provided for mean velocities and species concentrations in tests with non-reacting, buoyant plumes. For the tubular furnace, the steady-state MTR is of the order of 0.02 at the two measurement points which are situated vertically above the right edge of the fire surface, in heights of 2cm and 4cm. The values at the measurement points are far below the recommended maximum mean value, in the slice contour some small regions are visible in which the criterion is >0.2 .

Input and output parameters for TF2.

For the study TF2, 144 different input parameter sets were defined by advanced Latin Hypercube Sampling, using the parameter ranges shown in table 4.2.

Table 4.2: Input parameters of the tubular furnace sensitivity study TF2 with finite rate combustion model. (Descriptions according to the FDS6 User's Guide [25]).

Input parameter name	Description	Units	Lower bound	Upper bound
TMPA	The fraction of fuel mass converted into CO.	kg/kg	450.00	900.00
IMF_O2	Ambient mass fraction of oxygen (default: 0.232428 kg/kg)	kg/kg	0.17	0.232428
IMF_CO2	Ambient mass fraction of CO ₂ (default: 0.0058 kg/kg)	kg/kg	0.0003	0.0006
A_R1	Pre-exponential factor of reaction 1	mol/cm ³ /s	7.00E+11	1.30E+12
E_R1	Activation energy of reaction 1	J/mol	87864.00	163176.00
N_S_C3H8_R1	Concentration exponent of propane in reaction 1	-	0.07	0.13
N_S_O2_R1	Concentration exponent of oxygen in reaction 1	-	1.16	2.15
HOC_R1	Heat of combustion of reaction 1	kJ/kg	32200.00	59800.00
A_R2	Pre-exponential factor of reaction 2	mol/cm ³ /s	2.80E+14	5.20E+14
E_R2	Activation energy of reaction 2	J/mol	117152	217568
N_S_O2_R2	Concentration exponent of oxygen in reaction 2	-	0.18	0.33
N_S_CO_R2	Concentration exponent of CO in reaction 2	-	0.70	1.30
N_S_H2O_R2	Concentration exponent of water vapour in reaction 2	-	0.35	0.65
A_R3	Pre-exponential factor of reaction 3	mol/cm ³ /s	3.50E+08	6.50E+08

Table 4.3: Output parameters of the tubular furnace sensitivity study TF2 with finite rate combustion model and Direct Numerical Simulation (DNS). The output parameter values are the statistical results of 144 simulations, each of them using a different input parameter set. Values in the same line generally originate from different variants.

Output parameter name	Description	Units	Results			
			Min	Max	Mean	Std.-Dev.
T_1	Gas temp., pos. 1	°C	453.5	1513.00	1097.94	312.6
T_2	Gas temp., pos. 2	°C	453.4	1019.00	784.04	144.6
T_3	Gas temp., pos. 3	°C	453.0	942.12	701.72	128.0
CO2_1	MF CO ₂ , pos. 1	kg/kg	2.33E-04	1.20E-01	4.28E-02	3.19E-02
CO2_2	MF CO ₂ at pos. 2	kg/kg	2.54E-04	9.26E-02	3.30E-02	2.61E-02
CO2_3	MF CO ₂ at pos. 3	kg/kg	3.09E-04	8.44E-02	2.99E-02	2.44E-02
CO_1	MF CO at pos. 1	kg/kg	1.09E-05	6.00E-04	4.18E-04	1.13E-04
CO_2	MF CO at pos. 2	kg/kg	1.02E-05	6.00E-04	4.17E-04	1.14E-04
CO_3	MF CO at pos. 3	kg/kg	1.08E-05	6.00E-04	4.16E-04	1.16E-04
O2_1	MF oxygen at pos. 1	kg/kg	2.33E-04	1.20E-01	4.28E-02	3.19E-02
O2_2	MF oxygen at pos. 2	kg/kg	2.54E-04	9.26E-02	3.30E-02	2.61E-02
O2_3	MF oxygen at pos. 3	kg/kg	3.09E-04	8.44E-02	2.99E-02	2.44E-02
C3H8_1	MF propane at pos. 1	kg/kg	3.31E-05	3.29E-02	4.62E-03	8.07E-03
C3H8_2	MF propane at pos. 2	kg/kg	5.32E-07	1.63E-02	2.86E-03	5.07E-03
C3H8_3	MF propane at pos. 3	kg/kg	7.52E-10	9.82E-03	1.21E-03	2.40E-03
FED_1	FED at pos. 1	-	9.69E-06	2.74E-01	9.90E-02	7.26E-02
FED_2	FED at pos. 2	-	9.56E-06	1.54E-01	3.64E-02	3.77E-02
FED_3	FED at pos. 3	-	9.06E-06	1.17E-01	2.48E-02	2.93E-02
total_HRR	Max. total HRR	kW	-1.39E-05	5.30E-02	2.96E-02	1.77E-02
GASTEMP_FIRE	Gastemp. near fire surface	°C	452.3	1205.40	829.94	203.2
Tmax_global	Global max. of gas temp.	°C	454.8	2296.10	1507.11	601.1

For total_HRR and Tmax_global, the global maximum over the simulation time of 5 s was recorded; for all other output parameters the mean value of the last 0.5 s of simulation was used. Positions 1-3 are marked in Figure 4.1. MF means mass fraction.

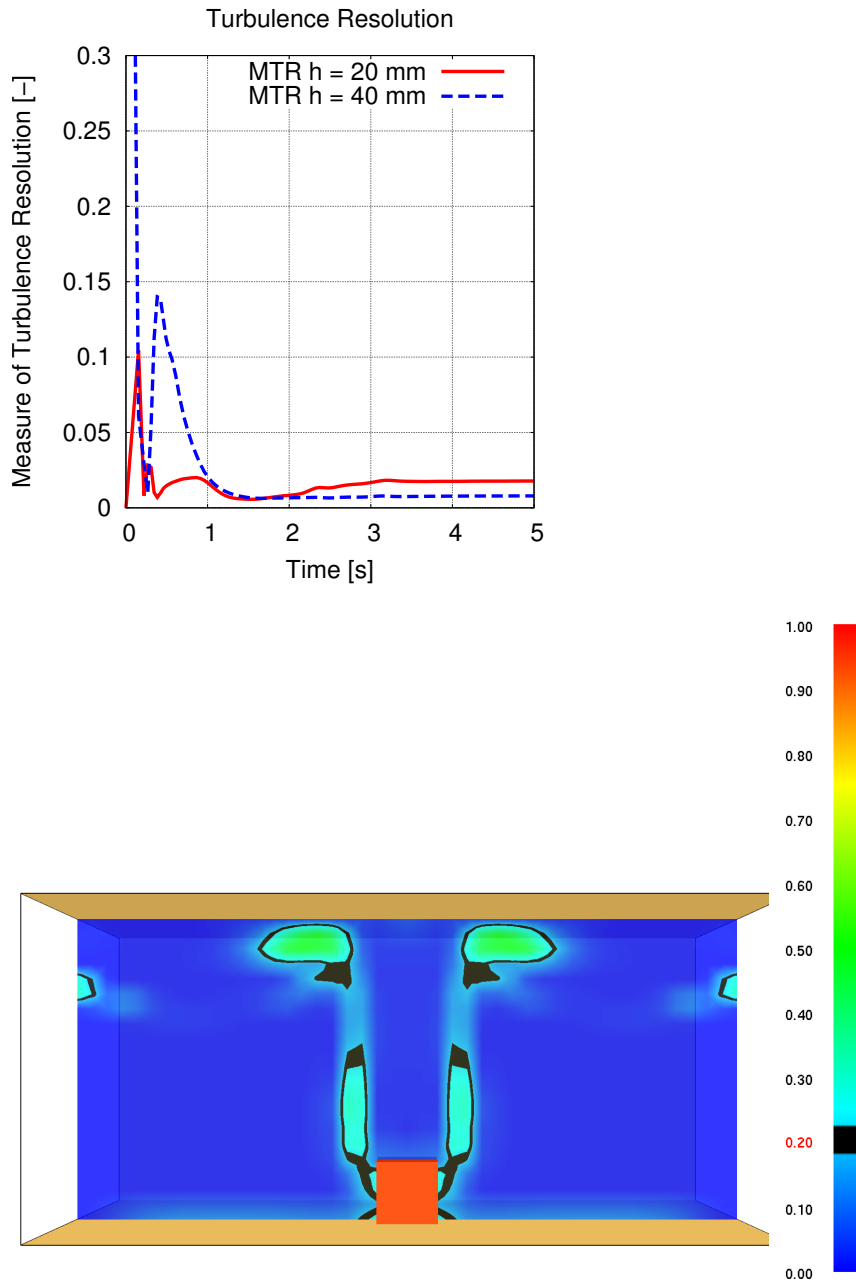


Figure 4.9: Tubular furnace analysis: *A posteriori* mesh quality metrics by the MTR criterion shown as time history for two measurement points which are situated vertically above the right edge of the fire surface, in heights of 2cm and 4cm and a centered MTR slice contour in the steady state after 5 s.

Sensitivity Analysis Results for TF2. The analysis TF2 with finite-rate combustion was carried out both with Large Eddy Simulation and with Direct Numerical Simulation in order to determine the difference arising from the different mixing models. Despite uncomplicated geometry, buoyant flow and relatively fine mesh of 2.5 mm, the differences in CoP results are significant (Figure 4.10). The two methods show very different statistical responses from the model. The DNS performs much better over this small scale. The conclusion of this result corresponds to the recommendation in the FDS User's Guide: The combination of finite-rate combustion with LES leads to significant changes in the mixing process; the reaction parameters would have to be adapted to adjust to this deviation. Also, the CoP values for the whole model (the values in parentheses in the CoP chart) are much higher for DNS compared to LES. The CoP values for the whole model indicate which portion of the variance in the specific response variable can be explained by the variation of all input parameters together. The portion of the variance of a response variable which cannot be explained by the variances of the input parameters is caused by other factors - for instance physical discontinuities or model defects, cf. section 3.2.4. So the low CoPs for the LES simulation could have their reason in the expected low quality of the mixing model for finite combustion in Large Eddy Simulation. In Figure 4.11, the influence of the variation of NS_O2_R1 (the concentration exponent of oxygen in the reaction R1) on the response variables is shown. It mainly influences the temperature and heat release rate but also has influence on the species mass fractions. The concentration exponent NS_O2_R1 controls the reaction rate of the propane combustion (cf. section 4.1.2), the bigger it is, the faster runs the reaction.

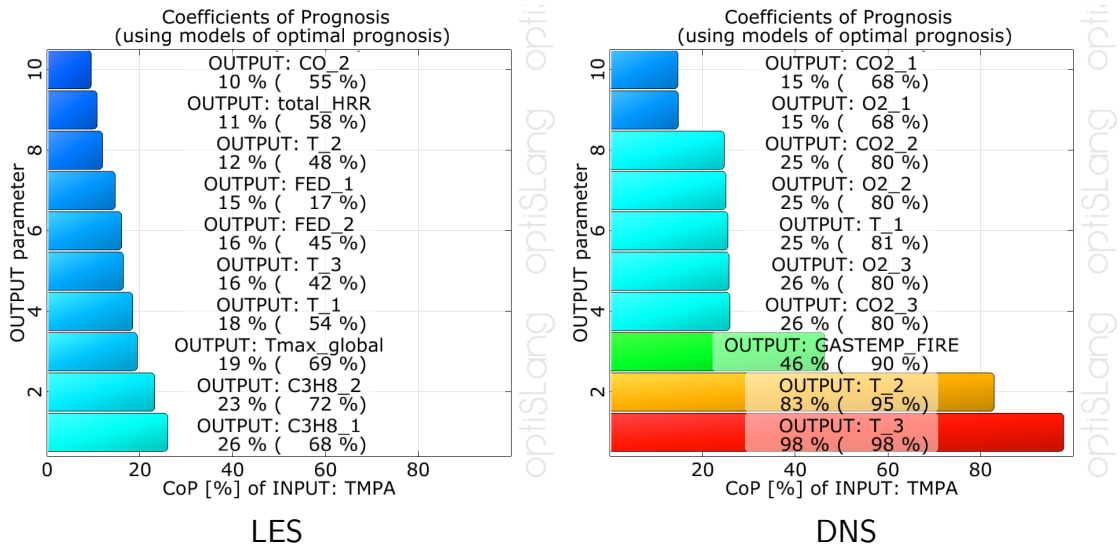


Figure 4.10: Tubular furnace analysis TF2: Coefficient of Prognosis for ambient temperature (TMPA). Comparison of finite-rate combustion with Large Eddy Simulation (LES), left vs. Direct Numerical Simulation (DNS), right, with 2.5 mm mesh resolution.

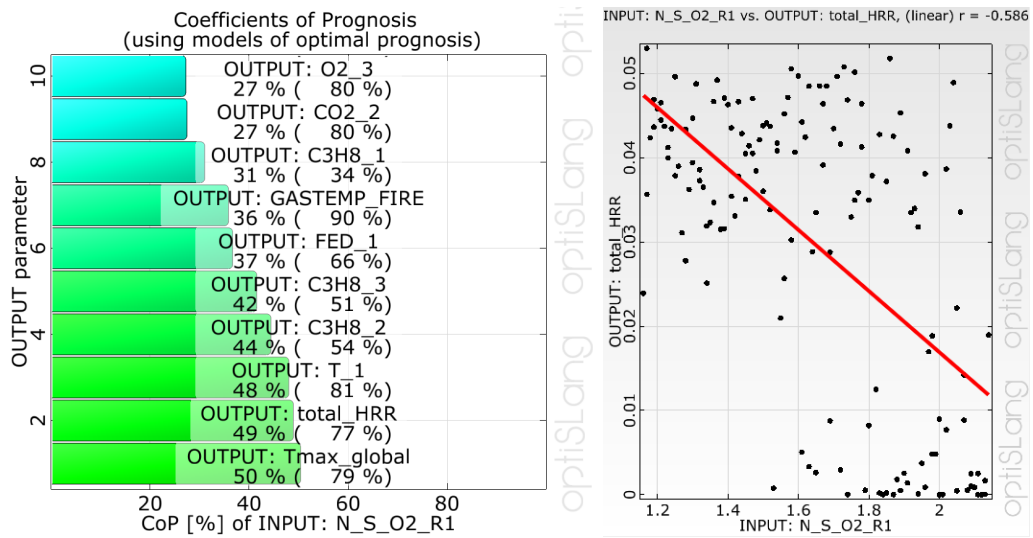


Figure 4.11: Tubular furnace analysis TF2: Coefficient of Prognosis for the concentration exponent of oxygen in reaction R1 of propane combustion, NS_O2_R1 (see 4.1.2), and anthill plot vs. max. total heat release rate.

In Figure 4.12 the Coefficient of Prognosis for the activation energy in reaction R1 of propane combustion, E_{R1} , is shown. The quotient of activation energy E_a and temperature influences the reaction rate in the Arrhenius equation. The reaction rate increases with increasing ambient (background) temperature. The sensitivity of the reaction rate versus the activation energy is stronger for lower ambient temperatures and decreases for higher temperatures, following the exponential function in the Arrhenius approach (see Figure 4.12b).

The relationship between the initial mass fraction of CO_2 and the mass fraction of CO at the three measurement points can be discussed with the data in Figure 4.11. The points which represent the highest concentrations of CO are grouped in the form of a linearly increasing function. The reason could be that more CO can be produced by reduction of CO_2 in reaction R3 when more CO_2 is available in the background. The reaction R1 is not influenced directly by the initial CO_2 mass fraction, because the initial O_2 mass fraction is independently specified. Thus the variance of the initial CO_2 only changes the initial mass fraction of the background species nitrogen.

The input parameters for reaction R2, $CO + 0.5 O_2 \rightarrow CO_2$ have a predominant influence on CO_2 , CO , O_2 and hence FED whereas the temperatures and heat release rate do not appear in the CoP diagrams in Figure 4.14 because the formation enthalpy of CO_2 and thus the heat of reaction are much lower than in the propane combustion reaction R1.

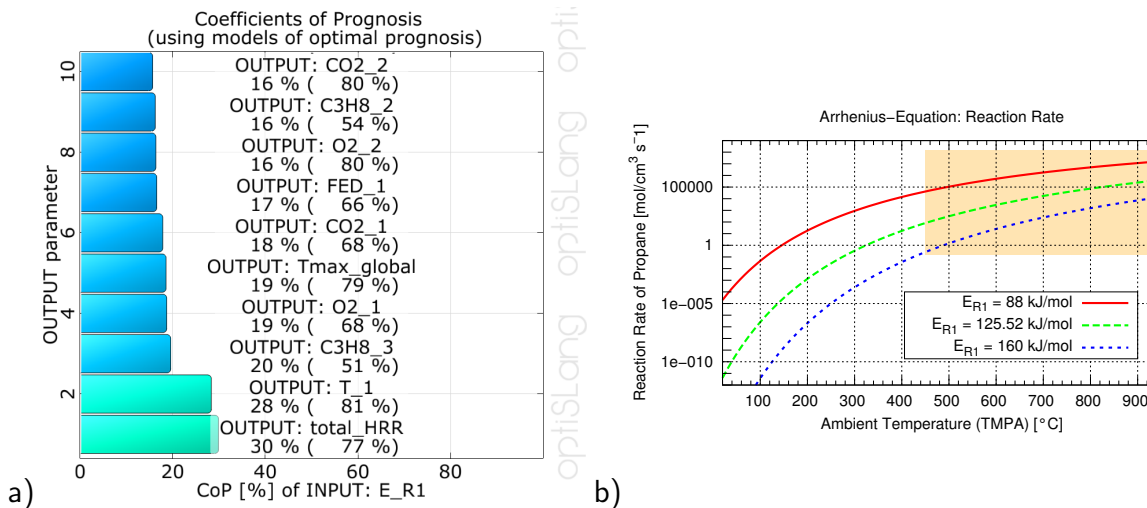


Figure 4.12: Tubular furnace analysis TF2: Coefficient of Prognosis for the activation Energy in reaction R1 of propane combustion, E_{R1} (see 4.1.2). The marked area in the Arrhenius graph is the parameter range covered in the sensitivity analysis TF2.

Figure 4.15 contains 3D response surfaces which illustrate some relationships between input and response parameters and the metamodel of optimal prognosis. The graphs 4.15a and b show the influence of the activation energy and the concentration exponent of O_2 on the mass fraction of CO_2 at position 2, and on the gas temperature at position 1, respectively. Both responses decrease with increasing activation energy E_{R1} , because there are more cells in which the high activation energy is not reached. The reaction rate in these cells is much lower. Hence CO_2 production and temperature are limited by higher activation energy. Whether the activation energy is reached also depends on the

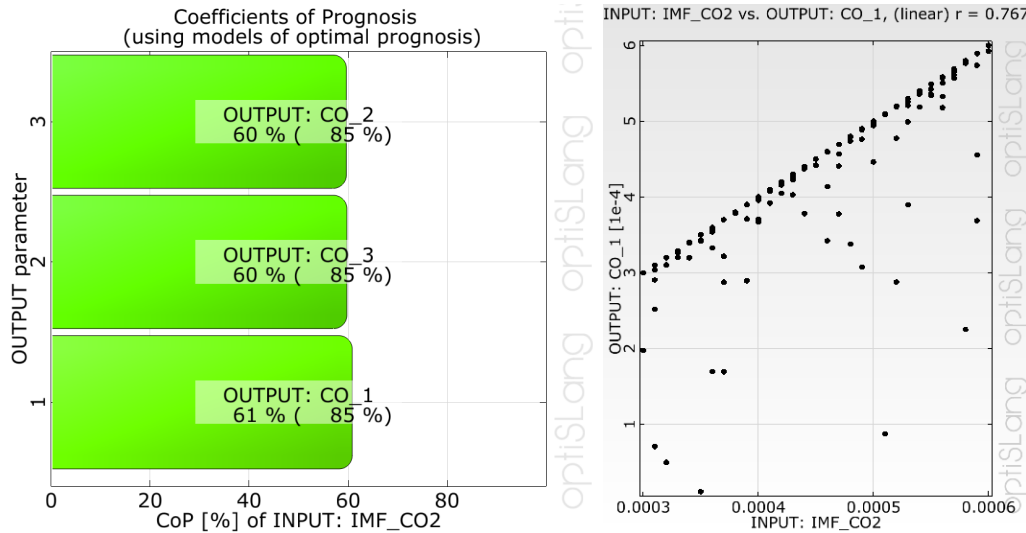


Figure 4.13: Tubular furnace analysis TF2: Coefficient of Prognosis for the initial mass fraction of CO₂, IMF_CO2, and anthill plot vs. the CO mass fraction at position 1.

background temperature, TMPA, which is realised by external heating in the real furnace test. In the Arrhenius equation, the temperature is in the denominator and the activation energy in the numerator of the negative exponent. An increasing ratio E_a/T therefore leads to slower reaction rates. This is also reflected by the response surface in Figure 4.15c, where the CO₂ mass fraction results decrease strongly for lower TMPA values. The width of the parameter range of the concentration exponent NS_CO_R2 was specified as $\pm 30\%$, and this large range produces large variations for CO2.2 and T.1. For samples with NS_CO_R2 values near the reference value of 1.65¹, the variance in CO2.2 and T.1 is obviously smaller. As a probability distribution function for this experimentally determined parameter was not available it was set to be uniformly distributed with a rather wide range.

4.3.6 Summary of findings from TF2

The sensitivity analysis TF2 of the tubular furnace model was carried out with two different numerical approaches to describe turbulence: 192 samples were simulated based on Large Eddy Simulation (LES) and 144 samples using Direct Numerical Simulation (DNS). In both cases more samples were simulated than required according to the recommendation given in section 3.2.2: For 14 input parameters and 21 output parameters, $2 \cdot (14+21) = 70$ samples are recommended with Latin Hypercube Sampling. For the analysis with LES, the coefficients of prognosis are very low, whereas for the DNS version, they lie in a reasonable range of 68 to 98 %. It can be concluded that the finite-rate combustion model will, within the investigated input parameter ranges, produce reliable results only if DNS is applied. Also in the DNS study, a portion of the variation in the output parameters cannot be explained by input parameter variations. It is assumed that the simplification of reality in the finite-rate combustion model is the main reason for

¹The reference value is given in literature, e.g. Westbrook and Dryer [83].

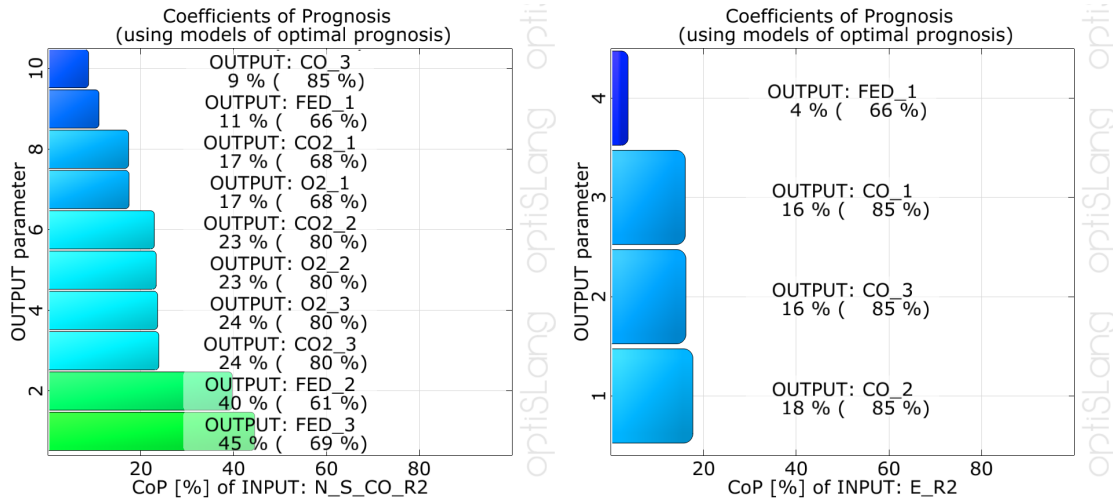


Figure 4.14: Tubular furnace analysis TF2: Coefficient of Prognosis for the concentration exponent of CO, NS_CO_R2, and for the activation energy for the reaction R2, E_R2 (right) (see 4.1.2)

this result. Unfortunately, DNS analyses require much longer simulation times and are therefore not applicable for real-scale fires with current simulation technology. For further conclusions, see also section 5.3.

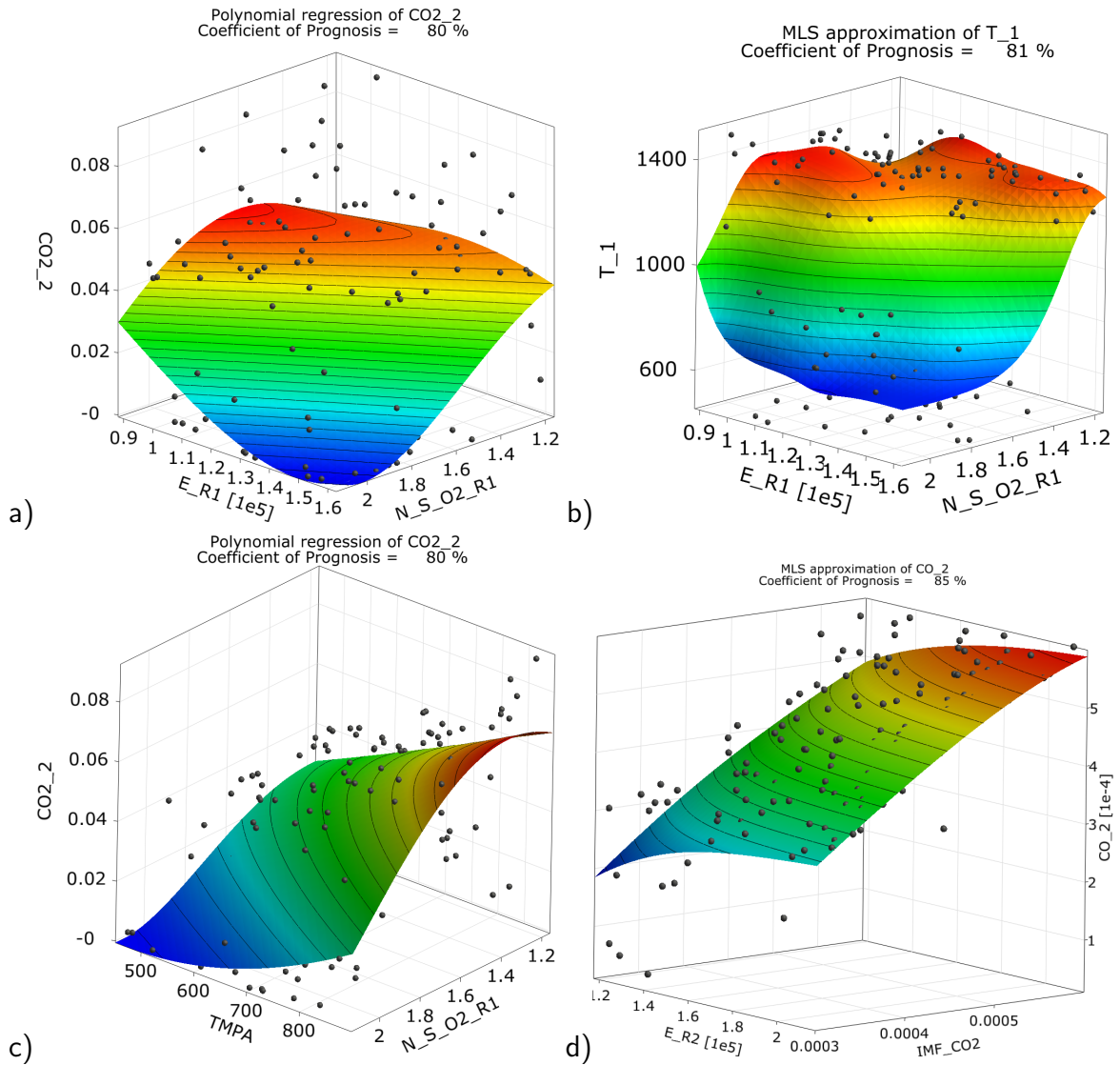


Figure 4.15: Tubular furnace analysis TF2: 3D response surfaces of the metamodel of optimal prognosis.

4.4 Sensitivity Analysis of ISO-9705 Room-Corridor test

4.4.1 Introduction

The background for the room corridor test setup is described in section [2.3.3](#).

4.4.2 Model description

The two parts of the test geometry were mapped into two meshes in the FDS model with cell size of 5cm. From the original measurement points, only a subset was included, shown in Figure [4.16](#). For the room corridor, the simulation of many samples with Direct Numerical Simulation (DNS) was not possible due to the very long simulation times; Large Eddy Simulation (LES) was used as turbulence model. Because the results from the tubular furnace simulation have shown that the finite-rate combustion model cannot be applied together with LES without significant modification of reaction parameters, the room corridor could only be investigated with the mixing-controlled simple chemistry combustion model. Equal input parameters like those in the tubular furnace study TF1 were used (see section [4.3.3](#)).

Input and output parameters for Room Corridor Test. For the room corridor analysis, 96 different input parameter sets were defined by advanced Latin Hypercube Sampling, using the parameter ranges shown in table [4.4](#).

Table 4.4: Input parameters of the room corridor sensitivity study with simple chemistry model. (Descriptions according to the FDS6 User's Guide [\[25\]](#)).

Input parameter name	Description	Units	Lower bound	Upper bound
CO_YIELD	The fraction of fuel mass converted into carbon monoxide.	kg/kg	0	0.02
SOOT_YIELD	The fraction of fuel mass converted into smoke particulate.	kg/kg	0	0.02
HOC	Heat of combustion of propane	kJ/kg	44018	48651
HRRPUA	Heat release per unit area	kW/m ²	150	300
Y_O2_INFTY	Ambient mass fraction of oxygen (default: 0.232428 kg/kg)	kg/kg	0.17	0.232428
Y_CO2_INFTY	Ambient mass fraction of carbon dioxide (default: 0.0058 kg/kg)	kg/kg	0.0003	0.0058

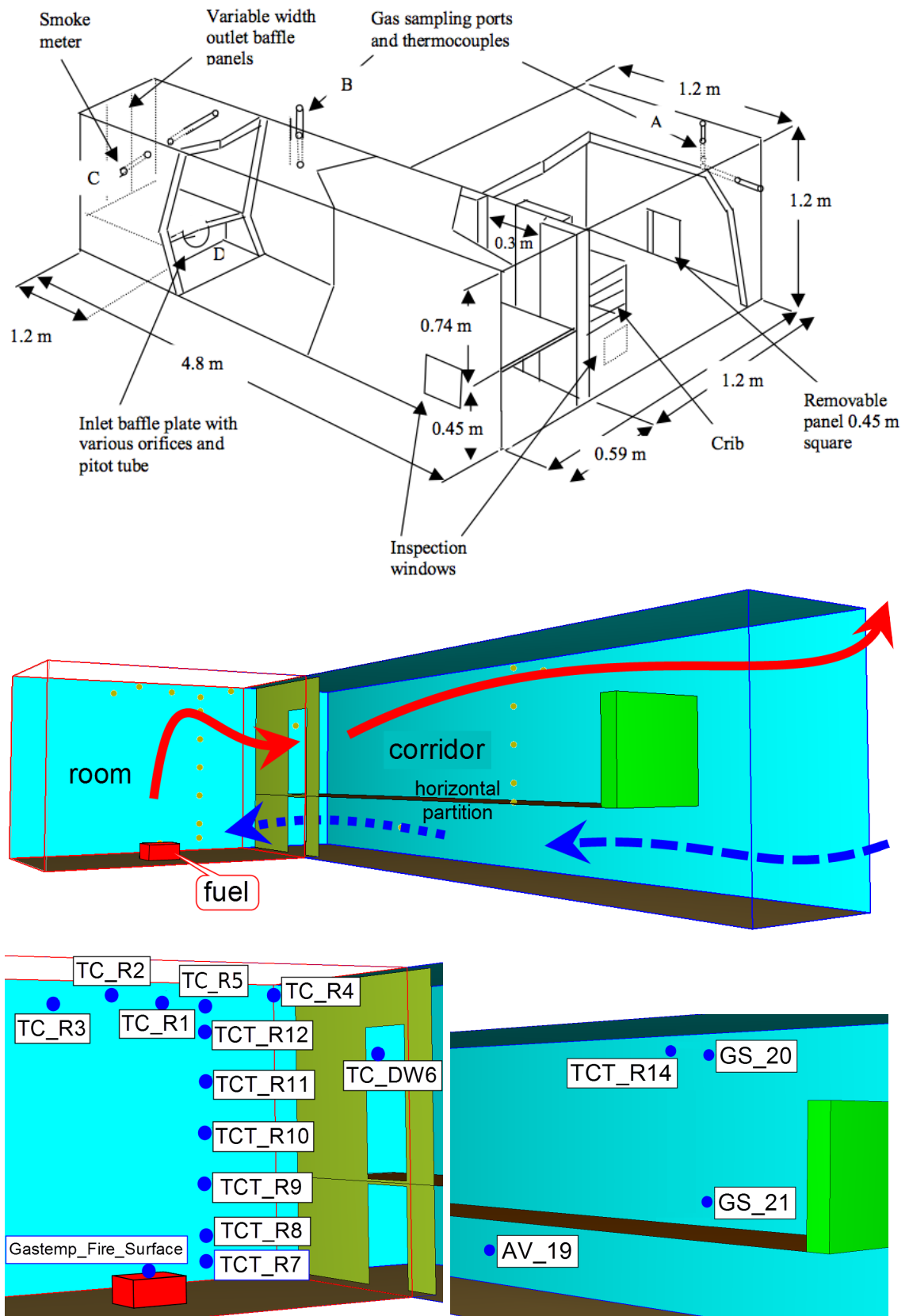


Figure 4.16: Geometry and measurement points of the room corridor simulation model

Table 4.5: Output parameters of the room corridor sensitivity study with simple chemistry model. (Descriptions according to the FDS6 User's Guide [25]). The output parameter values are the statistical results of 96 simulations, each of them using a different input parameter set. Values in the same line generally originate from different variants.

Output parameter name	Description	Units	Results			
			Min	Max	Mean	Std.-Dev.
TC_R1	T _{Gas} at TC 1	°C	66.25	96.15	81.44	8.80
TC_R2	T _{Gas} at TC 2	°C	66.72	97.58	82.16	8.87
TC_R3	T _{Gas} at TC 3	°C	69.62	104.88	87.27	9.54
TC_R4	T _{Gas} at TC 4	°C	63.78	92.18	78.26	8.40
TC_R5	T _{Gas} at TC 5	°C	64.81	93.99	79.44	8.50
TC_DW6	T _{Gas} at TC 6	°C	41.19	63.52	50.92	5.30
TCT_R7	T _{Gas} at TC 7	°C	22.40	25.01	23.53	0.58
TCT_R8	T _{Gas} at TC 8	°C	26.28	31.18	28.54	1.20
TCT_R9	T _{Gas} at TC 9	°C	36.93	49.18	43.23	3.18
TCT_R10	T _{Gas} at TC 10	°C	51.93	76.65	64.01	6.45
TCT_R11	T _{Gas} at TC 11	°C	57.71	84.72	71.27	7.39
TCT_R12	T _{Gas} at TC 12	°C	61.76	88.65	75.35	7.93
TCT_R13	T _{Gas} at TC 13	°C	64.81	93.99	79.44	8.50
TCT_R14	T _{Gas} at TC 14	°C	33.09	42.24	37.46	2.54
AV19	Flow velocity AV19	m/s	-0.45	-0.32	-0.38	0.03
GS20_CO	MF of CO at GS20	kg/kg	7.32E-08	2.00E-05	9.55E-06	5.61E-06
GS21_CO	MF of CO at GS21	kg/kg	1.47E-08	3.75E-06	1.79E-06	1.04E-06
GS20_CO2	MF of CO ₂ at GS20	kg/kg	2.64E-03	8.91E-03	5.84E-03	1.64E-03
GS21_CO2	MF of CO ₂ at GS21	kg/kg	8.09E-04	6.34E-03	3.56E-03	1.59E-03
GS20_O2	MF of O ₂ at GS20	kg/kg	1.66E-01	2.27E-01	1.97E-01	1.80E-02
GS21_O2	MF of O ₂ at GS21	kg/kg	1.69E-01	2.30E-01	1.99E-01	1.80E-02
GS20_C3H8	MF of Propane at GS20	kg/kg	3.34E-11	3.66E-11	3.50E-11	6.71E-13
GS21_C3H8	MF of Propane at GS21	kg/kg	5.85E-12	7.65E-12	6.87E-12	3.45E-13
GS20_FED	FED at GS20	–	3.40E-04	4.75E-02	1.60E-02	1.23E-02
GS21_FED	FED at GS21	–	5.24E-05	3.98E-02	1.26E-02	1.08E-02
GASTEMP_FIRE_SURFACE	Gas temp. near fire surface	°C	272.9	437.0	353.8	42.8
maxT_part1	Max. gas temp, part 1	°C	606.5	1182.6	782.1	92.1
maxT_part2	Max. gas temp, part 2	°C	74.58	118.22	96.73	11.45

For maxT_part1 and maxT_part2, the global maximum over a simulation time of 350 s was recorded; for all other output parameters the mean value of the last 50 s of simulation was used. Positions AV19, GS20 and GS21 are marked in Figure 4.16. MF means mass fraction.

Reference Run Results for Room Corridor Test. The time histories of the output parameters of the reference run were constant or slightly oscillating about a constant value after around 300 s. The simulation end time was set to 350 s. For \max_T_part1 , \max_T_part2 and FED, the global maximum over the simulation time of 350 s was recorded; for all other output parameters the mean value of the last 50 s of simulation was used. Figure 4.17 shows temperature slice files of the reference run.

Sensitivity Analysis Results for Room Corridor Test. The figures 4.18, 4.19, 4.20, 4.21, 4.22 contain the most important results of the sensitivity analysis of the room corridor with 96 samples, based on the simple chemistry model and Large Eddy Simulation. As expected the results show clearly that the specified heat release per unit area (HRRPUA) is the predominating input parameter for all temperature outputs, as displayed in the overview in Figure 4.18. This shows that all CoPs for temperature variables have high values between 78 and 100%, apart from the measurement point TC_7.

The Metamodel of Optimal Prognosis identified a linear dependency (CoP = 100 %) between HRRPUA and the temperature results and between the ambient mass fraction of CO₂ and the CO₂ concentration results (see Figure 4.20). The linear dependency is also found in the 3D response surface of the MOP between HRRPUA, the ambient mass fraction of CO₂ and the CO₂ concentration. This response surface forms a plane (CoP = 100 %), cf. Figure 4.21 (right). Similar to this behaviour of the model is the dependency between HRRPUA, CO_yield and the CO concentration. About 98 % of the results can be explained by the planar response surface.

The measurement point TC_7 near the floor and the statistical maximum Temperature for Part 1 (room of fire origin), T_{max_part1} (see Figure 4.20). This temperature is calculated as the average over the last 50 s of simulation time from the maximum gas temperature occurring in part 1. This means the location of this maximum will differ for different time steps which worsens the comparability of values recorded for the average. Conclusions cannot be drawn from this result; a better approach would be to repeat the analysis and to record the gas temperature at the location of the global maximum for part 1 over all samples and time steps. This could increase the CoP for this variable.

70% of the variance in the flow velocity AV_19 can be explained by HRRPUA in the metamodel (see Figure 4.20). The CoP of this velocity, including all input parameters, is 70% and also the Coefficient of Importance (CoI) is only 69 % for the full model. This means that 30% of variance in AV_19 cannot be predicted by the Metamodel and cannot be explained based on the CoI. Reasons could be that the flow field was not completely in steady state yet when the average was recorded, too coarse a mesh was used or model flaws.

The output parameters for gas species correlated to the input as follows:

- Oxygen mass fractions depend 100% on the initial mass fraction of O₂ (Figure 4.19d).
- The CoP for carbon monoxide mass fractions is 93% for the CO_YIELD input variable, which defines the portion of fuel which is transformed to CO in the fire (Figure 4.19c and e).

- The carbon dioxide mass fractions depend with 97% and 100% on the initial mass fraction of CO₂ (Figure 4.19a and b).

An example for a variable with low importance for all response variables is the soot yield. It is not correlated with any of the output variables investigated. Thus, soot yield could be left out in subsequent optimisation runs and efforts to determine precise input data for this parameter will not improve the precision of the results (see Figure 4.22).

4.4.3 Summary of findings from Room Corridor Test

The sensitivity analysis of the room corridor test was carried out with 96 samples based on the "simple chemistry" model and Large Eddy Simulation (LES). The 6 input and 28 output parameters would require $2 \cdot (6+28) = 68$ samples only to produce statistically reliable results, according to the recommendation given in 3.2.2. The results allow similar conclusions like for the analysis TF1 which was also performed with the mixing-controlled simple chemistry model. Most Coefficients of Prognosis (CoP) were relatively high (78–100 %), hence most variations in the output parameters can be explained by variations of the input parameters. It can be concluded that the simple chemistry model in connection with Large Eddy Simulation is also appropriate for larger compartment fires, provided that the mesh density is sufficient.

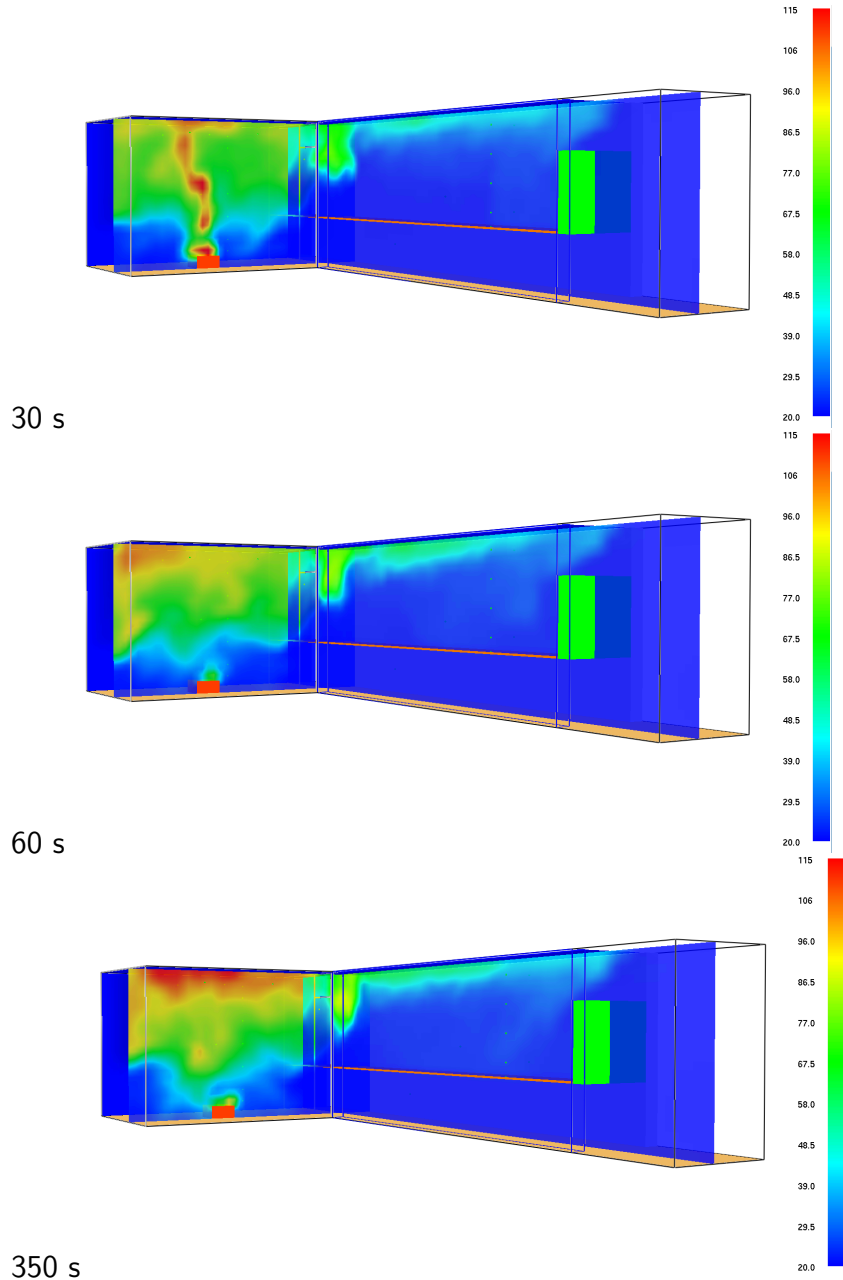


Figure 4.17: Gas temperature results (in °C) for the reference run of the room corridor model after 30, 60 and 350 s.

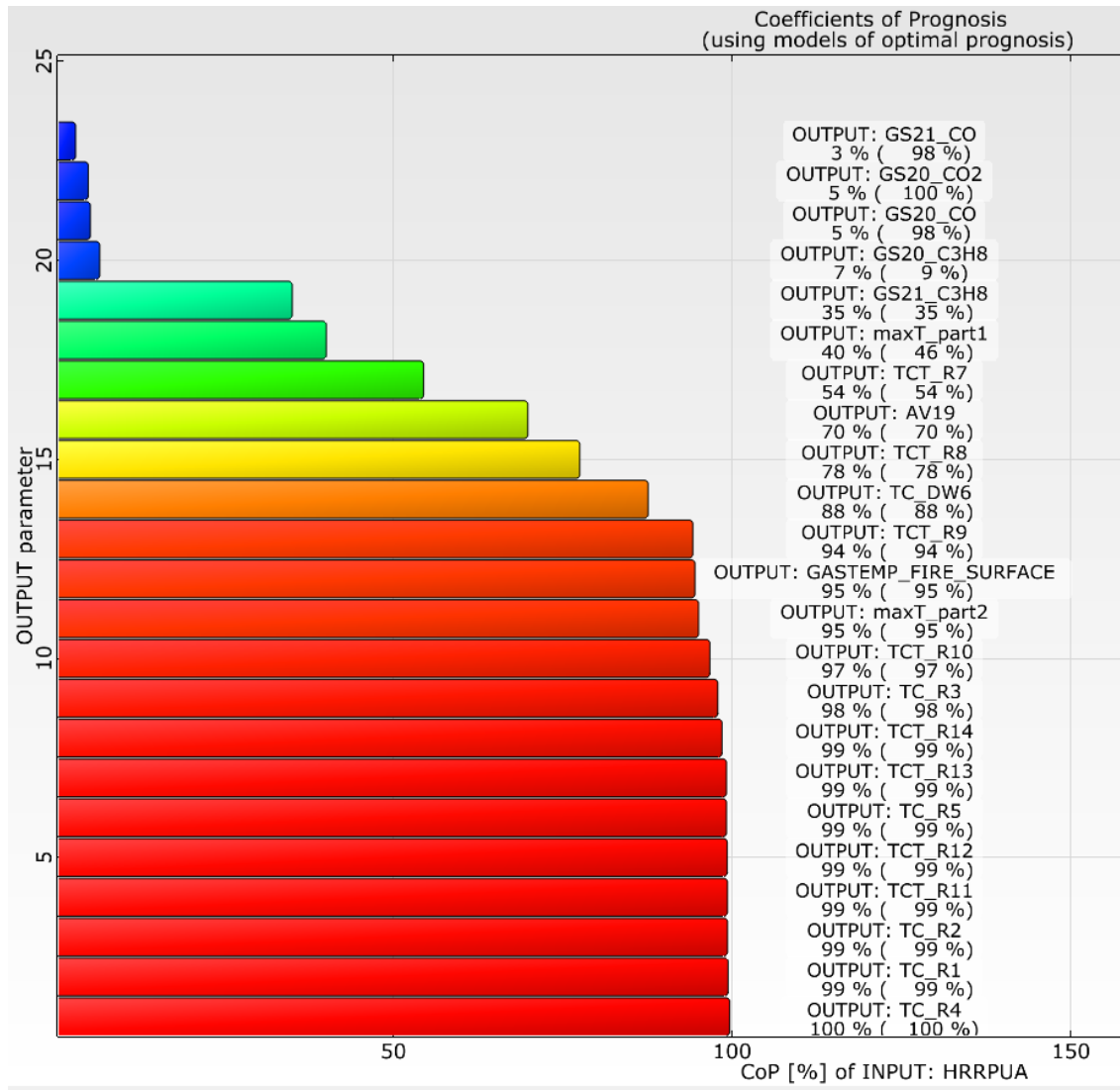


Figure 4.18: Room corridor sensitivity analysis: Coefficients of Prognosis for HRRPUA calculated with the metamodel of optimal prognosis.

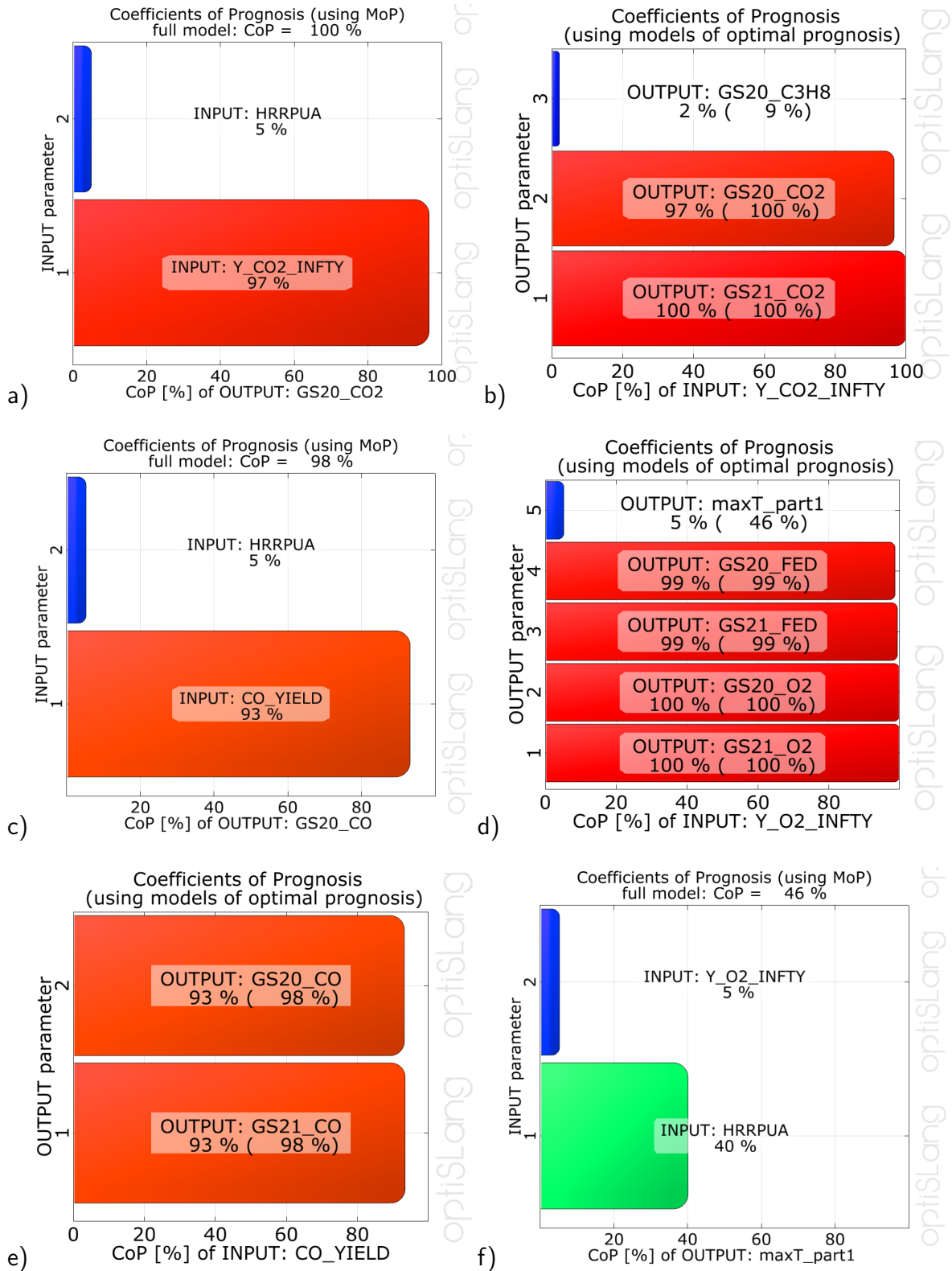


Figure 4.19: Room corridor sensitivity analysis: Coefficients of Prognosis calculated with the metamodel of optimal prognosis.

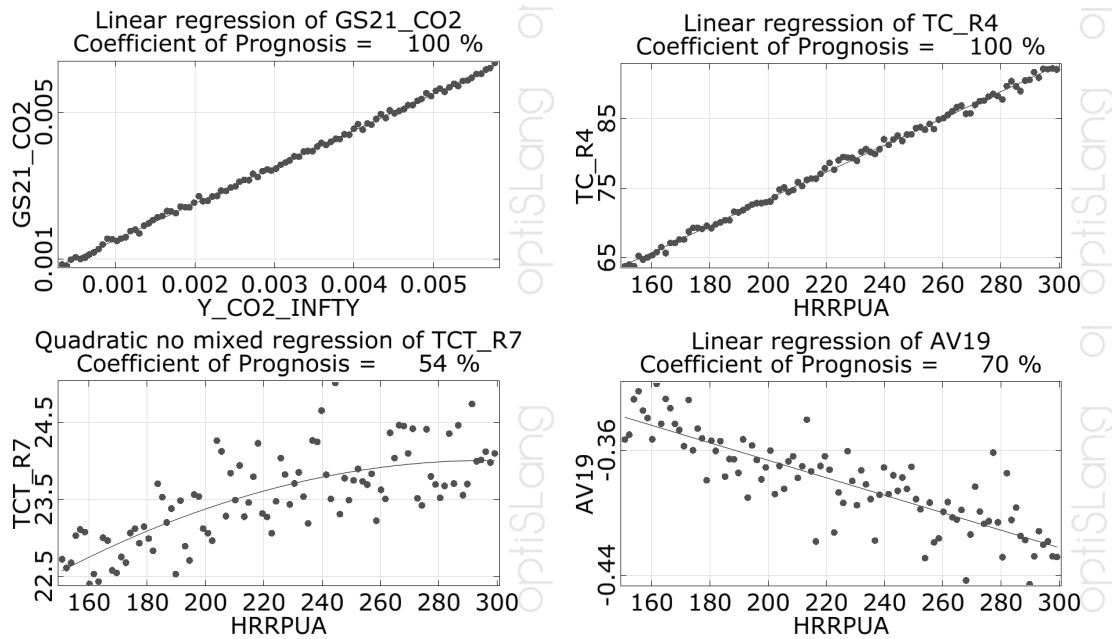


Figure 4.20: Room corridor sensitivity analysis: MOP Response Graphs.

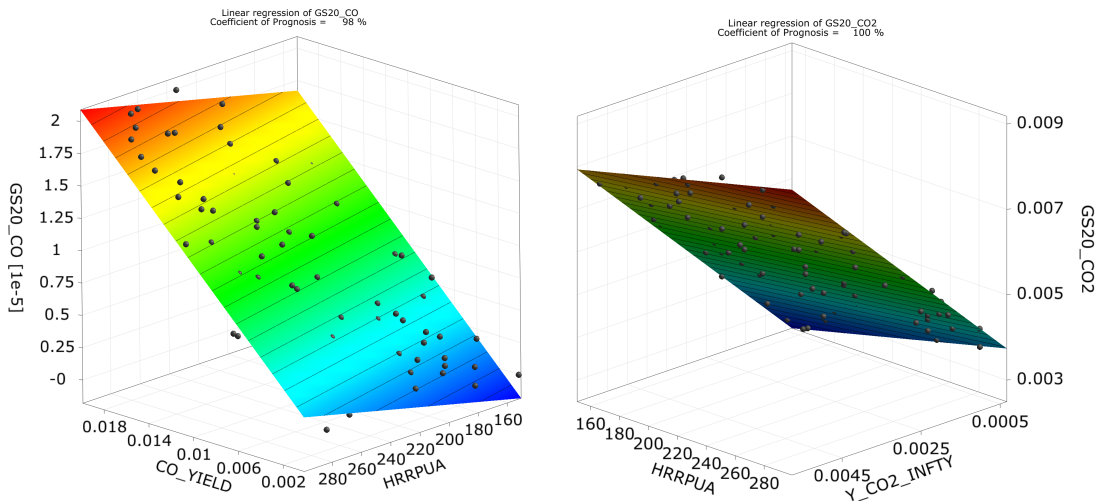


Figure 4.21: Room corridor sensitivity analysis: 3D Response Surfaces of the MOP for CO (left) and CO2 (right) at measurement point GS_20.

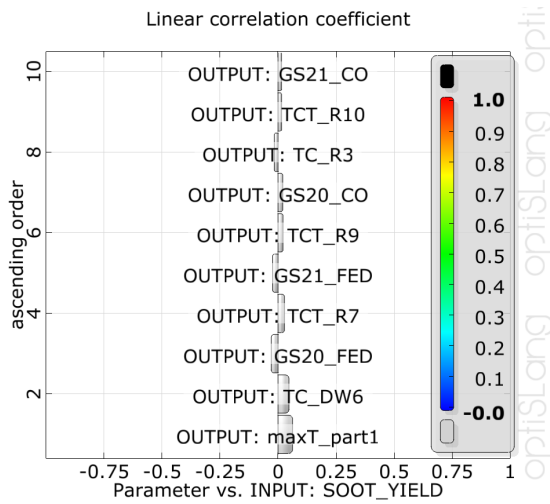


Figure 4.22: Room corridor sensitivity analysis: Linear correlation coefficients of soot yield.

Chapter 5

Conclusions

5.1 Uncertainties and Probabilistic Sensitivity Analyses

The objective of this thesis is to investigate how toxic hazard simulation for fire science can be improved. An important step towards this improvement is to identify weaknesses in the simulation model. One such weakness is the reliability of input parameters which are subject to scatter. Understanding the influence of the uncertainties in the input parameters on the results is a key to identify which parameters deserve more precise determination before being employed for predictions. Due to the numerous non-linear relationships between input parameters and responses, answers to this question can only be found by multiple simulations of the same model while varying the input parameters. An appropriate approach to examine statistically relevant response of the model on variations in input data are sensitivity analyses which are based on probabilistic methods. In chapter 4 "Simulation", results of different sensitivity analyses were presented which are based on Latin Hypercube Sampling, a method which allows a significant reduction of required samples compared to classical Monte Carlo Simulation.

The sensitivity analyses presented in chapter 4 were based on two different model scales: First, a small furnace of 5 x 11 x 5 cm with a specimen of 1 cm³ was simulated as a bench-scale investigation. Second, the half-scale room corridor test with outer dimensions of 2.30 x 4.80 x 1.20 m was subject to a sensitivity study.

Two options of gas-phase chemistry were applied: the mixing-controlled simple chemistry model and finite rate combustion based on Arrhenius equations. Further, two different numerical methods have been used: Direct Numerical Simulation (DNS) and Large Eddy Simulation (LES). As fuel, propane was used in all simulations.

In all three sensitivity studies, which are documented in chapter 4, a large number of input and output parameters were involved. The influence of 6 to 14 input parameters on 21 to 28 different output variables was investigated. Advanced Latin Hypercube Sampling was applied to generate the input parameter sets. This method minimises systematically the linear correlation between input parameter sets. This allowed statistically relevant results to be obtained with about one hundred to five hundred random samples only. Compared to other studies found in literature (cf. section 3.2.1) which are based on

deterministic sampling with few samples (between 3 and 25), the probabilistic approach ensures systematic coverage of the whole parameter space.

The aim of this approach was to acquire an understanding of the input parameters with the biggest influence on the results. For each analysis, the Metamodel of Optimal Prognosis (MOP) was calculated by searching the best approximation for the response surface. The Coefficient of Prognosis (CoP) which is determined by this model, evaluates whether the metamodel is able to predict any additional results generated with different input parameter sets. Therefore it can be applied as a measure of model quality, and also to detect potential areas of improvement. High CoP values are an indicator for reliable modelling.

5.2 Simple Chemistry or Single Mixing-Controlled Reaction

One numerical model to describe gas phase reactions in the Fire Dynamics Simulator (FDS) is the "simple chemistry" model. The basic approach of simple chemistry is a single step mixing-controlled model. It simulates a simple burner that releases heat at a predefined constant rate. Fire effluents released from this simple model are controlled by the amount of carbon atoms in the fuel, undergoing a stoichiometric burning process, with additional control parameters like CO yield and soot yield or heat of combustion of the fuel.

For the "simple chemistry" model it can be expected that the given heat release rate per unit area (HRRPUA) is the all-dominant input parameter for temperature and heat energy outputs. This was confirmed by the results both of the bench-scale simulation with the tubular furnace model and with the half-scale room corridor test.

The variance in the temperature results could be explained almost completely by the variance of HRRPUA input. The results for CO₂ confirm the expectation that CO₂ concentration depends on the ambient mass fraction of CO₂ and the amount of available fuel which is provided by the software to reach the desired heat release rate. The metamodel of optimal prognosis (MOP) for these results demonstrated an excellent ability for prediction, visible in high CoP values of 79 – 99 %.

The results of the room corridor simulation with the same combustion model also show that the predictability of the mixing-controlled combustion model by MOP is almost equally high if turbulence is simplified by Large Eddy Simulation, provided that mesh density is sufficient.

Overall these results show that with precise input data for HRRPUA and CO yield, the model will predict reliable results, whereas the initial mass fraction of O₂ and the heat of combustion of propane are only of importance when they approach the limits of their parameter ranges. The variance in soot yield had no significant effect on the selected output parameters.

Based on the sensitivity analyses it can be expected that predictability of gas temperature, CO and CO₂ mass fractions by the simple chemistry model is very good, provided that fundamental requirements for mesh density and geometric modelling are respected. This result confirms experimental validation studies which were performed by Rinne et al. [73],

where, in a single room, good correlation between simulation and test was documented. The basis for the experimental correlation was the precise measurement of the heat release rate as input parameter of the CFD model.

5.3 Finite-Rate Combustion.

In the finite-rate combustion model, the reaction is not infinitely fast, as in the mixing-controlled model, but controlled by Arrhenius equations. Here, the reaction rate depends on mass fractions of species involved, activation energies of the different reactions and temperature. It is possible to take multiple reaction steps into account and to track the different gas species which are involved in each reaction step. Because the 3-step reaction of propane is described by 3 Arrhenius equations, the number of input parameters increases considerably in comparison to the simple chemistry model. 14 input parameters were involved in the sensitivity study of the finite-rate reaction. The Arrhenius approach only works for propane if high background temperatures are set in order to keep the reaction running. The external energy input for the model is needed because of the high activation energy.

In the finite-rate combustion model, temperatures are smeared out over the mesh cell and lead to lower average temperatures for the cells if the default Large Eddy Simulation (LES) is used. Therefore it is recommended that finite-rate combustion is only used in Direct Numerical Simulation mode (DNS), or the input parameters are adapted for use in Large Eddy Simulation mode (LES). For the tubular furnace, both approaches - DNS and LES - were analysed using finite rate combustion. The results differ significantly. For the LES case, CoP values are low and the input parameters with high coefficients of importance are different from those found by DNS. Therefore only the results based on DNS will be discussed.

Despite the values of most Coefficients of Prognosis (CoP) being somewhat smaller for finite-rate combustion than for the mixing-controlled model, they are still at a level which indicates high predictability.

In Table 5.1, a comparison of different combustion and turbulence models is shown with regard to their applicability on different scales. Unfortunately, current simulation technology does not yet allow DNS simulations with real-scale fires to be carried out because very long simulation times would be required. Thus, simulations of buildings cannot yet be performed using finite-rate combustion, but are limited to simple chemistry in connection with LES. However, the rapid development of cluster computation, numerical methods and code parallelisation can create the conditions to apply this method in future. Due to these restrictions the simple chemistry model is presently used for real-scale fire simulations. Provided that heat release rate and CO yield are well defined, this model can deliver reliable predictions for gas temperatures and concentrations of carbon monoxide, carbon dioxide and oxygen. The prediction of mass fractions of other toxic combustion products with FDS 6 requires to use Direct Numerical Simulation method in combination with the finite-rate combustion model.

Table 5.1: Comparison of different combustion and turbulence models with regard to their applicability on different scales

Method	simple chemistry		finite-rate combustion	
	small scale	real scale	small scale	real scale
LES	T/R	T/R	T/–	T/–
DNS	T/R	–/R	T/R	–/R

Legend: T: Feasible with current simulation technology; R: High reliability of results; "–" not feasible or results not reliable, respectively.

5.4 Further Evaluation of Turbulent Combustion

For correct numerical modelling of combustion processes the interaction between the chemical reactions within the flame and the flow field and the effects of turbulence in both areas are important. Different régimes of turbulent combustion can be visualised in the Borghi-Peters diagram 5.1, where combustion régimes are visualised by the ratio of velocity scales v'_n/s_L and length scales l/l_F . The velocity scales are the fluctuations of the flow field v'_n and the adiabatic burning velocity or laminar flame speed, s_L . l is the length scale of the largest flow structures and l_F the laminar flame thickness. If it is known which area of the diagram is valid for the investigated scenario, useful conclusions can be made for fire simulations, e.g. on the required mesh resolution. If, for example, the chemical processes occur on a slower time scale than the eddies of the Komolgorov scale in a DNS, then the small eddies of the Komolgorov scale do influence the chemical reaction. Or, if the chemical time scale is significantly faster than large eddy turbulence time scale, the simplification of an infinitely fast reaction is justified. For the investigated scenarios of the half-scale room and the tubular furnace, laminar flame thickness, laminar flame speed and flow field fluctuations could be determined experimentally and by numerical simulation in order to assign these cases to an area in the Borghi-Peters diagram. The diagram can then also be applied to evaluate the filter effect of the mesh resolution [21, 60, 61].

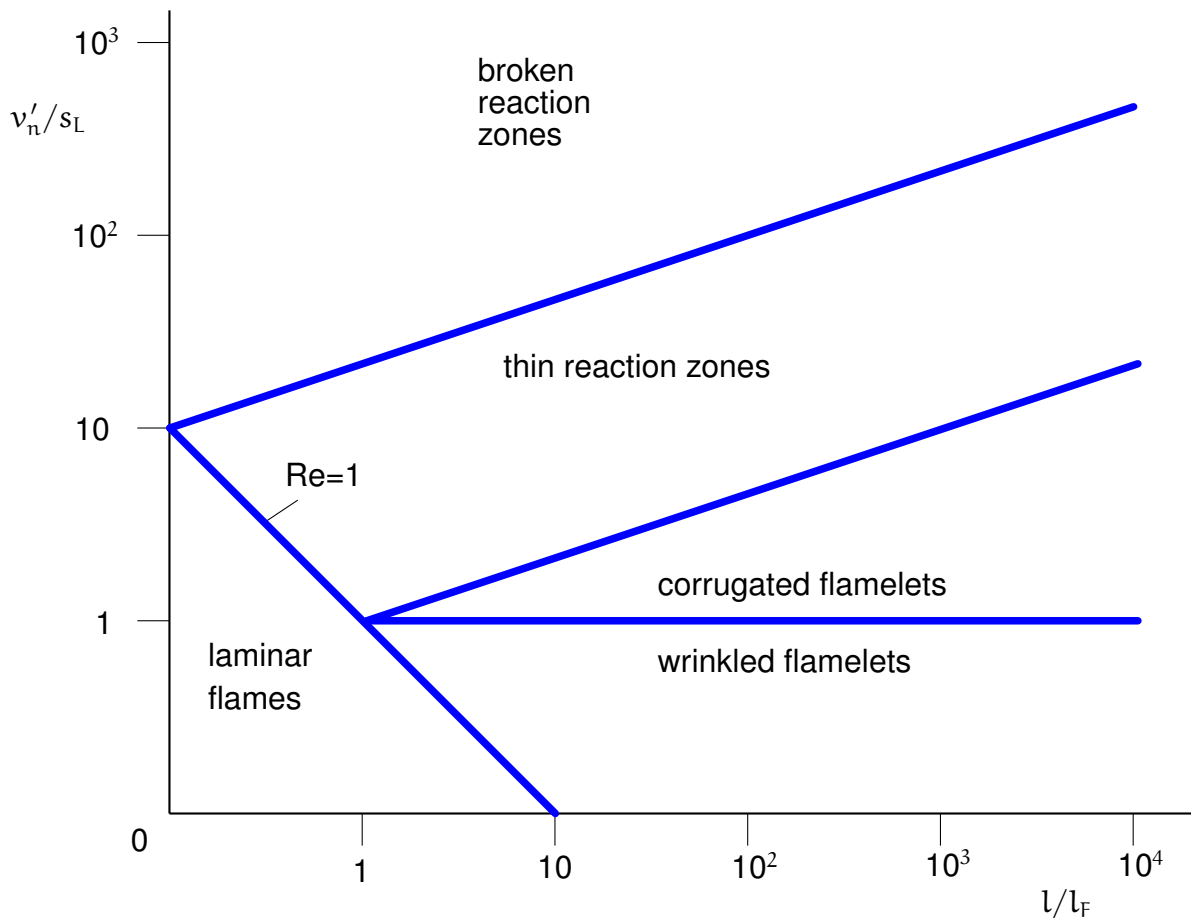


Figure 5.1: Borghi-Peters Diagram

Chapter 6

Guideline to sensitivity analyses

Based on the findings from the sensitivity analyses in this work, a general guideline is proposed below which describes how sensitivity analyses can be applied to increase the reliability of fire simulations. This includes improvement of the accuracy of simulation results for toxic combustion products. For the application of probabilistic sensitivity analysis to fire simulation as a new method, the following points are important:

- Sensitivity analysis based on probabilistic simulation can be applied to gain basic understanding of the relationships between uncertainties in input parameters and the results.
- Based on the sensitivity analysis, the number of important parameters can be reduced considerably for subsequent simulations.
- The correct simulation of toxic gases from solid fuels requires the identification of the parameters in the combustion model which are important for the toxic gas production. The identification can be performed based on sensitivity results and with simulation-based numerical optimisation methods. By use of these methods, the optimal input parameter set should be searched which allows good reproduction of test results.
- For real-scale fires, this methodology is limited to the simple chemistry model at present.
- Further development of this technology will be supported by hardware acceleration, parallelisation (use of supercomputers with high numbers of CPU cores) and advanced numerical methods.
- The proposed process how to generate simulation models with high predictability is shown in figure [6.1](#).

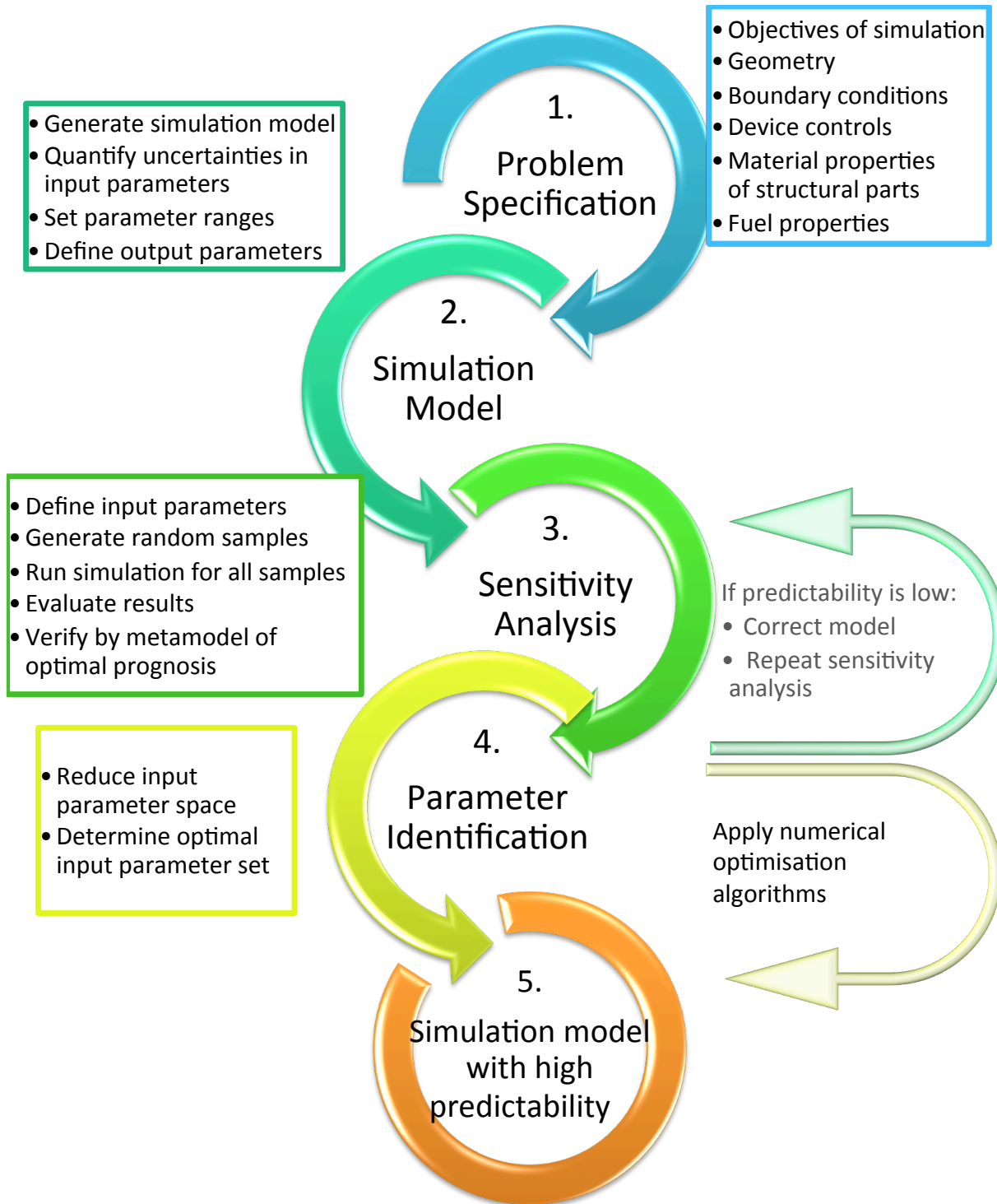


Figure 6.1: Process of sensitivity analysis and parameter identification.

References

- [1] Y. Alarie. Toxicity of fire smoke. *Critical Reviews in Toxicology*, 32(4):259–289, 2002.
- [2] C. Albrecht and D. Hosser. A response surface methodology for probabilistic life safety analysis using advanced fire engineering tools. In B. Karlsson, editor, *Fire Safety Science - Proceedings of the ninth International Symposium*, pages 1059–1072. International Association for Fire Safety Science, 2011.
- [3] ASTM E 1355. *Standard Guide for Evaluating the Predictive Capabilities of Deterministic Fire Models*. ASTM International, West Conshohocken, Pennsylvania, 2012.
- [4] J. Axelsson, P. Andersson, A. Lönnermark, P. Van Hees, and I. Wetterlund. Uncertainties in measuring heat and smoke release rates in the room or corner test and the sbi test (nt tr 477). Nordtest technical report, SP Swedish National Testing and Research Institute, 2001.
- [5] J. Axelsson, P. Andersson, P. Lönnermark, P. Van Hees, and I. Wetterlund. Uncertainties in measuring heat and smoke release rates in the room/corner test and the sbi. Technical report, SP Swedish National Testing and Research Institute, April 2001. NT Techn. Report 477 - NORDTEST Project No. 1480-00.
- [6] V. Babrauskas. Generation of co in bench-scale fire tests and the prediction for real-scale fires. In *Proceedings of the First International Fire and Materials Conference*, volume 1, pages 155–177. Inter Science Communications Ltd., London, 1992.
- [7] V. Babrauskas and R. D. Peacock. Heat Release Rate: The Single Most Important Variable in Fire Hazard. *Fire Safety Journal*, 18:255, 1992.
- [8] V. Babrauskas, R. H. Harris, Jr., E. Braun, B. Levin, M. Paabo, and R. G. Gann. The Role of Bench-Scale Test Data in Assessing Real-Scale Fire Toxicity. National Institute of Standards and Technology, Gaithersburg, Maryland, USA, and VTT Technical Research Centre of Finland, Espoo, Finland, January 1991. NIST Technical Note 1284.
- [9] V. Babrauskas, R. G. Gann, B. C. Levin, M. Paabo, R. H. Harris, Jr., R. D. Peacock, and S. Yusa. Methodology for obtaining and using toxic potency data for fire hazard analysis. *Fire Safety Journal*, 31:345–358, 1998.

- [10] C.L. Beyler. Major Species Production by Solid Fuels in a Two Layer Compartment Fire Environment. In *Fire Safety Science – Proceedings of the First International Symposium*, pages 431–440. Hemisphere Publishing Company, 1986.
- [11] C.L. Beyler. *SFPE Handbook of Fire Protection Engineering*, chapter Flammability Limits of Premixed and Diffusion Flames, pages 2–172 – 2–187. National Fire Protection Association, Quincy, Massachusetts, 3rd edition, 2002.
- [12] P. Blomqvist and M. Simonson-McNamee. Large-scale generation and characterisation of fire effluents. In A. Stec and T. R. Hull, editors, *Fire toxicity*, chapter 13, pages 118 – 198. Woodhead Publishing, Cambridge, UK, 2010.
- [13] A. Bounagui, N. Bénichou, C. McCartney, and A.H. Kashef. Fire performance of houses – part 1 – basement fires. Technical report, National Research Council Canada, 2004.
- [14] H. Brohus, P. V. Nielsen, A. J. Petersen, and K. Sommerlund-Larsen. Sensitivity analysis of fire dynamics simulation. In *The International Conference on Air Distribution in Rooms - Proceedings of Roomvent*, page 10. FINVAC, 2007.
- [15] R. A. Bryant. New Approach to Ventilation Measurements in Enclosure Fires. In *International Interflam Conference, 11th Proceedings.*, pages 453–463. Interflam, September 3-5 2007.
- [16] R. W. Bukowski. Fire Hazard Assessment for Transportation Vehicles, pages 5/227 – 5/233. National Fire Protection Association, 2002.
- [17] R. W. Bukowski, R. D. Peacock, W. W. Jones, and C. L. Forney. Example Cases for the HAZARD I Fire Hazard Assessment Method. Volume 3. Final Report. NIST Handbook 146/III, National Institute of Standards and Technology, 1989.
- [18] M. F. Bundy, A. P. Hamins, E. L. Johnsson, S. C. Kim, G. Ko, and D. B. Lenhert. Measurements of Heat and Combustion Products in Reduced-Scale Ventilation-Limited Compartment Fires. National Institute of Standards and Technology, July 2007. NIST Technical Note 1483.
- [19] N. Bénichou, J.Z. Su, A.C. Bwalya, G.D. Loughheed, B.C. Taber, P. Leroux, A.H. Kashef, C. McCartney, and J.R. Thomas. Fire performance of houses. Technical report, National Research Council Canada, 2009.
- [20] M. Clyde and E. I. George. Model uncertainty. *Statistical Science*, 19(1):81–94, 2004.
- [21] L.P.H. de Goeij. Introduction to combustion. In J.A. van Oijen, editor, *Course on Combustion*. J. M. Burgerscentrum, 2010.
- [22] E.L. Droguett. Methodology for the Treatment of Model Uncertainty. PhD thesis, University of Maryland, College Park, 1999.

- [23] D. Drysdale. An Introduction to Fire Dynamics. John Wiley & Sons, 3rd edition, 2011.
- [24] K. Fischer, J. Kohler, M. Fontana, and M. H. Faber. Wirtschaftliche Optimierung im vorbeugenden Brandschutz. Institut für Baustatik und Konstruktion, ETH Zürich, IBK Bericht Nr. 338, 2012.
- [25] J. Floyd, G. Forney, S. Hostikka, T. Korhonen, R. McDermott, and K. McGrattan. Fire dynamics simulator (version 6.0), user's guide. National Institute of Standards and Technology Special Publication 1019, February 16 2013.
- [26] B. Forell. A Methodology to assess Species Yields of Compartment Fires by means of an extended Global Equivalence Ratio Concept. PhD thesis, Technische Universität Braunschweig, 2007.
- [27] A. Galgano, C. Di Blasi, and E. Milella. Two-model Monte Carlo Simulation of Fire Scenarios. *Polymer Degradation and Stability*, 95(12):2430 – 2444, 2010.
- [28] D. T. Gottuk and B. Y. Lattimer. SFPE Handbook of Fire Protection Engineering, chapter Effect of Combustion Conditions on Species Production. National Fire Protection Association, Quincy, Massachusetts, 3rd edition, 2002.
- [29] K. Grewolls and G. Grewolls. Praxiswissen Brandschutz - Simulationen: Schneller Einstieg und kompaktes Wissen. Feuertrutz GmbH, 2012.
- [30] K. Grewolls, T.R. Hull, A. Stec, and D.A. Purser. Fire effluent toxicity: Possibilities and limitations of modelling hazard. In 6th International Seminar on Fire and Explosion Hazards, 2010.
- [31] G. E. Hartzell, D. N. Priest, and W. G. Switzer. Modeling of Toxicological Effects of Fire Gases: II. Mathematical Modeling of Intoxication of Rats by Carbon Monoxide and Hydrogen Cyanide. *Journal of Fire Sciences*, 3:115, 1985.
- [32] L. Hatton. The T Experiments: Errors in Scientific Software. *IEEE Computational Science and Engineering*, 4(2):27–38, 1997.
- [33] L. Hatton and A. Roberts. How accurate is scientific software? *IEEE Transactions on Software Engineering*, 20(10):785–797, 1994.
- [34] B.J. Holland and J.N. Hay. The value and limitations of non-isothermal kinetics in the study of polymer degradation. Plastic Materials Laboratory, School of Metallurgy and Materials, The University of Birmingham, 2001.
- [35] D. Hosser and G. Blume. Brandschutz in chemikalienlagern -experimentelle und theoretische untersuchungen zur optimierung von nachweismethoden und schutzkonzepten. Technical report, TU-Braunschweig, Braunschweig, 2000.

- [36] S. Hostikka, T. Korhonen, and O. Keski-Rahkonen. Two-model monte carlo simulation of fire scenarios. In B. Karlsson, editor, *Fire Safety Science - Proceedings of the eight International Symposium*, pages 1241–1252. International Association for Fire Safety Science, 2005.
- [37] T. R. Hull. Bench-scale generation of fire effluents. In A. Stec and T. R. Hull, editors, *Fire toxicity*, chapter 12, pages 424 – 460. Woodhead Publishing, Cambridge, UK, 2010.
- [38] A.F.M. K. Islam. *Modelling of Fire and Toxicants Formation - Measures to Reduce Risks*. PhD thesis, Technische Universität Braunschweig, 2008.
- [39] ISO 13571. *Life-threatening components of fire – Guidelines for the estimation of time to compromised tenability in fires*, 2012.
- [40] W. Jahn, G. Rein, and J.L. Torero. The Effect of Model Parameters on the Simulation of Fire Dynamics. In *Fire Safety Science*, volume 9, pages 1341–1352. International Association for Fire Safety Science, 2009.
- [41] T. Jin. *SFPE Handbook of Fire Protection Engineering*, chapter *Visibility and Human Behaviour in Fire Smoke*. National Fire Protection Association, Quincy, Massachusetts, 3rd edition, 2002.
- [42] T. Jin and T. Yamada. Experimental study on human emotional instability in smoke filled corridor: Part 2. *Journal of Fire Sciences*, 8:124–134, 1990.
- [43] S.-H. Koo, J. Fraser-Mitchel, R. Upadhyay, and S. Welch. Sensor-linked Fire Simulation using a Monte-Carlo Approach. In B. Karlsson, editor, *Fire Safety Science - Proceedings of the ninth International Symposium*, pages 1389–1400. International Association for Fire Safety Science, 2008.
- [44] C. Lautenberger and A. Fernandez-Pello. Optimization algorithms for material pyrolysis property estimation. *IAFSS, Fire Safety Science*, 10:751–764, 2011.
- [45] B. C. Levin, E. Braun, M. Navarro, and M. Paabo. Further development of the n-gas mathematical model -an approach for predicting the toxic potency of complex combustion mixtures. In Reprinted from ACS Symposium Series No. 599, Chapter 20, *Fire and Polymers II: Materials and Tests for Hazard Prevention*, 1995. Gordon L. Nelson, the American Chemical Society.
- [46] J. Li, Z. Zhao, A. Kazakov, and F. L. Dryer. An updated comprehensive kinetic model of hydrogen combustion. 2004.
- [47] A. Lock, M. Bundy, E. L. Johnsson, A. Hamins, G. H. Ko, C. Hwang, P. Fuss, and R. H. Harris, Jr. Experimental Study of the Effects of Fuel Type, Fuel Distribution and Vent Size on Full-Scale Underventilated Compartment Fires in an ISO 9705 Room. National Institute of Standards and Technology, October 2008. NIST Technical Note 1603.

- [48] A. Lönnermark, P.O. Hedekvist, and H. Ingason. Gas temperature measurements using fibre bragg grating during fire experiments in a tunnel. *Fire Safety Journal*, 43(2):119–126, 2008.
- [49] D. M. Marquis and E. Guillaume. Modelling Reaction-to-fire of Polymer-based Composite Laminate, Nanocomposites with Unique Properties and Applications in Medicine and Industry. InTech, 2011.
- [50] T. McAllister, W. Luecke, M. Iadicola, and M. Bundy. Measurement of Temperature, Displacement, and Strain in Structural Components Subject to Fire Effects: Concepts and Candidate Approaches. National Institute of Standards and Technology, November 2012. NIST Technical Note 1768.
- [51] R.J. Moffat. *The Gradient Approach to Thermocouple Circuitry, from Temperature - Its Measurement and Control in Science and Industry*. ASTM, 1962.
- [52] G.W. Mulholland, M.L. Janssens, S. Yusa, W. Twilley, and V. Babrauskas. The effect of oxygen concentration on co and smoke produced by flames. In *Fire Safety Science*, volume 3, pages 585–594. International Association for Fire Safety Science, 1991.
- [53] M. Münch. Brandsimulation / cfd-simulation: Einführung. <http://www.inuri.de/index.php/de/fachinformationen/brandsimulation.html>, 2012. Accessed 02 July 2012.
- [54] National Institute of Standards and Technology (NIST) of the United States Department of Commerce. https://code.google.com/p/fds-smv/wiki/FDS_Release_Notes/, 24 Feb 2012. Accessed 24 Feb 2013.
- [55] NIST. Fire Dynamics Simulator, Technical Reference Guide. National Institute of Standards and Technology, Gaithersburg, Maryland, USA, and VTT Technical Research Centre of Finland, Espoo, Finland, February 16 2013. NIST Special Publication 1018 (Four volume set).
- [56] K.A. Notarianni. Uncertainty, chapter 5-4. SFPE, 2008.
- [57] optiSLang Documentation. optiSLang - the Optimizing Structural Language, Sensitivity Analysis, Multidisciplinary Optimization, Robustness Evaluation, Reliability Analysis and Robust Design Optimization, Version 3.2.1, July 8 2011.
- [58] T. Paloposki, L. Liedquist, and Valtion teknillinen tutkimuskeskus. Steel Emissivity at High Temperatures, volume 2299 of VTT research notes. Technical Research Centre of Finland, 2005.
- [59] J. Pauluhn. Animal exposure experiments. In A. Stec and T.R. Hull, editors, *Fire toxicity*, chapter 7, pages 229 – 281. Woodhead Publishing, Bayer Schering Pharma, Germany, 2010.
- [60] N. Peters. *Turbulent Combustion*. Cambridge University Press, Cambridge, 2000.

- [61] N. Peters. Premixed turbulent combustion: The regime diagram. <http://www.princeton.edu/cefr/Files/2010%20Lecture%20Notes/Norbert%20Peters/Lecture11.pdf>, 2010. Accessed 20 July 2013.
- [62] W. M. Pitts, E. Braun, R. D. Peacock, H. E. Mitler, E. L. Johnsson, P. A. Reneke, and L. G. Blevins. Temperature uncertainties for bare-bead and aspirated thermocouple measurements in fire environments. Technical report, National Research Council Canada, October 1998. NIST Interagency/Internal Report (NISTIR) - 624.
- [63] W.M. Pitts. The Global Equivalence Ratio Concept and the Formation Mechanisms of Carbon Monoxide in Enclosure Fires. *Progress in Energy and Combustion Science*, 21:197–237, 1995.
- [64] D.A. Purser. SFPE Handbook of Fire Protection Engineering, chapter Toxicity Assessment of Combustion Products. National Fire Protection Association, Quincy, Massachusetts, 3rd edition, 2002.
- [65] D.A. Purser. Toxic hazard calculation models for use with fire effluent data. In A. Stec and T. R. Hull, editors, *Fire toxicity*, chapter 19, pages 619 – 636. Woodhead Publishing, Cambridge, UK, 2010.
- [66] D.A. Purser. Application of human and animal exposure studies to human fire safety. In A. Stec and T. R. Hull, editors, *Fire toxicity*, chapter 8, pages 282 – 345. Woodhead Publishing, Cambridge, UK, 2010.
- [67] D.A. Purser. Hazards from smoke and irritants. In A. Stec and T. R. Hull, editors, *Fire toxicity*, chapter 3, pages 51 – 117. Woodhead Publishing, Cambridge, UK, 2010.
- [68] D.A. Purser and J.A. Purser. HCN yields and fate of fuel nitrogen for materials under different combustion conditions in the ISO 19700 tube furnace and large-scale fires. *IAFSS, Fire Safety Science*, 9:1117–1128, 2008.
- [69] J. Qu. Response Surface Modelling of Monte-Carlo Fire Data. PhD thesis, Victoria University, Australia, 2003.
- [70] J. G. Quintiere. *Fundamentals of fire phenomena*. John Wiley & Sons, University of Michigan, 2006.
- [71] J.G. Quintiere, B.S. Grove, Building, Fire Research Laboratory (U.S.), and College Park. Dept. of Fire Protection Engineering University of Maryland. Correlations for Fire Plumes. NIST GCR. National Institute of Standards and Technology, Building and Fire Research Laboratory, 1998.
- [72] G. Rein, J.L. Torero, and et al. W. Jahn. Round-robin study of a priori modelling predictions of the Dalmarnock Fire Test One. *Fire Safety Journal*, 44(4):590 – 602, 2009.

- [73] T. Rinne, J. Hietaniemi, and S. Hostikka. Experimental Validation of the FDS Simulations of Smoke and Toxic Gas Concentrations. Technical report, VTT, Espoo, 2007. URL <http://www.vtt.fi/inf/pdf/workingpapers/2007/W66.pdf>.
- [74] A. Saltelli, K. Chan, and E.M. Scott. Sensitivity Analysis. Wiley series in probability and statistics. Wiley, 2000.
- [75] R. Shepherd. Effects of fire effluents on fire victims. In A. Stec and T.R. Hull, editors, Fire toxicity, chapter 5, pages 199 – 216. Woodhead Publishing, Royal Liverpool Hospital, UK, 2010.
- [76] A. Stec. Toxicity toxic product yields in fire: Influence of material, temperature and ventilation condition. Symposium "Fire Safety Engineering in the UK: The State of the Art.". BRE Centre for Fire Safety Engineering, University of Edinburgh, 2010.
- [77] A. Stec. Estimation of toxicity during burning of common materials. In A. Stec and T. R. Hull, editors, Fire toxicity, chapter 15, pages 541 – 558. Woodhead Publishing, Cambridge, UK, 2010.
- [78] A. Stec and T. R. Hull, editors. Introduction to fire toxicity. Woodhead Publishing, Cambridge, UK, 2010.
- [79] S. I. Stoliarov, N. Safronava, and R. E. Lyon. The effect of variation in polymer properties on the rate of burning. Fire and Materials, 33(6):257 – 271, 2009.
- [80] B. N. Taylor and C. E. Kuyatt. Guidelines for Evaluating and Expressing the Uncertainty of NIST Measurement Results, 1994. NIST Technical Note 1297.
- [81] J. Troitzsch. Plastics Flammability Handbook: Principles, Regulations, Testing and Approval. Hanser Verlag, Munich, 2004.
- [82] J. M. Watts, Jr. and J. R. Hall, Jr. Introduction to Fire Risk Hazard Analysis, pages 5/1 – 5/7. National Fire Protection Association, 2002.
- [83] C.K. Westbrook and F.L. Dryer. Simplified Reaction Mechanisms for the Oxidation of Hydrocarbon Fuels in Flames. Combustion Science and Technology, 27:31–43, 1981.
- [84] A. Witkowski. The use of Numerical Methods to Interpret Polymer Decomposition Data. PhD thesis, University of Central Lancashire, 2012.